AD_____

GRANT NUMBER DAMD17-94-J-4242

TITLE: Electrically Mediated Trauma Repair

PRINCIPAL INVESTIGATOR: Richard B. Borgens, Ph.D.

CONTRACTING ORGANIZATION: Purdue Research Foundation
West Lafayette, Indiana 47907

REPORT DATE: September 1998

TYPE OF REPORT: Final

PREPARED FOR: Commander
U.S. Army Medical Research and Materiel Command
Fort Detrick, Maryland 21702-5012

DISTRIBUTION STATEMENT: Approved for public release;
distribution unlimited

The views, opinions and/or findings contained in this report are
those of the author(s) and should not be construed as an official
Department of the Army position, policy or decision unless so
designated by other documentation.

REPORT DOCUMENTATION PAGE

Public reporting burden for this collection of information is estimated to average 1 hour per response, including the time for reviewing instructions, searching existing data sources, gathering and maintaining the data needed, and completing and reviewing the collection of information. Send comments regarding this burden estimate or any other aspect of this collection of information, including suggestions for reducing this burden, to Washington Headquarters Services, Directorate for Information Operations and Reports, 1215 Jefferson Davis Highway, Suite 1204, Arlington, VA 22202-4302, and to the Office of Management and Budget, Paperwork Reduction Project (0704-0188), Washington, DC 20503.

1. AGENCY USE ONLY (Leave blank)	2. REPORT DATE September 1998	3. REPORT TYPE AND DATES COVERED Final (22 Aug 94 - 21 Aug 98)

4. TITLE AND SUBTITLE
Electrically Mediated Trauma Repair

5. FUNDING NUMBERS
DAMD17-94-J-4242

6. AUTHOR(S)
Borgens, Richard B., Ph.D.

7. PERFORMING ORGANIZATION NAME(S) AND ADDRESS(ES)
Purdue Research Foundation
West Lafayette, Indiana 47907

8. PERFORMING ORGANIZATION REPORT NUMBER

9. SPONSORING / MONITORING AGENCY NAME(S) AND ADDRESS(ES)
U.S. Army Medical Research and Materiel Command
Fort Detrick, Maryland 21702-5012

10. SPONSORING / MONITORING AGENCY REPORT NUMBER

19990127 081

11. SUPPLEMENTARY NOTES

12a. DISTRIBUTION / AVAILABILITY STATEMENT

Approved for public release; distribution unlimited

12b. DISTRIBUTION CODE

13. ABSTRACT (Maximum 200 words)

As an external application to injured or developing systems, steady voltage gradients can alter the dynamics of such processes in a predictable and polarized way. We have exploited this in ways designed to enhance the regeneration of nervous tissue with small current regulated implantable devices. We have facilitated regeneration of nerve fibers within the lesioned adult mammalian spinal cord following acute application of DC fields. Further tests proved that a recovery of function in a normally permanent sensorimotor defects secondary to severance of the relevant intramedullary spinal cord tracts could be induced. This research employed the cutaneus trunci muscle reflex (CTM) of the adult guinea pig where functioning of skin musculature is dependent on long afferent projections within the ventrolateral spinal cord. Evaluation of skin movement and electrophysiological evaluation of the reflex proved that up to 25% of electrically treated animals recovered reflex functioning while 100% of the sham treated population remained permanently impaired. Further development of devices designed to affect both ascending and sescending nerve fiber projections have been tested to be effective in restoring variable levels of functional recovery in clinical cases of naturally produced, and neurologically complete paraplegia in canines. We believe this technique provides a relatively simple medical intervention to recover lost functions following severe traumatic CNS injury.

14. SUBJECT TERMS
Electrical Fields, Central Nervous System Trauma, Spinal Cord Injury, Functional Recovery, Bioimplants, Paraplegia

15. NUMBER OF PAGES
139 pages

16. PRICE CODE

17. SECURITY CLASSIFICATION OF REPORT	18. SECURITY CLASSIFICATION OF THIS PAGE	19. SECURITY CLASSIFICATION OF ABSTRACT	20. LIMITATION OF ABSTRACT
Unclassified	Unclassified	Unclassified	Unlimited

FOREWORD

Opinions, interpretations, conclusions and recommendations are those of the author and are not necessarily endorsed by the U.S. Army.

_____ Where copyrighted material is quoted, permission has been obtained to use such material.

_____ Where material from documents designated for limited distribution is quoted, permission has been obtained to use the material.

_____ Citations of commercial organizations and trade names in this report do not constitute an official Department of Army endorsement or approval of the products or services of these organizations.

_____ In conducting research using animals, the investigator(s) adhered to the "Guide for the Care and Use of Laboratory Animals," prepared by the Committee on Care and Use of Laboratory Animals of the Institute of Laboratory Resources, National Research Council (NIH Publication No. 86-23, Revised 1985).

_____ For the protection of human subjects, the investigator(s) adhered to policies of applicable Federal Law 45 CFR 46.

_____ In conducting research utilizing recombinant DNA technology, the investigator(s) adhered to current guidelines promulgated by the National Institutes of Health.

_____ In the conduct of research utilizing recombinant DNA, the investigator(s) adhered to the NIH Guidelines for Research Involving Recombinant DNA Molecules.

_____ In the conduct of research involving hazardous organisms, the investigator(s) adhered to the CDC-NIH Guide for Biosafety in Microbiological and Biomedical Laboratories.

_____   _____
PI - Signature   Date

Table of Contents

I. INTRODUCTION

The behavioral loss following severe neurotrauma results from the inability of nerve fibers within the central nervous system (CNS) to regenerate significantly to form new, functionally meaningful connections as well as the physiological dysfunction of intact, yet demyelinated axons within white matter[19,91,12]. At present there is no known approach to altering the biology of this injury to significantly change the axis of behavioral deficits. For example, the administration of "high dose" methylprednisilone following spinal trauma must be made within the first 8 hours of injury and is only effective in neurologically "incomplete" cases[44]. In spite of other advancements[70], we should view the opportunity for significant recovery following severe CNS neurotrauma as limited, and the quality of life for those affected as impoverished.

Our approach to an experimental treatment involves the imposition of a weak (300-400 μV/mm) electric field across the long axis of the spinal cord and its injury site. This procedure originally emerged from well described growth and directional responses of neuronal processes to applied DC electric fields in culture.

When exposed to weak extracellular voltage gradients, nerve fiber responses include: an increase in the growth rate of regeneration when fibers face the cathode of the applied field; a decrease in growth rate when fibers face the anode of the applied field; resorption of neurites into the cell body when they project toward the anode; an inhibition of axonal degeneration (retrograde "dieback") when transected fibers face the cathode; an increase in retrograde degeneration when transected fibers face the anode; an increase in axonal branching when regenerating axons face the cathode; an increase in neurite outgrowth from cultured ganglion on the "cathodal" side; an induced oriented neurite growth towards the cathode and away from the anode in these same ganglion; an increased rate of growth (2-3 fold) when fibers turn towards the cathode and away from the anode; an increase in growth cone filapodia and cytoplasmic spines in the presence of a cathodal field; the respecification of oriented growth of neurites along the DC potential gradient and away from cues provided

by "contact guidance" mechanisms. These observations have recently been reviewed[85,97,98,56,28,29,40,99] and summarized in several reports in addition to the responses of several non-neuronal cell types (embryonic fibroblasts, myoblasts, neural crest) to applied DC fields[28,29,26,124].

Lastly, observations of growth responses to applied DC fields are strengthen by the fact that developing neurons <u>reside</u> in a weak, polarized extracellular voltage gradient during ontogeny[102]. This may help explain the curious and striking responses of neurons and their processes to artificially applied weak extracellular gradients of potential.

<u>Axonal Regeneration in the Mammalian Spinal Cord.</u>

For a decade, we have been testing the responses of *completely transected ascending (sensory) nerve fibers* in adult guinea pig to the imposition of distally negative applied fields. We developed an implantable current regulated circuit to accomplish this - complete with "wick" electrodes to eliminate the possible confusion produced by effects mediated by electrode products[28]. To precisely determine the original plane of transection we developed the use of a "u" shaped marker device made of tantallium that was inserted into the hemisection[36].

Tract tracing was accomplished by anterograde labeling of ascending dorsal columns with horseradish peroxidase (HRP), the site of application on the order of 2-3 vertebral segments caudal to the original transection (approximately mid thoracic)[36,37]. Our three main observations in electrically treated animals (made approximately 50 days post-transection) were: 1) a strikingly elevated number of ascending HRP loaded fibers terminated deep within the caudal aspect of the lesion, many terminating *at the exact plane of the original transection*, 2) a smaller number of ascending fibers in only field-treated animals had circumnavigated the lesion by projecting around its lateral or ventral border into the *rostral spinal cord segment.* 3) the character of the anatomical response to the field was dependent on field strength. Few fiber termination's were within the lesion at the lowest

magnitude of field (1 μA units), more numbers and deeper penetrations in the intermediate field strength (5 μA units) but without evidence of fiber projection into the rostral segment of the spinal cord. Such deviating fibers were observed in only the experimental group using 10 μA applied current (ca. 100μV /mm). All of these groups were compared to a comparable number of sham treated control animals that were implanted with non-functional (internally short circuited) implants. In the past work plan we proposed to evaluate these sensory projections using modern tract tracing with fluorescent intracellular probes such as rhodamine conjugated dextrans.

Applied Fields May Reduce "Secondary" Injury Following Spinal Trauma

The notion that trauma to the brain and spinal cord results in a two stage injury process is accepted by most investigators in the field. The first stage is an instantaneous destruction of parenchyma followed by so called "secondary injury" pathology. This next stage is perceived as a slower time course of auto destructive events - clearly superimposed on the continued degenerative phenomena caused by the initial insult. Secondary injury is correlated to the loss of free radical scavengers, the accumulation of lactate and peroxides within the lesion, and post traumatic ischemia[16,19] all of which appear to be involved with progressive histological dissolution of tissue at the site. *A particular cellular species directly implicated in this process is the macrophage.* Quantification of the density of macrophage invasion following contusion injury to the spinal cord demonstrates as much as 30% of the lesion volume at 2 weeks post injury <u>can be accounted for by these cells</u>[16,19]. The role of inflammatory processes and the particular role of the macrophage have been recently reviewed[19,119,18,17,115]. It may be possible that fields applied *soon after injury* may create conditions where macrophage infiltration of the lesion could be impaired or redirected in some predictable way. Since these cells constitute the single largest immigrant to the lesion site, they should be considered as a possible target of the applied field. This can be determined by identification of macrophages with immunohistochemical technique followed

by computer assisted sampling and cell counting, comparing control and experimental (electrically-treated) animals.

Field Induced Recovery of Function in Canine Paraplegia

Severe traumatic spinal cord injury in the canine produces the same clinical deficits observed in Humans: loss of function, both motor and sensory, below the level of the lesion, spasticity, incontinence, and atrophy of the affected hind limbs. These problems produced by neurological "complete" trauma show very little response to conventional medical and surgical intervention (including acute administration of steroids)[29,42]. We employed a clinical protocol to isolate such severely injured animals from possible "incomplete" injuries presenting at the clinic. This included tests for superficial and deep pain cognition, standard reflex testing (to identify upper motor neuron sequelae), a regimen of evoked potential tests (including SSEP, MEP, and SEP), studies of ambulation, and tests for the loss of proprioceptive placing. To meet study criterion, a dog was required to be negative on all measures of neurological functioning. We further subdivided incoming candidates on the basis of injury type (fracture dislocation or severe traumatic disc herniation) and time post injury (hours to 1 month post injury, 1 month-1 year post injury , and >1 year). The acute traumatic disc herniation group was extremely interesting due to its direct comparison to the human injury mode - namely severe compression of the spinal cord followed by extreme central hemmoragic necrosis[29,41]. One should not confuse this injury (which involves acute direct explosion of disc material into, sometimes laceration of, the spinal cord) in canine chondrodystrophic breeds with human "slipped" discs - which is rarely a spinal cord injury[29,41].

Since the resolution of behavioral deficits in a clinical injury might involve interaction of the applied field with ascending and descending tracts, we developed a methodology called "oscillating field stimulation" (OFS) born of an interesting observation by McCaig[99]. He noted that when neurites in culture experience an imposed DC field, growth responses

towards the cathode may be immediate, while degenerative changes in neurites facing the anode take on the order of 45 minutes. The differing latency in the response to either polarity of the applied field may allow a window of opportunity where field imposition produces growth towards the cathode, with relatively short exposure—but less than the time necessary to induce degenerative changes at the anode. We developed an implantable circuit which would reverse the polarity of application every 15 minutes (described in reference 28). The current regulating and timing circuitry to accomplish this have been published elsewhere[28] (see methods below). Active OFS units and indistinguishable "sham" units were produced in our laboratory, coded and provided the clinic for use in a randomized, blinded trial of their effectiveness in naturally produced canine paraplegia. All neurological exams were video taped at prespecified times: prior to surgery, just post-surgery, at the 6-8 week and 6 month recheck. Some neurological evaluations (deep pain and ambulation) were scored at the end of the experiment by comparison of video records for all dogs in the trial by a panel of investigators blinded to their status. Briefly our results were; 1) a strong trend for recovery of function *in all neurological categories* was evident in the experimental group *with no reverse trends*, compared to the sham-treated canines. 2) Only 15% of OFS treated dogs failed to recover in some category of evaluation compared to 60% of the sham-treated controls. 3) Approximately one-third of the OFS treated dogs recovered in all 4 categories of behavioral evaluation - *none of the sham treated animals did.* 4) The combined neurological score was significantly different between these groups at 8 weeks ($p< 0.033$) and at the 6 month ($p< 0.035$) recheck period.

In summary OFS stimulation appears to be an effective technique to accomplish recovery of function in clinical cases of spinal trauma if applied within 1 month of the injury (most convincing results were achieved when the application was within 2 weeks of injury[41]. Further advancement must depend on a deeper understanding of these mechanisms of action at least at *the cell and tissue level of inquiry.* The USAMRDC embodies just such an important evaluation of these relevant anatomies following DC

stimulation using a defined guinea pig spinal cord lesion and further canine clinical trials intended to determine if an increased magnitude (3 fold) of oscillating field stimulation will a) extend the effective time frame of acute treatment and b) lead to a greater level of behavioral recovery in all cases, and c) prove to be more effective in promoting recovery than that provided by decompressive surgery and acute administrations of steroids.

II. Body

1. Methods

A. Sensory Projections, DC Fields, and Flourescent Tract Tracing

<u>Experimental Animals</u>

Adult guinea pigs (ca. 400-500 g) of the Hartley strain were used for these experiments. Animals were divided into two groups, those receiving active stimulator units and those receiving sham (inoperative) units. Following surgery, animals were housed two per cage, fed ad libidum and monitored daily. All animals were sacrificed 2 months post surgery (Table 1). The surgical procedures, stimulator fabrication, and preparation of tissues used in this study are very similar to previously described techniques in this series[36,37,38,40,41]. Only a brief summary will be repeated here, emphasizing the departures from earlier methods.

	Operated	Surviving	Days to Sacrifice	Range	Lost to Histology
Experimental	25	18[1]	60 ($\pm$0.56)[2]	57-64	4[3]
Control	19	15	60 ($\pm$0.57)	57-63	1

Table 1

1. *Difference in mortality between the groups is not significant (P=1.0, Fisher's exact test)*
2. *SEM is shown within the parenthesis*
3. *Number lost due to technical error, and/or failure in label uptake.*

<u>Surgical Procedures</u>

Anesthesia was performed with an intramuscular injection of a mixture of 60 mg/kg ketamine HCL, 0.6 mg/kg acepromazine maleate, and 12 mg xylazine. The spinal cord was exposed by a dorsal and partial laminectomy, and a dorsal hemisection performed. The spinal cord was cut transversely slightly ventral to the level of the central canal, and the lesion confirmed, by previously described techniques. A small marker device was inserted into this cleft as in Fig. 1, and the lesion covered by a small rectangular piece of silastic

sheet (Dow - Corning 500 - 1). The marker device was fashioned from platinum-iridium wire and was left *in situ* for the duration of the experiment. When removed, following perfusion/fixation, the marker provided index holes in the parenchyma of the spinal cord. These holes allowed a determination of the original plane of transection (Fig. 1). The silastic sheet was used to help maintain the position of the marker device, and to keep it from being displaced upward and out of the lesion by movement of the animal within the first week or so following surgery. The surgery was completed by closing the tissues in layers following the implantation of the stimulator and positioning of the electrodes.

The stimulator unit (see below) was subcutaneously located beneath the substantial fat pad on the animals' back between their shoulders. Electrodes were routed from this location and affixed to paravertebral musculature with 3-0 silk suture, rostral and caudal of the hemisection by approximately 2 vertebral segments. A colored suture was knotted into the paravertebral muscle adjacent to the hemisection to help locate this site at a later date. The cathode (negative pole of the circuit) was always positioned rostral to the lesion. In this way, the proximal segments of severed ascending afferent fibers within the white matter would experience a distally negative imposed electrical field.

Figure 1 Legend

This artists drawing shows the shape, size, and placement of the marker device into a dorsal hemisection of the spinal cord. The marker is left in situ during the experiment and only removed following fixation of the tissues (see methods).

To the right, and clockwise, are illustrations of the general appearance of longitudinal/ horizontal histological sections of the spinal cord following the removal of the marker. In more dorsal sections, two holes may mark the lateral boundaries of the lesion (top right), while a transverse hole marks the ventral boundary of the lesion. Many times there may be movement of the marker producing index holes that are slightly oblique compared to usual (3rd from top right), or where one index hole is missing because the edge of the marker device extended out of the spinal cord on one side (bottom, right). A natural marker for the plane of transection is the closely opposed tips of the severed and swollen central canal. The canal does not reunite, and usually forms a large syrinx causing even more damage in surrounding parenchyma.
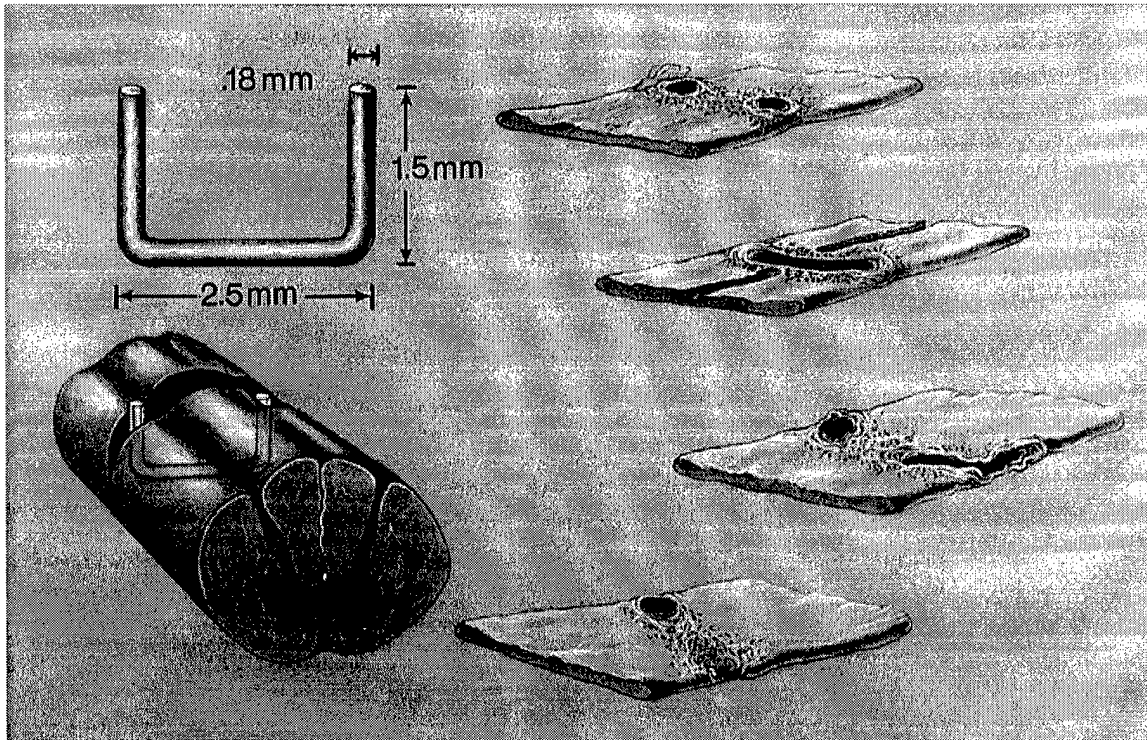
Figure 1

Stimulator Units

The stimulator units were powered by two 3 Volt Lithium Cells (Ray o Vac 1225 BR), connected to a National Semiconductor LM 334 Z Constant Current Source used to maintain regulated current, and a single 1/8th Watt resistor which set the current level to 45 μA. This level of current would be associated with an electrical field imposed across the spinal cord lesion of approximately 0.4 mV/mm (based on earlier in vivo measurements, Borgens et al., 1990). With 39 mA hr capacity, the voltage would be exhausted at approximately 36 days. Sham stimulators were fashioned to be identical to the active units but rendered inoperative through the use of exhausted voltage sources and other nonfunctional components. Electrodes were fashioned from 30 gauge multi-strand stainless steel, insulated with silicone rubber (Cooner Wire, Chatsworth, CA). A longer anode (14 cm vs. 10 cm, cathode)) was used to differentiate the electrodes for the surgical technician. The completed electronics were potted in Beeswax and then a medical grade elastomer

(Dow Corning 382). Prior to implantation, about 5 mm of the silicone insulation was stripped from the terminal of the electrode wire, and the individual 40 strands (each 46 gauge) were coiled. These multi-strand electrodes provided a comparatively large surface area which lowers the current density at the electrodes. Additionally about 15 mm of heat shrink Teflon was affixed near the terminal of the electrode forming a small tab used to facilitate fastening the electrodes to musculature with suture.

Anatomical Procedures

Anterograde tract tracing was accomplished using a rhodamine conjugated dextran (Fluoro Ruby; Molecular Probes Inc.) of 10,000 molecular weight. The injected concentration was 50% in 2% DMSO in double distilled water. Approximately 24 hours prior to the scheduled time of sacrifice, animals were reanesthetized with ketamine/xylazine as previously described, and the spinal cord surgically exposed by dorsal approach. The original site of the lesion was determined, and Fluoro Ruby was injected into the dorsal spinal cord (using a Hamilton syringe and integral needle) *approximately 2 vertebral segments caudal to the hemisection.* Following this procedure the wound was closed, and the animal was sacrificed the next day by perfusion/fixation using previously described technique[36,40]. We have since found it useful to fix tissues with 6% paraformaldehyde containing 0.1% glutaraldehyde. The small amount of glutaraldehyde does not compromise viewing of the fluorescent tracer, or significantly increase background fluorescence, however it significantly increases the degree of fixation, ease of sectioning, and overall section integrity over that of paraformaldehyde alone.

Following fixation, the spinal cord was removed by dissection and then additionally immersion fixed in paraformaldehyde/glutaraldehyde for a minimum of 1 hour. If it was felt that the perfusion procedure was not ideal, the immersion was extended overnight. The marker device was carefully removed from the fixed spinal cord by cutting it at the base of one of the "legs", and gently removing each of the two segments from the fixed spinal cord

with watch maker's forceps under stereoscopic magnification. Spinal cords were then placed in 10% sucrose buffered with Mono/Di Basic Phosphate (pH 7.4), and sectioned on a freezing microtome at approximately 60 μm. Horizontal/longitudinal sections (Fig. 1) were affixed to slides, and cover slipped using DPX mountant (Fluka Chemical). Viewing and epifluorescent darkfield photography was accomplished using an Olympus VanOx Universal microscope.

Confocal Laser Microscopy

Laser microscopy employed a Bio-Rad MRC 1000 Laser Scanning Confocal Microscope using a Krypton/Argon emission source (Ion Laser Tech Corp). The excitation wavelength was usually at 568 nm while emissions were collected at about 585 nm and acquired to the computer using Comos® software (Bio-Rad). The digitized images were transferred to a Silicon Graphics Indigo 2® work station. Three dimensional reconstruction and pseudocolor rendering was performed using Voxelview® software and managed as plates with Powerpoint® software. These finished plates were transferred to an automated 35 mm camera (Laser Graphics personal LFR). Automated scanning of a region of interest within the spinal cord section was accomplished using the Z axis scanning function of the MRC 1000, which collected serial 2 μm thick optical planes through the thickness of the specimen. Such Z scans were then later reconstructed as three dimensional images. In regions of dense scar, the visualizations of axons, and the tracing of these axons, was accomplished using two methods: First, the visualization of axons within the reconstructed scar was achieved by eliminating the most dorsal and most ventral optical planes of the Z axis scan containing few–or no–axon profiles. This reduced the opacity and the background (non neuronal cells of the scar) of the image. Next, individual axon profiles were traced from a chosen–to an end–point by reconstructing and emphasizing pixels that were 1) of a similar value, and 2) that were connected. This was performed using Voxelviews'® automated seed fill algorithm. These two methods allowed visualization of fine axonal

processes and their branches buried within the region of glial scar or within the capsular connective tissue surrounding some cysts or the marker (index) holes.

Darkroom techniques

Darkfield epifluorescent color images were photographed using conventional 35 mm color slide film. Black and white film was not used (see below). Working prints and final color plates were developed in the darkroom using the Unicolor® 3 step developing procedure (Photo Systems Inc.), Kodak Radiance 3 paper, and a Beseler 45 S Dichro color head enlarger. We found that commercial printing did not allow sufficient choice in magnification, or in critical focus, during production of the print. Some darkfield color slides were used as a negative to produce a reverse black and white image on conventional photographic paper. We have found these " reverse positive" prints, in which the axon is dark against a light background, to be much superior in contrast and resolution to the conventional darkfield B & W image (where the axon is light against a black background)[35].

B. Two and Three Dimensional Morphometry of SCI

Animals

Fully adult (300 - 400 g) laboratory rats (Sprague-Dawley) were used in the subsequent experiments (see next section). Rats (but not guinea pigs), provide better models for the use of monoclonal antibodies such as ED-1 (see below). Following surgery, they were housed two animals per cage, fed ad libidum, and their health monitored daily. All animals in this study were sacrificed 3 weeks (21 ± 1 days) post-surgery by an overdose of Sodium Pentobarbital (0.8 ml of 1 g/ml standard injectable) immediately followed by perfusion/fixation with 6% paraformaldehyde, 0.1% glutaraldehyde in a phosphate buffer. The spinal cords were dissected free and immersion fixed in the above fixative for about 18 hours.

Surgical Procedures

Anesthesia was performed using an intraperitoneal injection of 1 ml/100 g body weight of a standardized solution of 10 ml Ketamine HCL (100 mg/ml) and 1.1 ml Xylazine (100 mg /ml). The spinal cord was exposed by a partial laminectomy (10th to 11th thoracic vertebrae; dura left intact), and the dorsal hemisphere crushed using blunted Watchmakers forceps. The incision was closed in layers with 3 - 0 proline suture, and the skin closed with wound clips. Immediately post-surgery each animal was subcutaneously injected with 3 ml lactated ringers to prevent dehydration, and the animal placed under a heat lamp for about 24 hours to reduce post-surgical mortality due to shock.

Immunocytochemistry

The segment of spinal cord containing the lesion was dehydrated in ascending concentrations of alcohol followed by xylene permitting infiltration and imbedding in Paraplast (paraffin) by conventional methods. The entire spinal cord was sectioned on a rotary microtome at approximately 15 microns, and horizontal longitudinal sections were affixed to microscope slides. Prior to use the slides were dipped in a 0.5% gelatin solution which aids in the adhesion of the sections to the slides during subsequent treatment. Paraffin was partially removed with a 1 hour treatment in a 60°C oven, and completely removed after a 1 hour immersion in 100% xylene. Sections were rehydrated by immersions in descending grades of alcohol to distilled water by conventional methods. Hydrated sections affixed to slides were first incubated in a commercial enzyme and tissue non specific antigen blocker (Endo/Blocker M69 and Tissue Blocker, Biomeda) for 5 minutes, with a 1 minute rinse in buffer (Automation Buffer, Biomeda). The sections are then exposed to the primary antibody for the macrophage, ED1 [MCA - 341, Serotech/Harlan Bioproducts (mouse antirat)] for 10 minutes, and rinsed with buffer. The secondary biotinylated antibody [rabbit - antimouse (Lab/Probe, Biomeda)] was

administered for 10 minutes, rinsed in buffer prior to exposure to the streptavidin peroxidase (10 minutes), rinsed, and exposed to a commercially prepared Diaminobenzidine reagent (Biomeda) for 5 minutes, and counter stained with hematoxylin. Stained sections were rinsed in distilled water and coverslips affixed with a warm glycerol gelatin (Sigma Chemical Co.). Two uninjured spinal cords served as controls for non-specific staining.

Photography and Image Reproduction

Viewing and conventional photography of spinal cord sections was accomplished with an Olympus Van Ox Universal Microscope. Morphometry was performed on digitized images acquired with a JVC TK-1070U color video camera mounted on the microscope. The acquisition of microscopic images was accomplished with RasterOps® MediaGrabber™ 3.2 software captured to a Macintosh Quadra 800 Computer. Working copies of digitized images and data spreadsheets were produced with an HP Laser Jet 5M printer, and final color plates used a Tektronix Phaser 400 dye-sublimation printer.

Computer Assisted Morphometry

The method used for the most accurate counting of macrophages within histological sections was based on the determination of an average number of pixels represented by a single macrophage at a standardized magnification (200x). To canvas the lesioned area, one field of view at 200 diameters was chosen within its center and acquired to the computer. Four additional (exactly adjacent) fields of view (rostral, caudal, right, and left) were also captured. In this procedure there is no attempt to systematically random sample cells (or parts of cells) within the reference space (the lesion)[52]. We estimate that in any one spinal cord section, an average of 90% (or more) of the lesion was acquired for cell counting in even the largest injuries. However, in most sections studied, the size of the region of injury was reduced such that 100% of the lesion was acquired, digitized, and managed for morphometry. By using software that can transform assigned color pixel

values (Color Look Up Tables) to a single color pixel value, the assigned colors (the area of interest) can be measured in pixels (Fig. 2C and D). By sampling every third section (approximately 15 μm), more target area comprised of labeled cells could be evaluated within the histological section than is practical by other sampling/counting techniques. Furthermore, once the visual data is digitized, color transformed for counting, and assigned a file name - the actual counting can be performed using a custom designed script (IPLab Spectrum™) that does not require human interaction with the acquisition of this data.

Macrophage Size in Pixels

At a standardized magnification of 200 diameters, an average of 14 ± 5 individual macrophage cells (full diameter and isolated from other cells) were chosen per histological section from a series of 12 slides. The mean, SD, and SEM of these 173 cells in pixels was 18.9, 4.27, and 0.3 respectively. The actual unit area of the pixel in micrometers at this same magnification was determined by capturing an index score of a haemocytometer to the computer. We also made measurements of the diameters of 61 similarly isolated macrophages, using an ocular micrometer for comparison of the means.

Algorithms for Three Dimensional Surface Reconstruction and Quantification

For 3-D reconstruction, the spinal cord segment containing the lesion was acquired to the computer at low magnification (20 diameters). All serial histological sections comprising a spinal cord were used for this purpose. During the digitization process, registration was accomplished by superimposing each successive image onto a tracing of the prior histological section made on the computer screen with a dry erase marker. The boundary of the cord, and other fiducial points or objects (such as cysts and irregularities of the lesion) served to aid in serial registration.

The algorithms used in this study construct planar contours of cord, lesion, and cysts as images via a process of segmentation. The constructed planar contours are polygons.
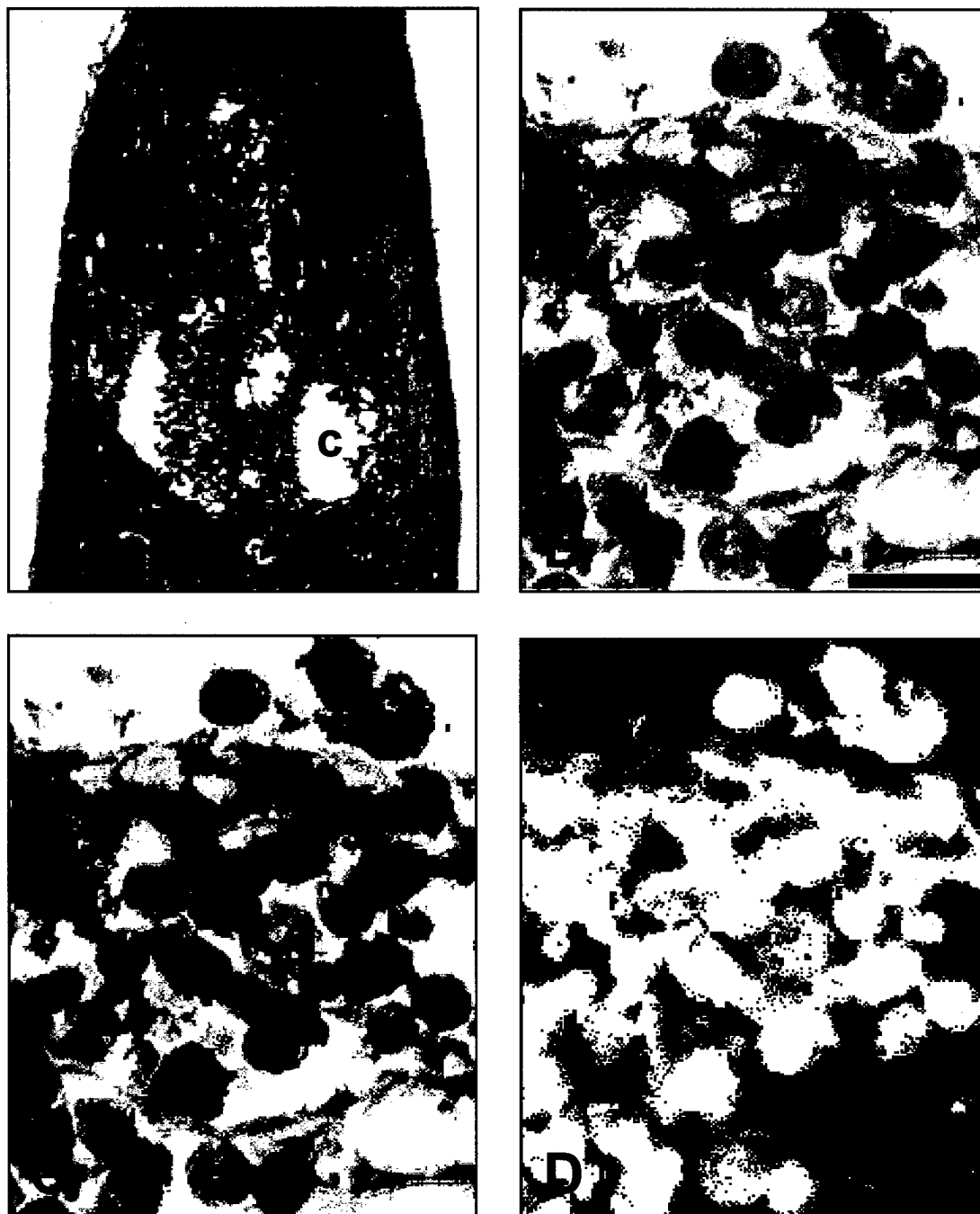
Figure 2 *ED1 Immunocytochemistry: Two Dimensional Morphometry. (A) Longitudinal horizontal section of a rat spinal cord, oriented rostral to the top and caudal towards the bottom. The section is 2.5 mm at its widest. This digitized image is as it appears on the video monitor following capture from the histological section (see methods). The dark purple/brown staining (arrow) is the region of labeled macrophages delineating the centrally located spinal cord lesion. The spinal cord is counter-stained with hematoxylin. Such compression lesions at 3 weeks were usually cystic (C). (B) A similarly digitized high magnification view of individual ED1 labeled macrophages within the injury site of the spinal cord shown in A. Note the vesiculated appearance of some of the labeled phagocytes and the blue background staining of strands of parenchyma. Scale Bar = 20 μm. (C) The identical image shown in B. The pixel values showing the overall range of brown staining (labeled macrophages and portions of macrophages) has been converted to a single pixel value (green) in preparation for binarization and computer assisted counting. Note the exclusion of the blue stained parenchyma shown in B. (D) The identical image shown in B and C. To facilitate counting, the image is binarized where the pixel value of 1 (white) is ascribed to the macrophages and all other color values = 0 (black). The computer assisted program of counting then derives the unit area in white pixels. At any given magnification, the unit area in pixels is further converted to the unit area in micrometers.*

The task is to construct surface meshes which interpolate the contours on two adjacent histological sections. Each section contains zero or more non-intersecting polygons which may be nested. The 3-D surface construction from planar contours requires a solution to *correspondence, tiling,* and *branching* problems.

The *correspondence* problem involves finding the correct connections between the contours of adjacent histological sections. *Tiling* refers to the use of boundaries to triangulate the strip lying between contours of adjacent sections into triangles. A *branching* problem occurs when a contour in one section may correspond to more than one contour in an adjacent section. The possibility of branching significantly complicates the task of tiling.

We approach the solution to all of these problems simultaneously[8.] This is accomplished by imposing a set of three mathematical constraints on the reconstructed surface and then deriving precise correspondence and tiling rules from these constraints. The constraints ensure that the regions tiled by these rules obey physical constructs and have a natural appearance.

Once a surface (wire frame or tiled mesh) is constructed, quantitative interrogation of the reconstruction to provide precise surface areas and volumes can be accomplished. The surface area of the 3-D image is simply the sum of all triangles. If the tiling process does not develop any untiled region, the reconstructed shape is a prismatoid which is a triangular tiled region between two parallel contours. If the reconstructed shape is not a prismatoid, it can be reduced into prismatoids[9]. A prismatoid is a polyhedron which consists of two planar contours in parallel planes and lateral triangles. The three vertices of each lateral triangle must be the vertices of both planar contours. The volume of a prismatoid is calculated as $V = \dfrac{h}{6} (B_1 + 4M + B_2)$ where B_1 is the area of the lower base, B_2 is the area of the upper base, M is the area of the midsection joining the bases and h is the separation between contours. With n parallel slices of contours equally spread, the composite volume computation results in: $V^1 = \dfrac{h}{6} (B_1 + 4\sum_{1}^{n-1} Mi + 2\sum_{2}^{n-1} Bi + Bn)$.

<u>Statistical Evaluation</u>

Comparison of data sets used Wilcoxon, Mann-Whitney U, and paired 2 tailed students' T tests of significance. Computations were performed using Instat© software.

C. Electric Field Effects on Secondary Injury

<u>Experimental Animals</u>

Fully adult (250 - 360 g) laboratory rats (Sprague-Dawley) were used in these experiments. Animals were divided into two groups, those receiving active stimulator units and those receiving sham (inoperative) units. Following surgery, they were housed two animals per cage, fed ad libidum, and their health monitored daily. All animals in this study were sacrificed 3 weeks (21 ± 1 days) post-surgery by an overdose of Sodium Pentobarbital (0.8 ml of 1 g/ml standard injectable) immediately followed by perfusion/fixation with 6% paraformaldehyde, 0.1% glutaraldehyde in a phosphate buffer. The spinal cords were dissected free and immersion fixed in the above fixative for about 18 hours.

<u>Surgical Procedures</u>

Anesthesia was performed using an intraperitoneal injection of 1 ml/100 g body weight of a standardized solution of 10 ml Ketamine HCL (100 mg/ml) and 1.1 ml Xylazine (100 mg/ml). The spinal cord was exposed by two small laminectomies placed two vertebral segments rostral, and two vertebral segments caudal to a centrally located partial laminectomy. A compression of the dorsal hemisphere of the exposed spinal cord was performed at this site using blunted watchmakers forceps[17,104]. After the dorsal half of the spinal cord, exposed by the central partial laminectomy was compressed for about 3 seconds, the wound was closed in layers with 3-0 proline suture. The uninsulated tips of

stimulating electrodes were inserted into the two laminectomies with the negative electrode (cathode) rostral to the lesion, and the positive electrode (anode) caudal to it. The electrodes were secured to the paravertebral musculature with silk suture in such a way that the uninsulated tips of the electrode did not touch the spinal cord, and all wounds were then closed in layers[36,37,38,40]. The body of the stimulator was placed in a deep subcutaneous fat pad at the base of the animals neck. The skin incision was closed with wound clips. Immediately post-surgery each animal was subcutaneously injected with 3 ml lactated ringers to prevent dehydration, and placed under a heat lamp for about 24 hours to reduce post-surgical mortality due to shock.

Experimental groups

The animals were divided into two groups: sixteen implanted with sham batteries (short-circuited and delivering no current), and 18 implanted with stimulators delivering 45 μA total current (associated with a field strength of approximately 400uV/mm at the spinal cord lesion; refer to citation 40). These units were functional during the entire duration of the study. Four experimentals and three controls were removed from the study population because of premature death, while two experimentals and one control animal were eliminated for poor health.

Immunocytochemistry

Following removal from the animal, the fixed segment of spinal cord containing the lesion was dehydrated in ascending concentrations of alcohol followed by xylene, permitting infiltration and imbedding in Paraplast (paraffin) by conventional methods. Spinal cords were sectioned on a rotary microtome at approximately 15 microns, and sections affixed to microscope slides. Prior to use the slides were dipped in a 0.5% gelatin solution which aids in the adhesion of the sections to the slides during subsequent treatment. Paraffin was partially removed with a 1 hour treatment in a 60°C oven, and completely removed after a 1

hour immersion in 100% xylene. Sections were rehydrated by immersions in descending grades of alcohol to distilled water by conventional methods. Hydrated sections affixed to slides were first incubated in a commercial enzyme and tissue non specific antigen blocker (Endo/Blocker M69 and Tissue Blocker, Biomeda) for 5 minutes, with a 1 minute rinse in buffer (Automation Buffer, Biomeda). The sections were then exposed to the primary antibody for the macrophage, ED1 (MCA - 341, Serotech/Harlan Bioproducts) for 10 minutes, and rinsed with buffer. The secondary antibody [rabbit - antimouse (Lab/Probe, Biomeda)] was administered for 10 minutes, rinsed in buffer prior to exposure to the streptavidin peroxidase (10 minutes), rinsed, and exposed to a commercially prepared Diaminobenzidine reagent (Biomeda) for 5 minutes, and counter stained with hematoxylin. Stained sections were rinsed in distilled water and coverslips affixed with a warm glycerol gelatin (Sigma Chemical Co.). Two uninjured spinal cords served as controls for non-specific staining. All of the prepared histology was coded such that all subsequent management of this material was performed by persons blinded to the experimental status. These codes were not broken until the completion of the morphometry.

Computer Assisted Morphometry

The method used for the counting of macrophages within histological sections was based on the determination of an average number of pixels represented by a single macrophage at a standardized magnification (200x). The determination of macrophage numbers from serial longitudinal sections is based on prior studies determining the average size of macrophages in pixels, and the use of software which color transforms only the labeled cells to be counted from background staining. The use of this methodology for the counting of macrophages (or other labeled cells) in spinal cord injuries, and various verifications of this method, is described in the previous section. To capture the lesioned area within a histological section, one field of view at 200 diameters was chosen within the lesion's center and acquired to the computer. Four additional (exactly adjacent) fields of

view (rostral, caudal, right, and left) were also acquired to the computer. Using this procedure, we estimate that in any one spinal cord section, an average of 90% (or more) of the lesion was acquired for cell counting in even the largest injuries. In most sections, however, 100% of the lesion was acquired, digitized, and managed for morphometry. By using software that transforms assigned color pixel values (Color Look Up Tables) to a single color pixel value, the assigned colors (specific staining of macrophages) was measured in pixels (Fig. 2C and D). By sampling every third histological section, more target area comprised of labeled cells can be evaluated than is practical by other sampling/counting techniques. Furthermore, once the visual data is digitized, transformed for counting, and assigned a file name—the actual counting was performed using a custom designed script (IPLab Spectrum™) that does not require human interaction with the acquisition of this data. Other regions of interest such as cysts can likewise be color transformed for the determination of their unit area within a histological section and summed to estimate the total unit area within the spinal cord lesion.

D. Electric Fields and Polymeric Guidance Channels

<u>The Implant</u>

The constant current (DC) Implant consisted of two components: the stimulator and a hollow silicone rubber guidance channel containing an active negative electrode (the cathode) or a sham electrode within its center.

The stimulator was similar to previously reported designs[30,40,38] using one 3V Lithium Cell (Ray o Vac 1225 BR) connected to a constant current source (National Semiconductor LM 334 Z), which regulates the DC output , and a 1/8 th watt resistor to set the total current to 0.1 μA. Electrodes were constructed of multistrand stainless steel wire (Cooner Wire, Chatsworth CA) insulated with silicone rubber. Anodal electrodes were

fashioned from 30 gauge multistrand, and cathodal electrodes from 50 gauge multistrand. The stimulator was potted in beeswax and subsequently medical grade elastomer (Dow Corning 382). About 3-5 mm of the distal tip of the positive electrode (anode, 14 cm long) was stripped with watchmakers forceps, and the individual strands of the multistrand wire were splayed out and coiled to provide a relatively large surface area. The distal tip of the cathode (negative electrode) was stripped of less than 1 mm of insulation and was inserted into the center of the silicone tube through a small hole made with a 20 gauge needle. The electrode, with its uninsulated tip within the center of the tube, was glued in place and the hole sealed with medical grade silicone based elastomer.

The guidance channel was fashioned from a 6 mm long piece of medical grade silicone rubber tubing (0.94 mm o.d. X 0.51 mm i.d., Dow Corning #602 - 135). With both ends of the tube open, and a centrally located cathode, current would enter both ends to complete the circuit from an externally placed anode (Fig 3). This would produce an electrical field of approximately 2.5 mV/mm within the tube. Outside of the tube, the field strength would fall off steeply to a level on the order of 100 μV/mm or less[40]. With approximately 40 mA/h capacity the units would be functional for about one month. Control or sham units were constructed from non functional components and were physically indistinguishable from active units.
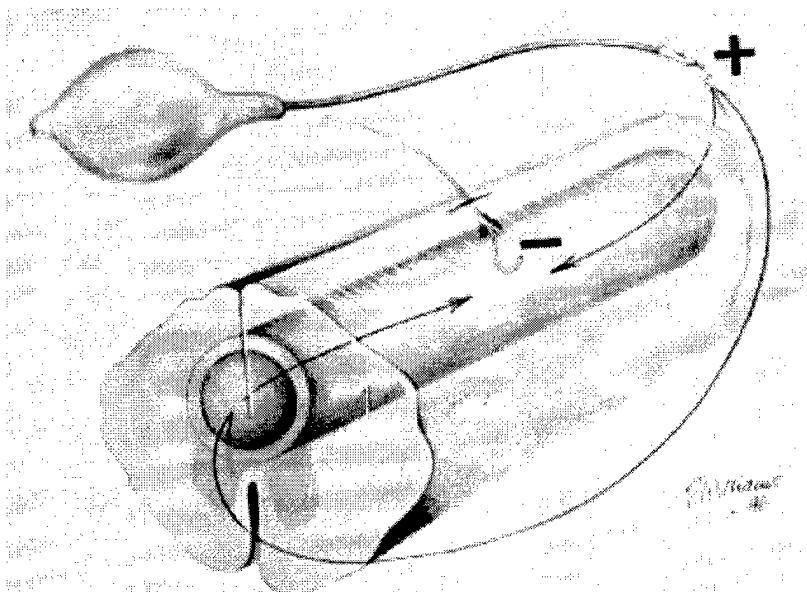
Figure 3
Artist drawing of the stimulator, silicone rubber tube or guidance channel, and the electrical circuit within the spinal cord. The tube was implanted into the dorsal spinal cord. The uninsulated tip of the cathodal electrode (negative) was sealed within the center of the tube, while the anodal electrode (positive) remained outside the vertebral column, sutured to paravertebral musculature. The body of the stimulator was surgically placed within the fat pad at the base of the guinea pig's neck. To complete a circuit, current must flow initially into each end of the hollow tube as diagrammed. For diagrammatic purposes, the drawing was not made to scale.

<u>Surgery</u>

Adult female guinea pigs (ca. 500 gm, Hartley strain) were used for these experiments. Anesthesia was performed with an intramuscular injection of a mixture of 60 mg/kg ketamine HCl, and 12 mg xylazine. The dorsal aspect of the spinal cord at a midthoracic level was exposed by a partial laminectomy. The spinal cord was incised with a fine cutting device (Moria microblade, 15 degree angle) along its midline for approximately 7 mm, and to the depth of the central canal. The guidance channel was inserted into this longitudinal fissure such that both ends of the tube were fully pressed into spinal cord parenchyma, with the electrode wire exiting the center of the tube. The stimulator body was placed within a subcutaneous fat pad, between the shoulders, approximately 5-7 cm from the spinal cord surgery. The stimulator electrodes were held in place with 3-0 silk suture, the positive electrode located about 1-2 vertebral segments caudal to the placement of the

tube, and sutured to paravertebral musculature. Subsequently, the wounds were closed in layers and the skin incision closed with wound clips. Three weeks following implantation, the animals were reanesthetized, and the implanted units were surgically removed by clipping both electrodes.

Experimental Design

Thirty-six experimental animals and twenty-five control (or sham treated) guinea pigs were evaluated following the implantation of the stimulator and guidance channel. Of the 36 experimental animals, 6 were sacrificed at 1 month post implantation, 20 at 2 months post implantation. Another 10 animals were later added to this group for retrograde labeling studies (see below). Sixteen control guinea pigs were sacrificed at 2 months post surgery. Nine other control guinea pigs (3 animals at 3 days, 3 at 2 weeks, and 3 at 1 month) were sacrificed for tract tracing as well as conventional histology (Masson's Trichrome and GFAP Immunocytochemistry) to evaluate the timing, and character of the cells and tissues entering the silicone rubber tube. Current (0.1 μA) was pulled into the tube with an indwelling cathode in all experimental animals . Preliminary trials using both indwelling anodes and cathodes at 0.1, 1.0, and 10 μA total current demonstrated that current levels higher than 0.1 μA, or anodes at any current level, prevented the ingrowth of any cells or tissues (data not shown). This is due to the growing concentration of toxic electrode products with time, trapped within the non permeable silicone tube. Table 2 provides a summary of the animals used in this study.

Total animals	Lost to study[1]	Exp.[2]	Cont.[2]	Retro FR[3]	Early sacrifice[4]
71	10	26	16	10	9

Table 2.
1. *Animals that died or were removed from the study due to weakened condition, and/or the complete loss of the implant.*

2. *Tract tracing with tetramethylrhodamine, (fluoro-ruby, FR), was performed on all of these animals.*

3. *Only active implants were studied using retrograde FR.*

4. *Masson's Trichrome, GFAP immunocytochemistry, in addition to tract tracing, was used to evaluate these spinal cords at 3 days, 1 week, and 1 month post-surgery.*

Spinal Tract Tracing

Approximately 24 hours prior to the scheduled time of sacrifice, animals were anesthetized, and the spinal cord was exposed by a partial laminectomy approximately 2 vertebral segments rostral, and 2 vertebral segments caudal, to the two ends of the tube. At these two locations, tetramethylrhodamine dextran (fluoro-ruby, Molecular Probes, Inc.) was injected into the dorsal half of the cord by previously described techniques. In this way, white matter projections directed towards both ends of the tube were anterogradely filled, allowing spinal long tract tracing. In a second group of animals, long tract tracing was not used. Instead a retrograde uptake procedure was utilized to help determine the cell bodies giving rise to axons that were found to enter the experimental tubes. In this procedure, the dorsal surface of the tube was surgically exposed, the electrode carefully withdrawn, and crystals of rhodamine dextran were inserted into this hole - into the center of the tube–using the sharp tip of a minutia pin. Immediately following insertion of the dye crystals, this area was dried with a small cotton swab and a small dab of silicone glue was applied to the hole to seal it. The glue was allowed to set up for about 10 minutes prior to closure of the wounds. If care was taken to keep the site relatively dry, this procedure could be performed without leakage of the dissolving marker into the interstitial environment surrounding the tube. In all cases, animals were sacrificed following deep anesthesia with ketamine/xylazine, and perfusion fixed by cardiac puncture with 6% paraformaldehyde and 0.5% glutaraldehyde. The spinal cord containing both sham and experimental tubes was dissected free for further immersion fixation prior to subsequent anatomical preparation, imbedding in paraffin, and longitudinal horizontal sectioning on a rotary microtome by previously described techniques[30,36].

Histological sections were viewed on an Olympus Van Ox Universal microscope. Fluorescent darkfield microscopy utilized several excitation and barrier filter combinations, the combinations used for the rhodamine dextran were 545/790 and 495/475 (Excitation/Barrier filter wavelength in nm). Darkfield images were viewed with an 3 CCD camera and a DEI-750 processor (Optronics, Inc.), and acquired to a Macintosh Quadra 800 computer with RasterOps® MediaGrabber™ software, or to a Symetra Dual Pentium Pro using Adobe Photoshop® software and FlashPoint ®128 hardware. Color Plates were produced using ColorIt™ and Microsoft® PowerPoint software. Working prints were produced on a Epson Stylus Color 800 printer, and final prints produced on a Textronix Dye sublimation color printer.

E. Effects of DC Fields on Canine Paralegia

<u>Admission Criteria</u>

All dogs used in this study were recruited from emergency admission to the Purdue University Veterinary Teaching Hospital (PUTVH) or by telephone contact with veterinarians from out of the Lafayette, Indiana vicinity, or from out of the State. These more distant recruitments were facilitated by advertisement for paraplegic dogs by University News Service press release and by advertisement of the clinical program on the Internet (www.vet.purdue/cpr). The initial evaluation of solicited cases required that the animal be completely paraplegic, show no ability to support the hindquarters or walk, and be urinary and fecal incontinent. We discouraged owners of very large or old dogs as these are both difficult to manage, and do not make good study candidates based upon our experience. Paraplegic dogs could not have received prior surgical management, or have received drugs such as phenyl-butazone or flunixin meglumine which could be deleterious to their health prior to entering the study. Of those animals brought to the clinic for evaluation, a

more strict criteria was to be met before an animal could be entered into the clinical trial without cost to the owner:

1.) The dog must have been diagnosed with <u>neurologically complete paraplegia</u> as defined by the complete lack of: i) superficial pain appreciation, ii) deep pain appreciation, iii) conscious proprioception - all below the level of the injury, iv) load bearing and voluntary walking using the hind limbs, and v) electrophysiological conduction across the zone of injury as measured by somatosensory evoked potential testing (SSEP). Examples of SSEP electrical records that eliminated animals as study candidates were previously provided in citation 41.

2.) Animals showing typical lower motor neuron (LMN) sequalae were excluded from participation. This was revealed by an LMN bladder as determined by Urological testing (urethral pressure profilometry and cystometry; described below), or the compromise of local spinal reflexes below the level of the injury (sciatic, tibialis cranialis, patellar, and flexor withdrawal).

3.) The pre-surgical or post-surgical radiographic examination had to demonstrate that the paraplegia was secondary to acute, explosive, Hansen type I intervertebral disc herniation (33 cases)[80]. Radiographic documentation of severe inter-vertebral disc herniation as well as intra-operative photography of disc removal were previously provided in citation 41. Three additional cases of paraplegia secondary to fracture/dislocation of the vertebral column qualified for the study, however these did not demonstrate sublexion of the vertebral column or transection of the spinal cord. Animals were excluded from the study for myelographic evidence of traumatic transection of the spinal cord at admission, or a failure to identify that the paraplegia was injury related. Examples of exclusions based on the latter criteria were two cases of paraplegia secondary to transverse myelitus, and one to a fibrocartilaginous embolism. Five cases were excluded from the study during the first week of evaluation due to evidence of spreading myelomalacia. These animals were euthanized

at the owner's request. Radiographic evidence for ascending / descending myelomalacia was previously provided in citation 41 (also see below).

4.) The extent of injury could not be more than 1 Vertebral segment (approximately 2 cm) as determined by the extent of uptake of contrast media by injured parenchyma during myelography.

5) The duration of paraplegia could not be greater than 18 days. Dogs that are rendered neurologically complete paraplegics by explosive disc herniation or by fracture dislocation do not usually respond to conventional management[83,86,69,136], retain substantial behavioral deficits for their lives, and thus are usually euthanized. It is this category of severely injured animals that were the focus of this investigation.

Owner Participation and Informed Consent

Owners participated in the clinical trial without medical costs following the signing of an informed consent agreement. Prior to their decision, they were provided a written description of the clinical trial and its procedures, including a description of their responsibilities to the animal and the Center's staff responsibilities to them. This included an agreement to return the dogs at approximately 6 weeks following surgery and again for a 6 month recheck. The owners were informed that they had an equal chance to receive a placebo treatment (i.e. a sham implantation), and that if this was the case, they could elect to receive a known active implantation at the end of the 6 month period of evaluation and/or other clinical procedures without medical costs. Participating owners were provided a cart for their dog (K–9 Carts, Big Sky, Montana), instructed on its use, as well as proper skin care and manual bladder expression. They were provided telephone numbers for emergency communication, and were regularly contacted by a veterinary technician. Owner compliance with their responsibilities was usually excellent. Of the 40 entering dogs, only one was lost to the study due to owner negligence , and three to lack of owner follow up.

Neurological Evaluation and the Combined Neurological Score

All neurological evaluations were performed by one of the three surgeons participating in the trial (J.P.T., G.B., D.W.), while evoked potential diagnostics were performed by either P.M. or R.B.B. (refer to participant list, last section) All neurological evaluations were composed of three parts: 1) a standard evaluation of spinal reflexes consisting of tibialis cranialis, patellar, sciatic, crossed extensor, flexor withdrawal, and the cutaneous trunci muscle (CTM) reflex, 2) a behavioral evaluation of ambulation, hindlimb load-bearing, superficial pain appreciation, deep pain sensation, and conscious proprioception (proprioceptive placing), and 3) physiological measurement of urethral pressure profillemetry, cystometry (performed by Urologist L.A.) , and somatosensory evoked potential (SSEP). All neurological evaluations were videotaped for later reference and evaluation (see below). The reflexes and behavioral tests were performed separately for each side of the body. We have described the details of each of these behaviours and reflexes and their clinical testing in a prior report, and direct the interested reader to this discussion[41]. The behavioral evaluations were scored in the following manner:

Ambulation

1 = no detectable ability to ambulate, coupled to the complete lack of spontaneous hindlimb load bearing. 2 = locomotion near the limit of detection: brief periods of stepping, some load bearing ability prior to falling. 3 = more marked ability to step in sequences, poorly coordinated, and unable to climb stairs. 4 = consistent effective locomotion, still with deficits in coordination, yet able to climb stairs. 5 = normal ability to walk or to climb.

Deep and Superficial Pain

These behaviors were scored similarly. 1 = no detectable response. 2 = at the limit of detection, usually accompanied by an increased interest or state of arousal, and increased respiratory rate and pulse. 3 = consistent attention to the site of stimulus without

a display of defensive behavior. 4 = mildly defensive response to stimuli including whining or sudden turns of the head to the site of stimulation. 5 = normal response to painful stimuli including aggressive behavior, yelping, biting. This test was scored for both hindlegs and averaged.

Proprioceptive Placing and Final Behavioral Assessment

The proprioceptive placing reflex was scored as present (2.5 points) or absent for each hindleg and averaged. The scores for each of the four behaviors were determined at the end of the study by a panel of 3 or 4 of the clinical investigators with reference to the original medical record. This is because the range of recovery could be more accurately assessed for one animal relative to the others (refer to discussion in citation 41). The panel met numerous times over a period of 2 months following the completion of all clinical rechecks for all animals. At each meeting the video taped neurological exam for each animal was played for the panel in random order by a technician. The panel was blinded to the identities of these animals, some of which had been admitted to the study as early as 1993. Each investigator scored every evaluation category independently, and could request the technician to replay any portion of the videotape as many times as required to decide a behavioral score. Half points were permitted when an evaluator deemed this to more accurately reflect the dog's performance. Inter-observer variability was minimal. For example, at the 6 week recheck, the scores for superficial and deep pain were identical between the panel members 65 % of the time, varied by 1 point or less in less than 20% of the total evaluations, and varied by more than 1 point in only 10% of the evaluations. The most relevant comparison of outcome between the groups was to average the combined scores for each animal (to produce a combined neurological score), and then compare the means of the total neurological scores between the groups. As in the previous study, the four individual measures of behavioral outcome (ambulation, deep pain, superficial pain, and proprioceptive placing) were each weighted equally, the largest total score achievable

was 5, and the complete absence of any functional measure being 1, as described above. (Transformation of the data is not required if "0" is not used as the lowest possible score). The total neurological score was constructed on a 1-20 point scale; neurologically complete paraplegia defined as 3, and animals that could not be determined to be different from uninjured dogs based on the functional criterion used here would score 20 points.

General Anesthesia

All surgical, radiological, electrodiagnostic, and occasionally urodynamic procedures required general anesthesia. This was accomplished using atropine (subcutaneous injection, 0.5 mg/kg) followed by the placement of an intravenous catheter in the cephalic vein. Anesthesia was induced by sodium pentothal (15 mg/kg, administered thorough the intravenous catheter). Following the onset of anesthesia, intravenous Ringer's lactate solution (10 ml/kg/hr) was maintained throughout the subsequent procedures. Anesthesia was maintained using endotracheal intubation to administer a mixture of oxygen and either isoflourine or halothane.

Electrophysiology: the Somatosensory Evoked Potential

The electrodiagnostic examination used in this clinical trial was simplified over the procedures used previously, which also included motor evoked and spinal evoked potential measurement[41]. We learned at that time that the most sensative indicator of recovered conduction in these clinical spinal cord injuries in dogs was the somatosensory evoked potential (SSEP). Thus only SSEP diagnostic procedures were used here. Animals admitted to the study could not reveal any indication of conduction through the injury on the basis of this test. Anesthetized dogs were evaluated using a Cadwell 7400 recorder, in the early part of the clinical trial. This instrument was replaced with a Nihon Kohden ME#B-5304K Neuropak 4 recorder. SSEPs were recorded using scalp needle electrodes placed over the contralateral somatosensory cortex from the stimulated tibial nerve. The reference

electrode was inserted into the pinna of the ear. Recorded SSEPs were usually measured using both a 30 ms and 50 ms time base. Stimulation was achieved with needle electrodes inserted through the skin at the distal popliteal space approximately 1 cm apart, the cathode proximal. Mild twitch of the hind limb digit was usually achieved with 0.1-0.2 mA square wave pulses. Three to four sets of 200 stimulations/set were averaged and stored on the computer for further reference and printing. Further details of the electrodiagnostic procedures can be found in citation 41.

Radiology and Myelography

Radiography of the vertebral column was performed using a 150 KVp (peak kilovoltage) 1200 mA (milliampere three phase, full-wave rectified x-ray generator. Fine intensifying screens, regular speed rapid process x-ray film, a 103 lines per inch focused grid with a bucky tray, and a 100 cm focal film distance were employed to give acceptable radiographic detail and contrast. A standard technique chart with the KVp varied according to patient thickness, and a constant mAs were used to ensure uniformity of the radiographic technique. Exposed x-ray films were developed with an automatic processor (RP XomatR Automatic Processor, Eastman Kodak Company, Rochester, NY). Ventrodorsal and lateral radiographic projections were obtained and examined for evidence of radiographic changes. Either general anesthesia (isoflurane following induction with sodium pentothal) or sedation (intravenous acetylpromazine and butorphanol) were used to facilitate positioning of the dog.

Lumbar myelography was performed to confirm suspected sites of intervertebral disc herniation, plan surgical approach and to identify malacic spinal cord. All animal patients were injected with 0.33-0.44 ml\kg of nonionic contrast medium (Omnipaque R (iohexol) Sterling Drug Co., New York, NY Winthrop). A 1.5-2.5 in 22 ga. spinal needle (MonojectR, Sherwood Medical Industries, St. Louis, MO) was used to puncture ventral subarachnoid space at L4-5 or L5-6. Nonionic iodinated contrast medium was injected over a period of 1-

2 minutes. Image intensified fluoroscopy was used to study to flow of contrast medium during injection when there was maximum distention of the subarachnoid space. In this way, areas of suspected cord swelling and subtle extradural lesions could be defined. Next, ventrodorsal and lateral radiographic projections were made with the same exposure factors as the survey radiographs. In some instances, to facilitate the surgical approach, oblique projections were used to further localize lateralized extradural lesions.

Following surgery, and at 6 week and 6 month re-evaluation, ventrodorsal and lateral radiographs were made to assess the integrity and location of the OFS device and leads. At each imaging session, all data were recorded on a standard radiographic evaluation form.

Urodynamics

Cystometry (CMG) and urethral pressure profilometry (UPP) evaluations were conducted using Urolab 1104 Urodynamaic equipment (Life Tech, Inc., Houston, Texas). Prophylactic antibiotics were administered prior to, and for about 5 days following urodynamic procedures.

Surgery and OFS Stimulator Implantation

Animals that met the restriction criterion, and that were still eligible for the study following electrodiagnostic and radiological testing were immediately taken to surgery. All dogs were administered Methylprednisilone sodium succinate (30 mg/kg slowly) and 22mg/kg/2hrs. i.v. throughout surgery.

All dogs were given Methylprednisolone sodium succinate (30 mg/kg slowly i.v.) shortly after induction of general anesthesia. Cefazolin sodium (22 mg/kg i.v.) was given approximately 10 minutes prior to the start of surgery and repeated at 2.5 hour intervals thereafter until the animal was fully recovered from anesthesia. The spinal cord injury site was exposed by hemilaminectomy ipsilateral to the lesion (with lateralized lesions) and by left hemilaminectomy when the lesion was purely ventral. The length of the surgical

decompression was determined by radiographic and surgical findings, with bone removal proceeding until epidural fat and grossly normal spinal cord were seen at both the rostral and caudal margins. The surgical site was intermittently lavaged with chilled isotonic saline solution throughout the procedure. Hemostasis was maintained with bipolar electrocautery in all cases. Adjunctive hemostatic methods used in some cases included focal application of bone wax to control bleeding from cut edges of bone and temporary placement of gelatin sponge to control hemorrhage from the ventral venous sinuses.

Surgical telescopes (2.5 x with expanded field) were worn while performing deeper portions of the dissection, including removal of the compressive mass of disc material and incision of the dura mater. Durotomy was performed with a #12 scalpel blade, and a final decision was made to include or exclude the dog based upon the visible extent of spinal cord malacia. Dogs with severe malacia, extending beyond one vertebral segment in length were excluded. An autogenous fat graft was placed over the exposed spinal cord to reduce the likelihood of constrictive fibrosis during the postoperative healing period.

Blunt dissection was used to create a pocket in the paravertebral musculature for the battery pack of the OFS unit. Two clusters of electrodes (one cluster of 3 rostral electrodes, and one cluster of 3 caudal electrodes were loosely sutured to the lumbodorsal fascia. The Uninsulated ends of the 3 platinum/iridium electrode leads were secured with polypropylene suture to each of the following locations just rostral and just caudal to the hemilaminectomy: 1) musculature attaching to the left articular facets; 2) musculature attaching to right articular facets; and 3) a small bone tunnel created through the base of the dorsal articular process. Distance of the electrodes from the dorsal aspect of the spinal cord varied with patient size but was within the range of 5-10 mm. The insulated electrode leads were routed through muscle layers to reach their rostral and caudal locations. Redundant portions were loosely coiled and sutured to the lumbodorsal fascia. Standard materials and techniques were used for closure of the surgical wound.

Post Surgical Care

A light pressure bandage was applied over the surgical site, postoperative radiographs for evaluation of stimulator placement were made, and dogs were taken to the intensive care unit of the Purdue University Veterinary Teaching Hospital (PUVTH). Here animals were followed closely during recovery from anesthesia, and received oxymorphone (0.1 mg/kg) or butorphanol (0.2 mg/kg) by intramuscular injection to control postoperative discomfort and pain. The urinary bladder was checked and expressed 3-4 times daily. Bladder infections, if present, were treated with appropriate antibiotic therapy.
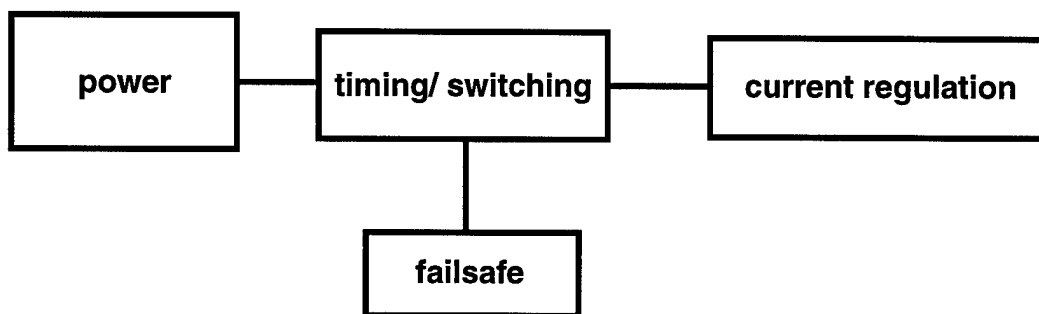
A minor surgical procedure was performed 48 to 96 hours after stimulator implantation. An incision (approximately 5 cm in length) was made over the rostral pole of the OFS battery pack. A teflon band which secured a magnet external to the battery pack was cut and the magnet and band were removed. This "activated" the unit by allowing a switch to close which was previously held open by the magnet. The surgical wound was closed in routine fashion and aftercare was as previously described. All dogs were kept under close observation for a total of 5-7 days following surgical decompression and OFS implantation. A postoperative neurological exam was videotaped shortly before discharging the dog to the owner's care. Recheck exams were scheduled for 6 weeks and 6 months following implantation.

Stimulator Design

We have previously provided details of the construction of a circuit that provides regulated current output from multiple electrodes and oscillates the polarity of the applied electric field at a predetermined time[28,41]. These designs have been further modified to produce a new generation of OFS stimulators that: 1.) produce a ca. three fold increase in current (~500-600 uA total current) over previous designs (at most delivering 200 uA total current; please refer to in vivo measurements described in citation 41), 2.) use three pairs of electrodes whose circuits are independently regulated but timed to invert their polarity in

synchrony, 3.) contain a switch that can be activated easily following surgical implantation of the unit. This allowed the unit to be activated at any time following the initial decompressive surgery, and 4.) contain "fail-safe" circuitry that terminates the application at non-nominal operation, particularly a failure in oscillation . Its other main features are small size and minimal quiescent power consumption.

Block diagram of OFS and Circuit Operation

```
┌─────────────┐     ┌──────────────────┐     ┌──────────────────────┐
│    power     │─────│ timing/ switching │─────│  current regulation  │
└─────────────┘     └──────────────────┘     └──────────────────────┘
                             │
                    ┌──────────────────┐
                    │     failsafe     │
                    └──────────────────┘
```

The OFS consists of main circuitry sections, or blocks. The first block covers the timing and polarity reversal functions of "oscillation." Its main timing component is a 4060 14-stage binary ripple counter with an onboard oscillator (refer to the circuit schematic, Fig 1, for the following description). The timing is set with an RC network and the output taken from the 14th stage (Q_{14}) for the maximum period. The output (Q_{14}, or the last stage of the 14 timing stages) acts as a reference that changes every 15 minutes. The output from Q_{14} serves two functions: 1. it drives one half of the current regulation circuit, and 2. it triggers an analog switch which, in turn, drives the other half of the current regulation circuit. The 4060 is a low-power complimentary metal oxide semiconductor (CMOS) device and consumes only a few microamps.

The second component in the timing/switching circuit is a Maxim DG319 analog single pole double throw (SPDT) switch. It uses the Vcc or power connector and ground as

inputs and is switched between these by the output of the oscillator timing action of the Q14. It is arranged such that the output of the switch is always the compliment of Q14, and is therefore used to drive the other half of the current regulation circuit. The DG319 is also a low-power CMOS device and consumes only a few microamps.

The analog switch operates down to a voltage of 2.5 volts. At that point, switching action stops and the output is locked in a DC state. The oscillator fail-safe utilizes a Maxim 921, which is a single integrated semiconductor chip containing a comparator and a 1.2 volt reference. A voltage divider sets the threshold voltage of the comparator to 2.6 volts and the output is connected to the VI input of the analog switch . When the power to the circuit falls to 2.6 volts, the output from the comparator changes from low to high and shorts out the analog switch. This short circuits the power to the circuit which subsequently shuts down any output to the electrodes.

The current regulation block of the OFS is based upon the LM334Z constant current source. The 334 is a stand-alone 3 terminal semiconductor device whose current output is programmed by a single resistor. That output is maintained until the resistance of the load exceeds the compliance of the voltage source or the voltage source falls below the operating voltage of the LM 334Z (ca. 1.8 V). The circuit has 2 arrays of 334s (one on each side) that feed the three sets of electrodes. Each pair delivers 200µA, producing a total current of 600µA (associated with a field of ca. 500-600 uV/mm given the standard array of electrodes used here; see citation 41). As seen in Fig. 4, the 334s are arranged in a "piggy back" fashion on both sides of the arrays. This is to provide accurate source/sink conditions for current delivery. This insures that the 600µA is distributed evenly across the lead pairs, none of them are delivering more or less current than the others in polarized synchrony. The set resistors of the 334s are integrated into dual inline packages (DIP) to keep the unit organized and modular.

The output leads are made of silicone rubber insulated stainless steel to minimize wire corrosion in the case of leakage around the electrode solder joint or a breach in the

leads' insulation. The electrodes themselves were a Platinum/Iridium (PlIr) alloy. 20 cm lengths of the PlIr wire were coiled in order to increase the surface area of current delivery further minimizing current density at the electrodes.

The overall circuit is provided in Fig.4 and a radiograph of the new design OFS unit in situ is provided in Fig 5. The hand fabricated circuit was inserted into a hollow tefelon cylinder and the electronic components and voltage source (3.6V,2400 mA/H Tadiran TL - 5903/T) perfused and sealed within the cylinder with epoxy. The end of the cylinder plus the electronic circuit was sealed with medical grade elastomer. The six electrodes exiting the other end of the tefelon cylinder were also sealed with medical grade elastomer. The two sets of three electrodes were insulated with two different colors for correct implantation by the surgeon to insure that polarity reversal for each set was symmetrical - one set of three electrodes being located rostral to the injury site, the other set caudal to it. Sham OFS stimulators were constructed from non functional components so as to be indistinguishable from active units by visual inspection or by radiography. All active and sham units were fabricated and tested by one electronics specialist (A. H.). At the beginning of the study, live and sham units were sterilized (ethylene oxide), packaged and coded by AH for blinded implantation. Early in the clinical trial this practice was discontinued. Subsequently live and sham OFS units were fabricated and tested, labeled as to their identity, and coded.

Figure 4 *Electrical Schematic of the OFS Circuit.*
The overall electrical circuit is shown, while an expanded view of the timing circuitry is provided at the bottom of the diagram. The latter inserts to pin 7 of switch IC 2 shown in the middle of the schematic. Refer to the circuit description, names and function of the various components in the accompanying text. Note the symmetrical array of three output electrodes at each end of the modular electronic circuit. Each pair of electrodes deliverd 200 μA total current (600 μA for the total output of the OFS unit), and the reversal of the polarity of all three electrode pairs was timed in synchrony by this design. All resistance numbers are given in ohms, the capaciter in Farads.
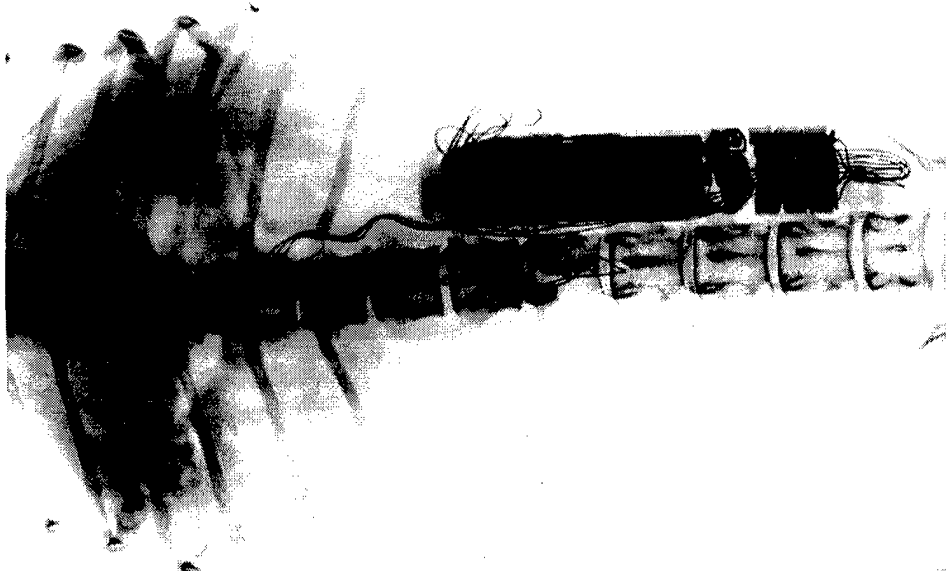
Figure 5
The OFS unit in situ, 6 weeks post surgery.
This ventrodorsal radiograph shows the OFS unit in place beneath the backskin in the lower thoracic region - and the placement of the three electrode pairs (large arrows) equidistant from the site of the disc herniation / compression of the spinal cord. The individual electrodes were sutured to paravertebral musculature, with one usually affixed dorsally, and the other two ventrolateral to this on either side, and at the same level, of the vertebral column. One set of three electrodes was positioned about two vertebral segments rostral, and the other set, two vertebral segments caudal to the lesion. The position of the voltage sources (arrowhead) and the regulatory and timing circuitry (small arrow) can be seen within the teflon covering (see text).

Study Design and Randomization

Prior to the recruitment of dogs to the study, sample size was an important

consideration since naturally occurring canine spinal injuries vary in position, severity,

pathophysiology, and response to conventional management. However, there was no

objective means to project the possible frequency of recovery in the control (sham-treated)

population on the basis of conventional management of the injury since there is no relevant

medical literature where multiple neurological evaluation procedures have been used as

exclusion criterion as we have performed. This exclusion procedure reduces the probability

that neurologically "incomplete" injuries (which respond better to surgical decompression)

enter the study population[41]. In this prior study, we were able to reach statistical

significance with a relatively low "n", which provides a more realistic rationale for recruitment numbers. Previously, 1/2 of the responding electrically-treated dogs achieved a combined neurological score of 6 of a possible 16. To detect a difference of 45 % in proportions (80 % power, alpha = 0.05, one sided test), 10 dogs per treatment category (OFS and Sham treatment) would be required to complete the study at 6 months post surgery. This study was completed with an "n" meeting this condition.

Of the 40 animals evaluated, 9 were implanted with units randomized and coded by one staff member of the study team as described above, the balance were randomized and coded by corporate colleagues as described above. In only 5 cases, the identity of an application was revealed prior to the end of the study. In these cases, owners whose dogs had received a sham implantation elected to continue treatment with a functional OFS stimulator. Since other owners of sham treated dogs did not elect to continue treatment, objectivity, and the identity of other dogs in the study was not compromised. Furthermore, the small group of "reimplants" did not adversely affect blinding and evaluation since these animals continued to be evaluated along with new admissions, animals that had not completed the 6 month period of evaluation, and other animals utilized in other types of clinical testing—all of whom were scheduled for examinations in the random order in which their owners returned to the PUVTH. The identity of all dogs was still unknown to team participants at the end of the clinical trial, and during the scoring of functional outcome by a panel of investigators. The identity of the implanted units was only made known following the assignment of functional scores, including the compilation of SSEP results.

In a previous investigation of OFS of paraplegic dogs, active OFS units were functional at the time they were implanted. In this study, 31 of the units were activated between 48-96 hours following surgical implantation. We had learned previously that the recovery of function in the experimental group could be achieved up to 18 days after surgery and application of the imposed electric field[41]. A short delay in unit activation thus allowed an opportunity to detect if the effect of the electrical stimulation might be isolated from the

early responses to decompressive surgery without adversely affecting the possibility of a good clinical outcome.

<u>Statistical Evaluation</u>

The comparison of individual categories of behavioral scoring and the total neurological scores utilized the non-parametric Mann Whitney test, which makes no prediction on the scatter of the data. The sham treated group never demonstrated a normal distribution in behavioral scores, while the actively treated group was more normally distributed. Fig.3 is a frequency plot of select control behavioural scores. This example is typical, showing infrequent and high outlier data points in the control population. Thus to facilitate recognition of trends in significance about the mode, one high outlier score was eliminated from the experimental and control group prior to a comparison of the groups with the Mann Whitney test. Instead of applying esoteric outlier analysis[62] or other little used statistical methods adapted to the problem of infrequent outliers[51], we simply provide the results of both comparisons : 1.) the complete data set for both controls and experimentals, as well as 2.) the data set with one (highest) outlier score deleted from each group. In some instances, and in the comparison of the SSEP data, an additional test of the proportions of responding and non- responding animals was used (Fisher's Exact Test, one tailed). The Student T evaluation was used to compare other data sets with an expected normal distribution such as animal age, time of admission, etc.

II. Results

A. Sensory Projections, DC Fields, and Fluorescent Tract Tracing

<u>General Procedures</u>

Twenty five animals were assigned to the experimental group, 19 to the sham treated control group. Over the years we have observed that the combined surgical procedures

stresses the animals. A total of 10 animals of 44 died during the conduct of the experiment (Table 1). This mortality included animals that did not recover from anesthesia at the beginning of the experiment to animals lost following the final anesthesia and injection of the intracellular tracer at the experiment's end. Losses between the groups were not statistically different. Table 1 summarizes these data as well as providing the days post surgery until sacrifice, and the numbers of animals in each group whose histological preparation was acceptable for study.

The use of a rhodamine conjugated dextran (Fluoro Ruby, Molecular Probes, Inc.) provided good detail of anterogradely labeled axons, both with Epifluorescent and confocal laser microscopy. Only one spinal cord was insufficiently labeled as to be useless (poor dye uptake). In a second, there was a complete failure in labeling. In this particular animal, excessive bleeding at the time of dye injection was noted, and this appears to have interfered with uptake of the dye at this site as labeled axons were not even visible at the location of the injection.

The dye spread evenly through the distal segments of axons and labeled the long tracts, both dorsal columns and components of ascending lateral tracts. These appeared as long, unbranched, columns of fibers of varying caliber, arranged parallel with the long axis of the spinal cord. The caliber spectrum labeled was not quantified, however we observed axons 1 μm or less in diameter filling with the dye over distances exceeding 1.5 cm. Confocal laser microscopy allowed even larger numbers of these very small afferents to be visualized - particularly at or within the lesion itself in experimentally treated spinal cords (see below). We are confident that axons that terminated caudal to the lesion represented the true terminal extent of these fibers, and not poor uptake of the intracellular marker, since a) many of these labeled axons possessed blunt terminal endings within the plane of section, and b) more lateral or ventral axonal tracts that were spared by the hemisection labeled beyond the plane of transection into the rostral segment.

Other than the tracts purposely labeled, two instances of extraneous labeling were occasionally observed, each easily delineated from the labeled long tracts. In the first case, injected Fluoro Ruby sometimes was found within the central canal of the caudal segment of spinal cord. This was taken up by interneurons, phagocytic cells, and possibly glia, lining the lumen. These very short lengths of axons (no longer than 20-35 μm) were clearly components of small neurons whose cell bodies also filled with dye. There was no mistaking the identity of these neurons, or their processes, with long tract axonal columns that were intentionally labeled. In the second case, dorsal roots were occasionally filled by dye escaping into the extradural compartment. These axons could easily be identified entering the spinal cord. Furthermore, when roots were labeled, these were near the injection site - we have no evidence of dorsal roots filling with dye at, or rostral to, the plane of transection in any spinal cord.

The use of the indwelling marker to determine the plane of transection was both effective and helpful. This technique, developed in our laboratory for use in dorsal and lateral spinal cord hemisection procedures[36,38], failed in only 3 cases. In these instances, the marker was displaced from the cord and could not be located following perfusion/fixation. In all other cases, the plane of transection could be determined by comparing the series of holes left in the tissue. Additionally other natural markers such as the swollen ends of the central canal, both rostral and caudal of the lesion, help determine the plane of transection when marker holes were absent.
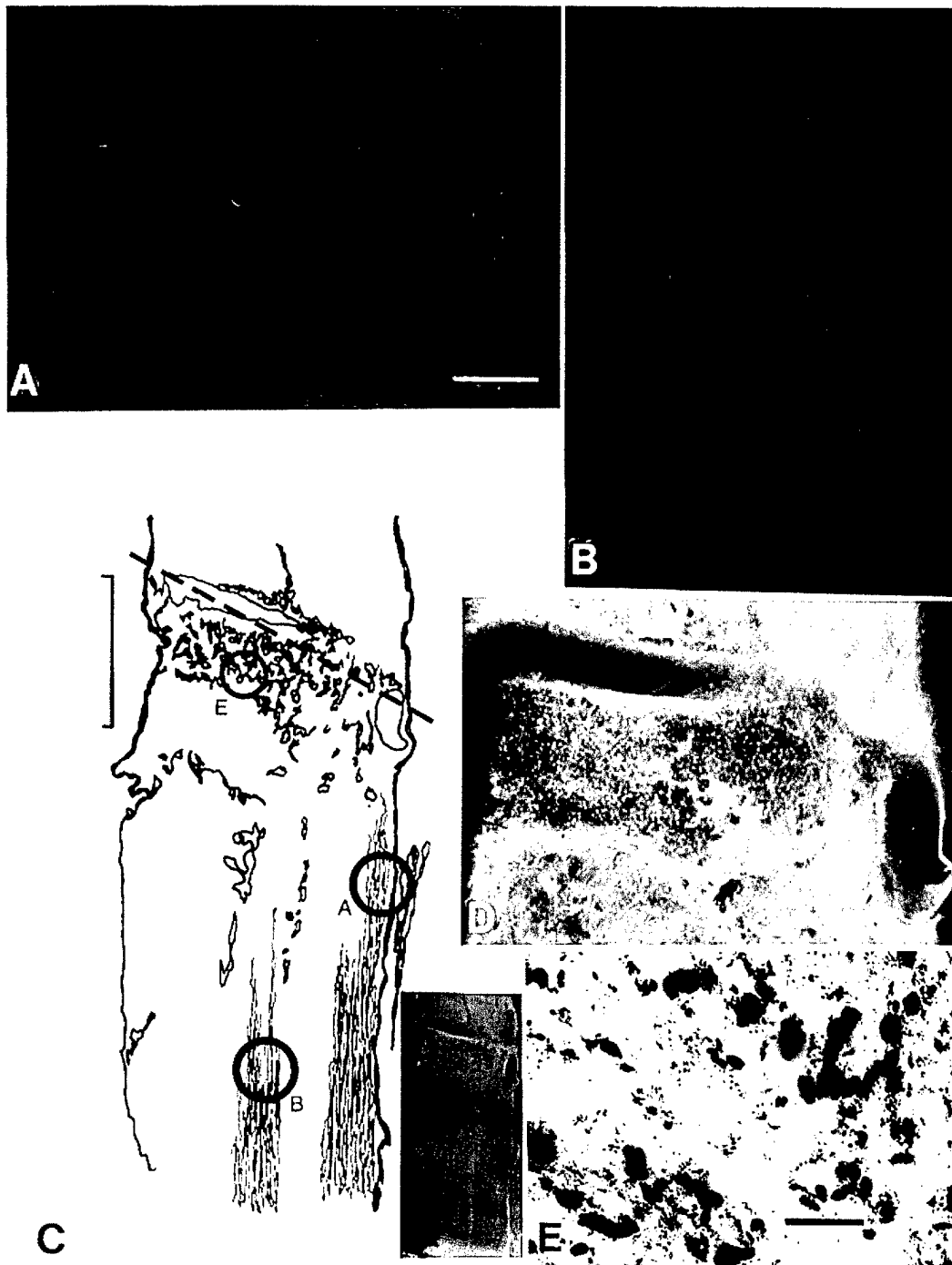
Sham-treated Spinal Cords

In sham treated animals it was indeed uncommon to trace axons to the caudal border of the zone of central hemorrhagic necrosis. This was expected, given our prior studies[36,37,40]. There were 19 animals in this group, 14 of which survived to provide clear

histology. In all but two of these cases (86%), labeled ascending fibers projected close to, but not into, the caudal region of the injury zone or lesion. This zone extended a variable distance rostral and caudal of the plane of transection. It was characterized by cavitated, destroyed parenchyma, containing blood cells, and large cysts. There are many cellular species occupying this area in large numbers two months post injury such as macrophages, leukocytes, and astrocytes (data not shown; refer to citations 123, 122, 101, 16, and 144). Only two sham treated chords (14%) showed axons that could be traced to enter the most caudal region of the lesion. In no case did we observe fibers projecting to the plane of transection, across it, or around it. Figure 6 depicts a spinal cord typical of the control group. Note a well filled lateral tract (Fig 6 A) and dorsal column (Fig 6 B) that do not project to the caudal boundary of the lesion (Fig 6 C and D), or the plane of transection identified by the marker holes (Fig. 6 C). We further evaluated the lesioned region of spinal cord in this and one other control cord with the laser confocal microscope. Scans of the lesion within the caudal segment of the spinal cord - that is, in the plane of projection of anterogradely filled fibers - never revealed the presence of even fine axonal branches or processes (Fig 6 E).

Electrically-Treated Spinal Cords

In most spinal cords in which an electrical field was imposed, the picture presented by intracellular tract tracing was different from control animals. In only three spinal cords (21%) were axon terminals restricted to a region caudal to the lesion, that was similar in appearance to the control spinal cords. The balance of the electrically treated cords showed labeled axons projecting not only to the plane of transection, but as well around it, and in 5 animals, *through* the plane of transection (between the marker holes) into the rostral segment of the spinal cord. We shall describe the appearance of axons found within each of these various locations in the following text.

Figure 6 *Epifluorescent photomicrographs and a laser confocal image of a sham-treated (control) spinal cord.*

Epifluorescent photomicrographs show an anterogradely filled lateral tract (A) and components of the dorsal column (B). The camera lucida drawing of this spinal cord (C) marks these approximate regions within the circles labeled A and B, and marks the plane of transection with a hatched line (the inset shows a low power view of this spinal cord for comparison). A darkfield fluorescent photomicrograph (D) of the region containing the lesion shows the absence of any axon profiles. Macrophages within this region have ingested the label and can be seen as the yellow cells peppering the lesion. The most rostral extent of anterogradely labeled axons is shown in the drawing. Scans of the lesion (circle marked E) more rostral to this were made with the confocal microscope, however axon profiles were not found. A high magnification, 2 μm optical section taken with the confocal microscope (E) is typical of all such scans. The index line in C is 500 μm; in A (as well B) = 50 μm; and in E = 150 μm.

Axonal Projections around the scar

In four electrically treated spinal cords (29%), we traced large and small caliber axons of the dorsal column to circumnavigate the scar by deviating away from the center of the spinal cord - that is, their original plane of projection - *towards the lateral edge of the spinal cord* . These axons followed a route curving with, or sometimes actually against, the capsule of scar surrounding the marker hole. Flattened and spear shaped axon terminals, characteristic of growth cones, were observed on these axons and their branches as they passed around the marker. The larger caliber axons deviating around the lesion within the undamaged parenchyma were usually observed to branch into numerous fine processes at about the level of the transection. These fine processes could also be traced into the rostral segment of the spinal cord to terminate in enlarged, flattened, endings. It is worth emphasizing at this juncture, two general characteristics of axons seen in this spinal cord that were characteristic of the other examples to be described below: 1) The production of numerous, small (< 1μm), branches from a single "parent" axons. Bifurcations of axons were common, but no more common than trifurcations (or even more numerous branches) developing from a single axon. Commonly these fine branches were seen to branch again at sites more distal. 2) Axonal processes were also seen to course near, or directly against, the scar tissue formed around the marker, the boundary of a cyst, a ribbon of dense scar tissue at the plane of transection, or in general, any region of discontinuity of the parenchyma. This was so common that inspection of these regions in experimentally treated spinal cords usually revealed the presence of fine axonal processes. This was in contrast to control spinal cords in which similar inspections at similar regions never revealed the presence of axons or their branches.

Axonal projections within and across the lesion

It was a simple matter to trace larger axons, components of the well marked ascending columns, deep into the lesion to the plane of transection (Fig. 7 A, B). We again

emphasize that when axons entered this region (or traversed it - see below) they usually branched into numerous small processes (Fig. 7D, E) - however this was not always the case. Sometimes axons projected transversely, running along the plane of the transection (Fig. 7B). In the example just noted, this well labeled axon projected along the caudal boundary of the transection for nearly 1/3 the width of the spinal cord. This projection was *perpendicular* to its original orientation. It was *not* a simple matter however to trace axons or their branches deep into the lesion, or across the plane of the original hemisection into the rostral segment. We were able to detect this in 5 of the 14 experimental spinal cords (36%). Ascending axons of the lateral and dorsal columns extended into these *as very fine processes* that were not easily revealed with low power magnification (< 20 diameters). Inspection of the plane of transection with the confocal microscope, the margins of cysts, or the edge of the swollen central canal increased our ability to resolve them. It was also characteristic that small axonal processes within the lesion were not organized in their projections. Figure 6 shows an experimentally treated cord in which a column of lateral tract axons projected to the level of the transection. Many of these axons branched repeatedly deviating their growth medially towards the boundary of a large cyst within the rostral segment of the spinal cord (Fig 8 A, B; compare with Fig. 7 A and B). Three dimensional reconstruction of a confocal Z axis scan of the entire depth of this lesioned area (approximately 60 μm) shows the especially dense mat of cells at the level of the hemisection. The ascending column of fibers projecting to this level was well labeled, however, only a very few labeled fibers were observed directly across from this region in the rostral segment of spinal cord (Fig 8 A). Furthermore, two micron thick confocal optical sections of this region did not allow one to trace the fibers through the ribbon of dense cells or "scar" in order to establish the continuity of these processes across the plane of the hemisection (Fig. 8 B), but better revealed the character of axonal branching at the level of the lesion. A three dimensional reconstruction of this region did allow tracing of individual
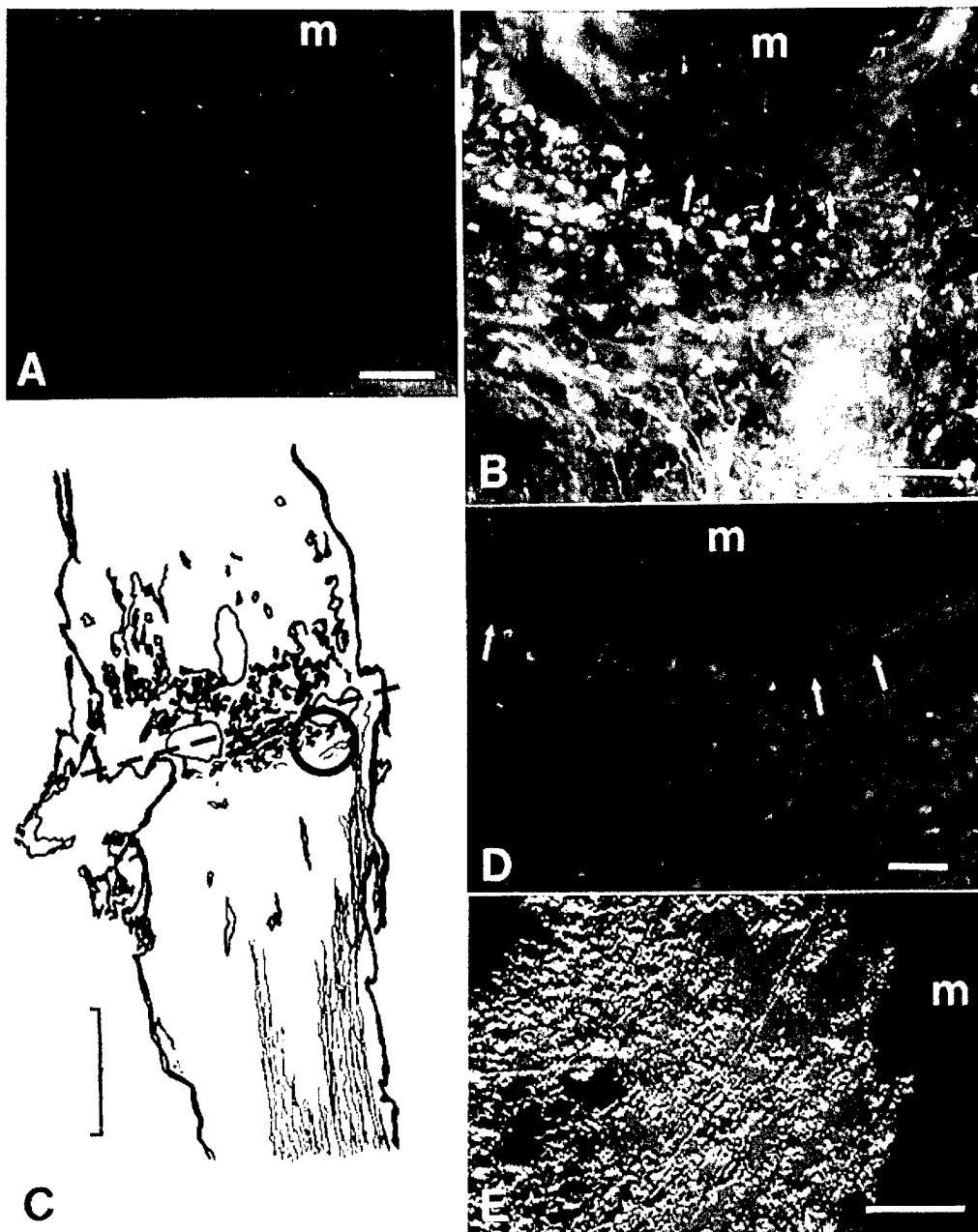
Figure 7 *Epifluorescent and laser confocal examination of axonal trajectories in an electrically treated spinal cord.*

The low power epifluorescent photomicrograph (A) shows the most rostral extent of a well filled column of right lateral tract ascending fibers where they project to the plane of the lesion at the right marker hole (m). A section 50 μm more ventral to this region is shown in B, but at a higher magnification. This approximate region is marked by the circle in the accompanying camera lucida drawing (C) as is the plane of transection (hatched line). Note in A that ascending lateral tract fibers project through the lesion to approximately 75 μm from the caudal edge of the marker hole. Some of these fibers curve abruptly, or gently, towards the center of the spinal cord. One of these axons, shown in B, projected to the level of the scar capsule surrounding the marker hole, turned towards the center of the spinal cord, and followed the transverse boundary of the scar for approximately 1/3 the width of the cord. A significant length of this axon is seen in the same plane of focus in B (arrows). Small processes (arrows) of this deviated group of axons could be detected following the capsular scar surrounding the marker hole (m) in photomicrograph D, some of which crossed the plane of transection. Examination of the medial face of this marker hole, situated over 100 μm within the rostral segment of the spinal cord, with the laser confocal microscope revealed fine (less than 0.5 μm diameter) processes ascending the spinal cord (E). The pseudocolor three dimensional image (E) was reconstructed using 20 two-micron thick optical sections. The scale in A = 80 μm; B = 25 μm; C = 600 μm; D = 10 μm; and E = 80 μm.
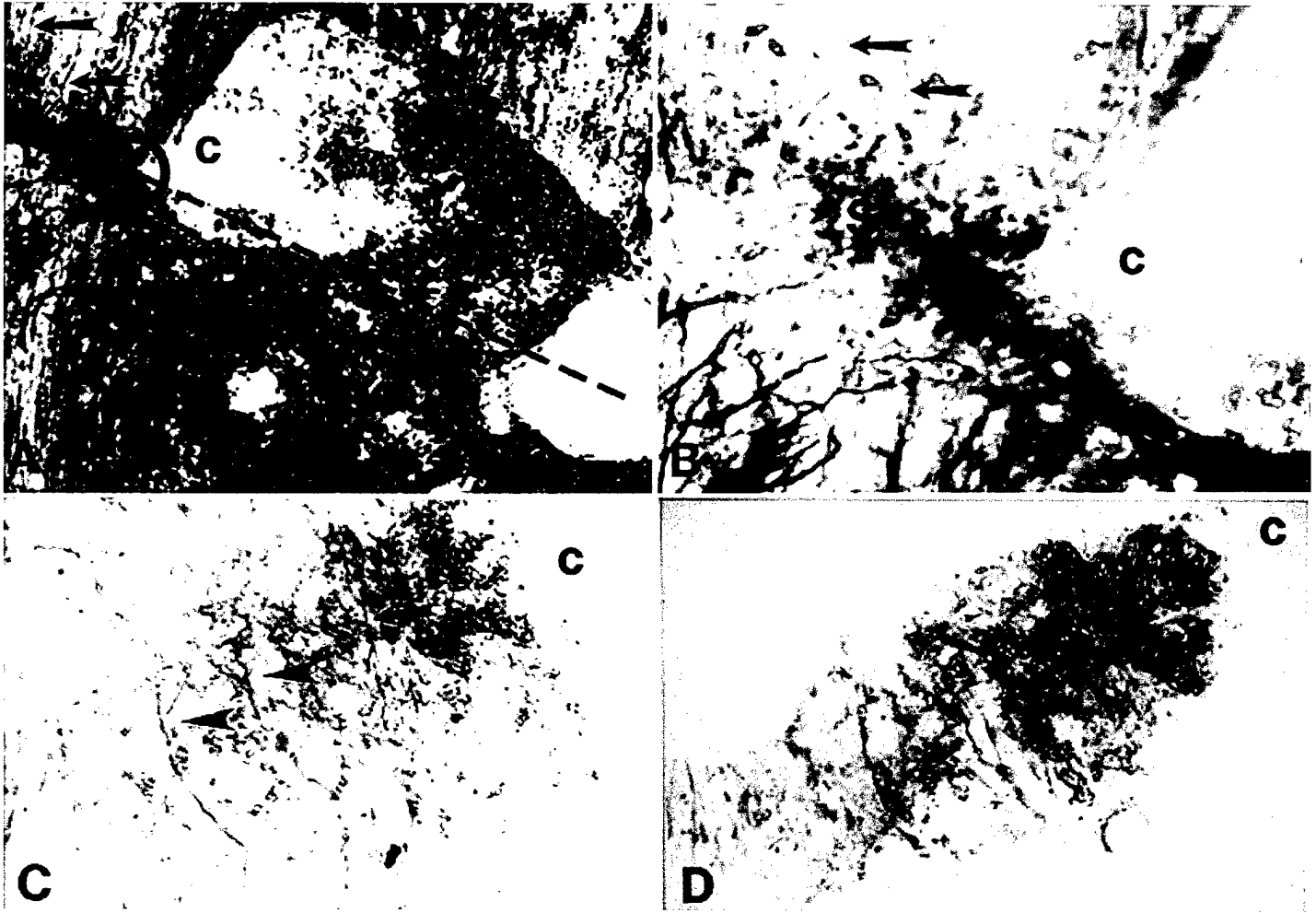
Figure 8 *Laser Confocal Images of Axons traversing the lesion.*

A.   This pseudocolor three dimensional reconstruction (60 µm deep) of the left region of a hemisection in an experimentally treated spinal cord. This region contained large cysts (c) within the rostral and caudal segments of the spinal cord. The hatched line marks the level of transection. A band of left lateral tract axons projected to the plane of transection (arrowhead) seen at the left hand boundary of the micrograph. Some of these axons branch and turn inward, towards the center of the spinal cord. A few labeled fibers are seen in the rostral segment of the cord (arrows), across a particularly thick region of scar tissue. These fibers could not be traced through the substance of the scar however. A single optical section of this region (2 µm thick) at a higher magnification is shown in B (the approximate region circled in A). Note the branching and turning fibers within the caudal segment of the cord project centrally, along the ribbon of scar (S) and/or toward the cyst (c). Though possible extensions of these fibers into the rostral segment is visible in this view (arrows), the individual processes could not be traced through the substance of the scar. C and D are three dimensional reconstructions of this same region, in which optical sections that did not contain axon profiles have been deleted from the reconstructed image (fewer deletions were made in C than D). In these images, axons can be seen traversing the substance of the scar (arrows), sometimes branching within it (arrowheads). (One indistinct fiber (arrow) at the margin of the cyst in C is more visible in D). The scale bar in A = 75 µm; B, C, and D = 25 µm.

fibers through the lesion at this boundary when optical planes of the scan *that did not contain axon profiles* were deleted (refer to methods). These fibers branched once, or even twice, within the substance of the lesion as they were traced into the rostral segment of the spinal cord (Fig. 8 C and D).

B. Two and Three Dimensional Morphometry of SCI

Verification: Macrophage Cell Diameter and Cell Counting

As described previously, the mean cell diameter in pixels of 173 individually measured cells was 18.9 ± 0.3, while the mean diameter by actual measurement was 12.5 ± 2.7 μm. We compared this average diameter with other histological examples of macrophages taken from the literature (11 - 21 μm;[16,18]), and we made micrometer measurements of the diameter of 61 individual and isolated macrophages as an additional check. In brief, our computer derived estimate of the macrophage cell diameter was very similar to the direct measurements and not significantly different (Table 3).

The accuracy of our computer assisted computation of macrophage number based on pixel values/macrophage was also verified by comparing computer assisted counts of macrophages within 10 different fields of view at our standard magnification with actual cell counts of these same fields of view made by a naive investigator. These numbers were also close, and were statistically similar (Table 4).

Table 3

| Type of Measurement	Animal Number	Number of macrophages measured	Mean cell diameter (pixels)	Mean cell diameter ± SEM (μm)	Mann-Whitney U (2-tailed, unpaired)
Visual	8	61	N/A	12.77 ± 0.50	P = 0.72
Computer	12	173	18.87*	12.47 ± 0.21	

* 1 μm = 1.51 pixels at 200x

Table 4

Type of Measurement	Animal Number	Fields of view counted	Mean macrophage count ± SEM	Wilcoxon (2-tailed, paired)
Visual	7	10	55.6 ± 16.1	P = 0.56
Computer	7	10	59.5 ± 21.3	

Macrophages of the Subacute Lesion

In every injured spinal cord, macrophages were the dominant cell type occupying the site of damage. Given the dorsal approach to the spinal cord during the laminectomy procedure, followed by compression of the dorsal spinal cord, one would reasonably expect the lesion severity to be most profound here in all eight spinal cords. This was true, and best exemplified by two spinal cords in which the tissue damage was completely confined to the dorsal half. Figure 9 shows the typical dorsal to ventral extent of lesioned parenchyma in two spinal cords where a variable amount of ventral grey and white matter destruction was evident. We measured the rostral to caudal extent of compromised spinal cord in all of the samples (measuring this in every third section beginning at the most dorsal). At T11 (the approximate lesion site in most cords) the length of the spinal cord segment is approximately 4.5 mm, at T12, 4.3 mm, and at T10, 4.6 mm[140]. The average measured rostral/caudal extent of the lesion for all 8 animals was 3.8 ± 0.7 mm (Table 5). Thus the longitudinal extent of the injury was somewhat less than 1 vertebral segment.

As discussed, labeled macrophages were of typical size (between 10 and 16 μm diameter), vesiculated with numerous inclusions, and positive for surface antigens derived from rat macrophage (ED1). We did not observe artifactual staining or labeling in control sections of two uninjured cords.
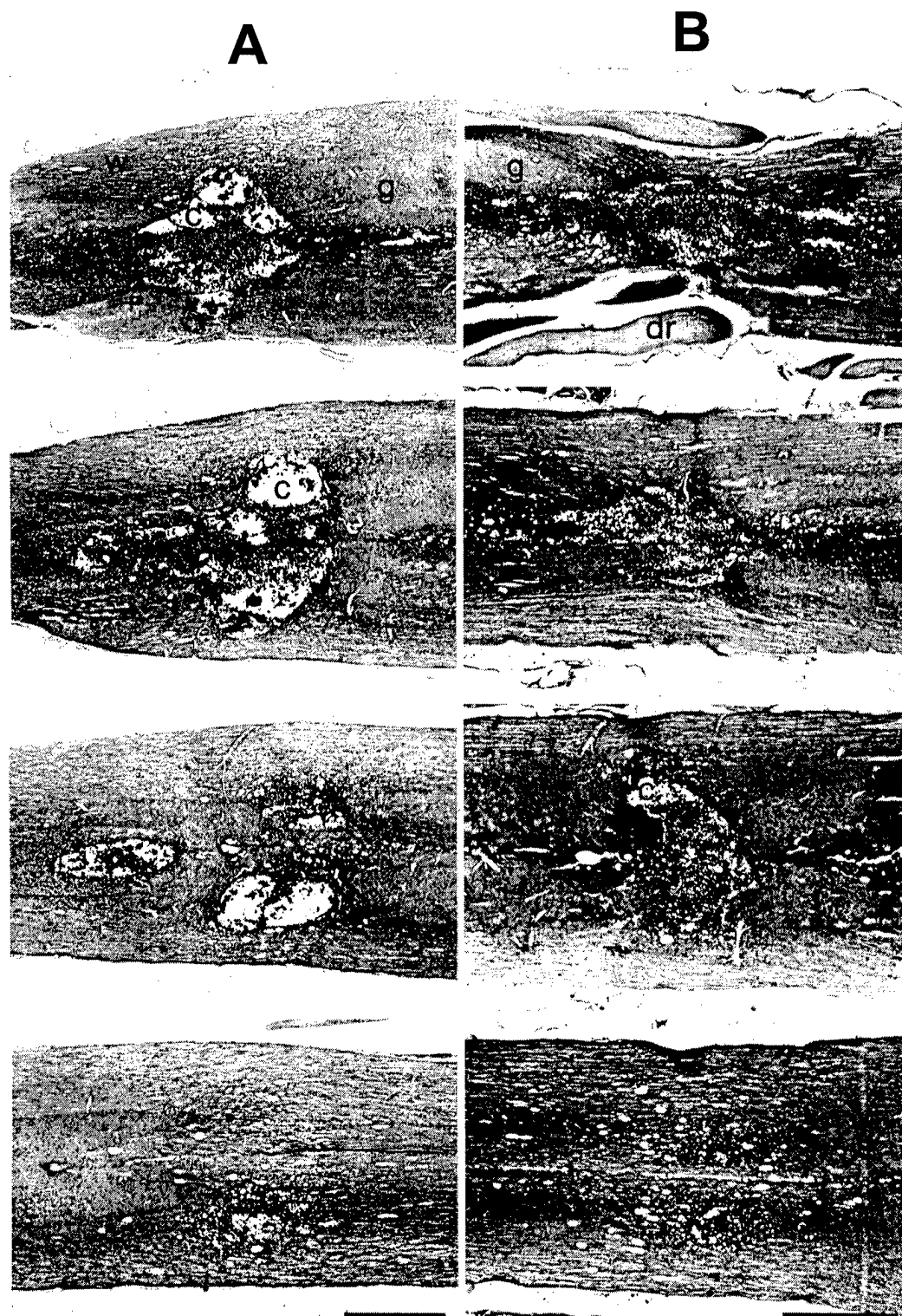
Figure 9 *Examples of Spinal Cord Injuries comprising the Data Set*
The four images in column A are individual sections of the same spinal cord showing the progression of a compression lesion from dorsal (top of page) to ventral (bottom of page), and similarly in B. Both cords are oriented rostral to the left and caudal to the right. One section of the spinal cord in column A was shown digitized in Figure 2. Note in both spinal cords the dark regions of macrophage staining in both white and grey matter is usually localized in and around cysts at the site of actual compression of the spinal cord. Note that the cord in column A is more cystic than the one in B. Note in both spinal cords, accumulations of macrophages are extensive in the dorsal white matter, and less extensive in both grey and white matter in more ventral regions of the spinal cord. This is probably due to the dorsal focus of compression. Scale bars in the bottom photomicrographs for column A and B = 1 mm. (dr = dorsal root, w = white matter, g = grey matter, and c = cysts.)

Table 5   2-D Morphometry of Cysts and Cavities

Rat #	Cysts mean diameter in mm		Rostral Cysts mean area in mm^2		Caudal Cysts mean area in mm^2		Microcavities mean diameter in μm		Lesion Length in mm
	n^1		n^2		n^2		n^1		
1	14	0.31	3	0.91	3	0.77	10	15.6	4.2
2	7	0.10	2	0.17	2	0.28	10	15.6	4.0
3	8	0.11	2	0.21	2	0.09	10	14.9	3.5
4	10	0.13	2	0.17	2	0.12	16	11.9	5.3
5	10	0.26	2	0.61	2	0.27	13	14.5	3.2
6	6	0.10	2	0.13	2	0.11	8	14.0	3.0
7	7	0.15	3	0.17	3	0.09	14	16.8	3.7
8	9	0.13	2	0.15	2	0.24	10	18.3	3.2
N	71		18		18		91		24
Population Mean	0.18		0.14		0.11		15.0		3.8
Population SEM	0.02		0.03		0.02		0.5		0.3

1. n = the number of cysts measured in each animal's spinal cord. The diameter for each cyst was obtained by averaging the major and minor axis.

2. n = the number of cysts measured in each animal's spinal cord. The area for each cyst was determined by Pixel transformation (as for macrophages) using IPLab Spectrum^{TM} (see methods).
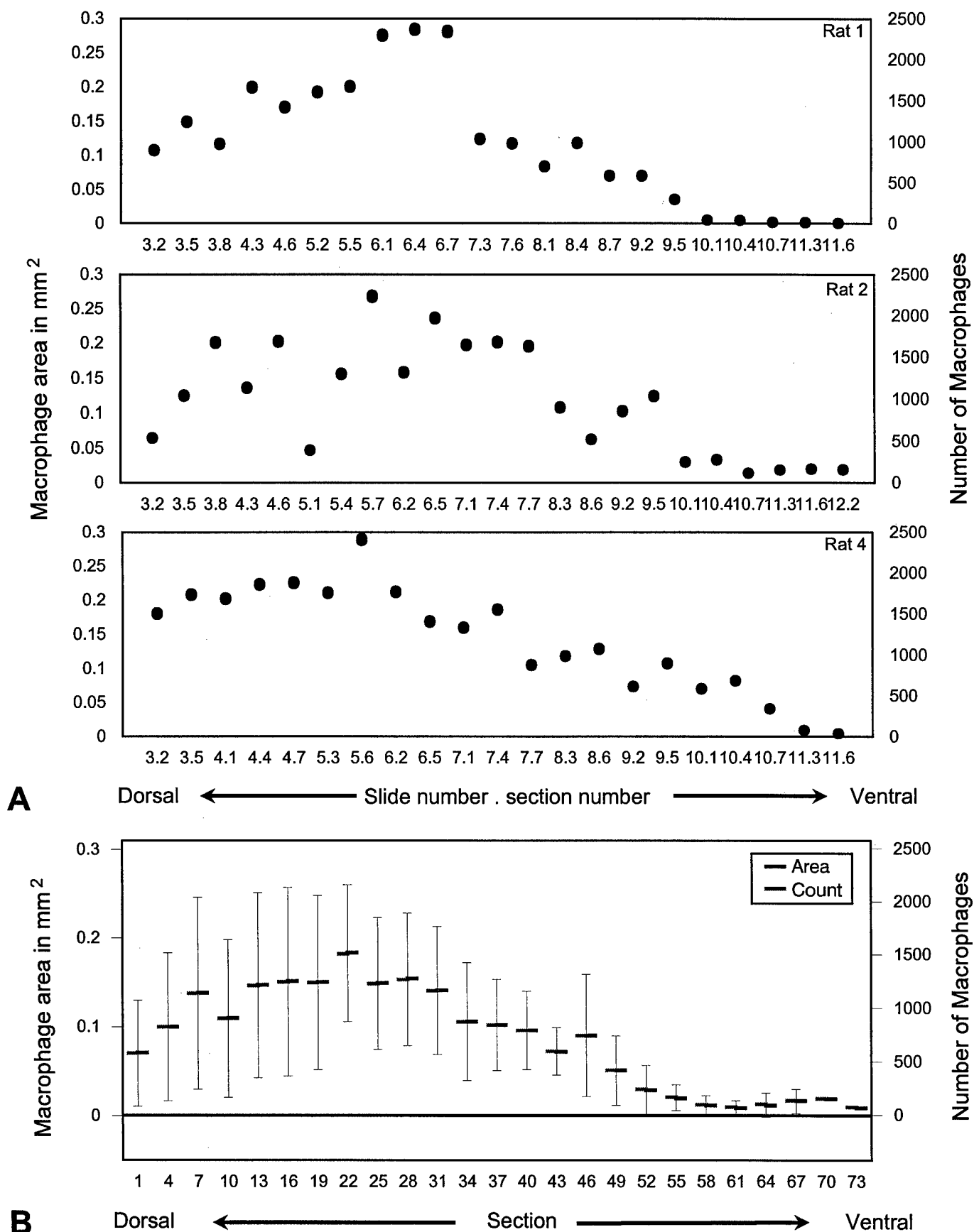
Lesion Boundary

The boundary of the injured region of spinal cord was well defined due to large accumulations of labeled macrophages separating relatively undamaged parenchyma (visualized by the counter stain) from macrophage filled and usually cystic spinal cord parenchyma. The integrity of adjacent "intact" spinal cord tissue showed well defined cell borders, homogeneous staining with hematoxylin, and was relatively free of phagocytes. These regions sometimes possessed variable amounts of cavitation, however. The boundary of the lesion and large cysts was circumscribed on the digitized image using a laboratory designated tracing program. This procedure was carried out on every digitized histological section of each cord as a first step in creating 3-D surface reconstructions.

Macrophage Counts

At three weeks post injury, macrophage numbers were quite variable between spinal cords as well as within individual histological sections of the same spinal cord. Individual sections contained numbers of macrophages ranging from a few hundred cells to over 2000, with means ranging from approximately 500 to 1500 cells per section. These counts were *confined to the lesioned region of spinal cord* and do not represent the numbers of macrophages that could be found at greater distances from the focus of injury (such as within degenerating white matter tracts). Additionally, we emphasize these numbers are conservative ones, or better said, underrepresent the actual numbers of cells in even the focal site of damage since in some sections less than 100% of the lesioned area was sampled by our technique. Figure 10 provides examples of macrophage counts and the unit area they occupy for three individual spinal cords (A) and a summary of all eight cords studied (Fig. 10 B). In spite of the large and expected variation in cell numbers, the greatest numbers of macrophage cells were found in the dorsal half of the spinal cord–that region associated with the greatest damage produced by dorsal compression of the cord (see methods). This is more evident when the macrophage counts are normalized by peak values (Figure 11), showing increasing cell counts peaking near the central–but still dorsal– region of the spinal cord, and decreasing sharply in ventral regions. The peak densities of macrophages represent a very significant fraction of spinal cord in regions where substantial numbers of these cells accumulate. The unit area occupied by macrophages in the lesioned segment ranged from 0.1 to 0.2 mm^2 within dorsal spinal cord segments of approximately 0.7 square mms.

Cystic regions within the injury zone

Though we made no comprehensive effort to quantitate the various fluid filled cavities that form in response to spinal cord compression, we did measure the diameters of two separate types of cavities that were common in all eight cords studied. Large cysts that

A

Rat 1

Rat 2

Rat 4

Macrophage area in mm^2

Number of Macrophages

0.3
0.25
0.2
0.15
0.1
0.05
0

2500
2000
1500
1000
500
0

3.2 3.5 3.8 4.3 4.6 5.2 5.5 6.1 6.4 6.7 7.3 7.6 8.1 8.4 8.7 9.2 9.5 10.110.410.711.311.6

3.2 3.5 3.8 4.3 4.6 5.1 5.4 5.7 6.2 6.5 7.1 7.4 7.7 8.3 8.6 9.2 9.5 10.110.410.711.311.612.2

3.2 3.5 4.1 4.4 4.7 5.3 5.6 6.2 6.5 7.1 7.4 7.7 8.3 8.6 9.2 9.5 10.110.410.711.311.6

Dorsal ⟵ Slide number . section number ⟶ Ventral

B

Macrophage area in mm^2

Number of Macrophages

— Area
— Count

0.3
0.2
0.1
0

2500
2000
1500
1000
500
0

1 4 7 10 13 16 19 22 25 28 31 34 37 40 43 46 49 52 55 58 61 64 67 70 73

Dorsal ⟵ Section ⟶ Ventral

Figure 10 Macrophage unit area and number by histological section. (A) shows examples of area and number plots for rats 1, 2, and 4. (B) shows the means and S.D.'s of all 8 rats.
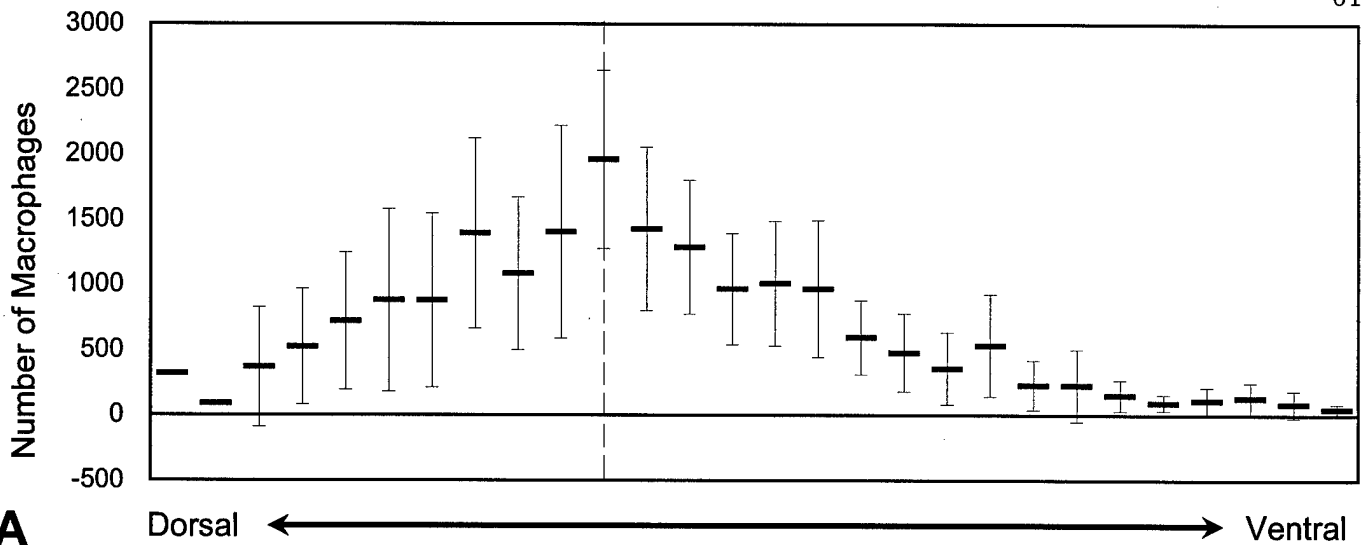
Figure 11 *Macrophage counts normalized by peak values. The hatched line representatives the section containing the maximum number of macrophages for each spinal cord. Means and S.D.'s for the sections dorsal and ventral are distributed on either side of this peak.*
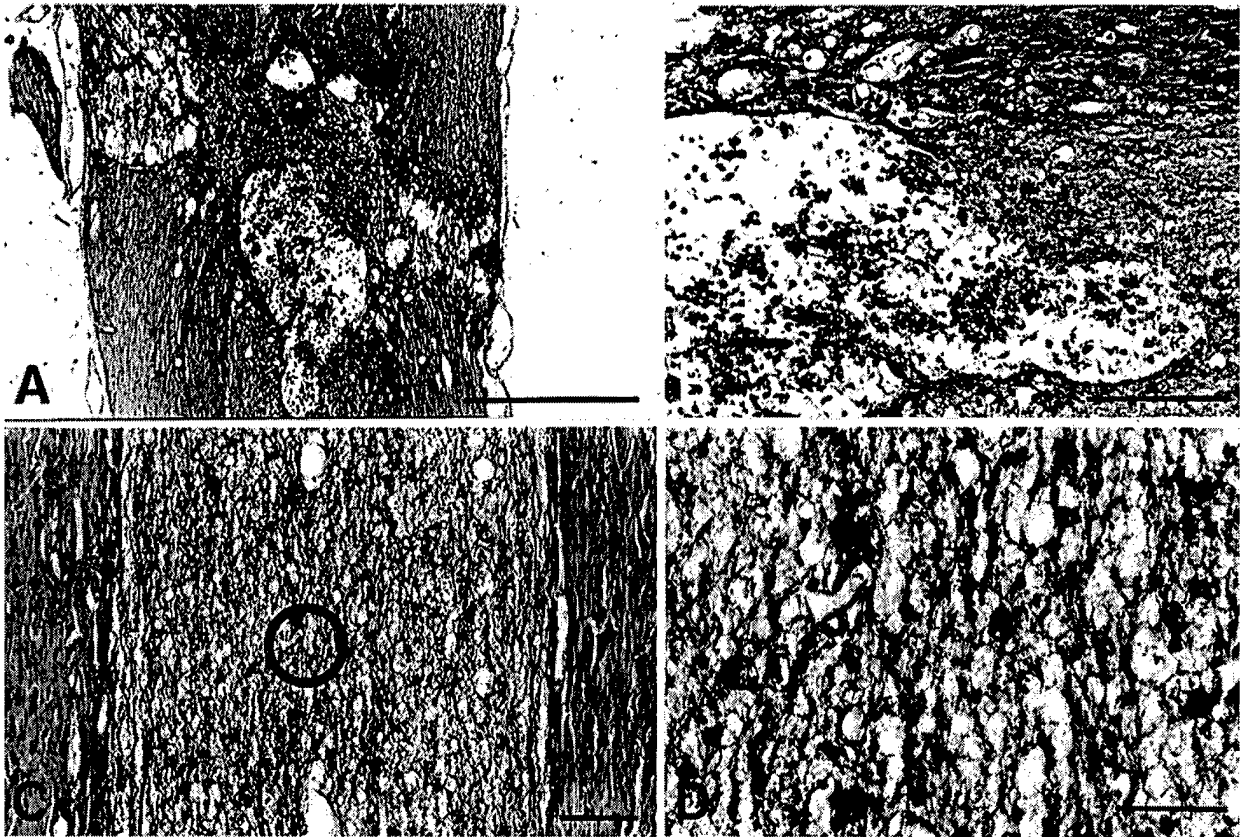

Figure 12 *Cyst and Microcavities in Damaged Spinal Cord Parenchyma A typical zone of compression injury is shown in A, containing numerous large and small cysts. It is likely that the large cysts located within the central cord are part of, or connected to, the central canal. The numerous smaller cysts in this locale (B) may or may not be connected as a cisternal system containing CSF. In regions far from the area of compression, white matter tracts undergoing Wallerian degeneration are always extensively cavitated (C and D). These small cavities are on the order of one cell diameter (10 - 15 µm). The defining of cysts and microcavities was not arbitrary in this report, but reflects a difference in the location, size, and significantly different range of diameters in the two groups of cavities quantitated by 2-D morphometry (Table 5). Scale Bar in A = 1 mm, in B = 250 µm, in C = 100 µm, and D = 50 µm.*

were centrally located within the region of injury and appeared to be in continuity with the swollen central canal (Fig. 12 A, B) were on the order of 0.2 mm in diameter (n=71) (Table 5). The largest cavities in central regions of grey matter were on the order of 25-30% of diameter of the uninjured spinal cord. In all spinal cords but two, these cavities were larger rostral to the injury than caudal. In spite of this trend, we detected no statistical difference relative to the rostral/caudal side of the injury in which the largest cysts occurred (P=0.06, Paired Students' T) (Table 5).

Another commonly observed form of cystic cavitation in all animals was so called "microcavitation." These cavities were not necessarily associated with the focal area of damage. Regions of microcavitation were sometimes extensive in white matter tracts undergoing Wallerian degeneration (Fig. 12 C and D). For example long tracts such as the ascending dorsal columns and lateral white matter tracts were intact on the caudal side of the injury, but degenerate on the rostral side - sometimes for the entire length of the histological segment examined. Phagocytosis of these distal segments produced expanses of cystic white matter where the average diameter of the individual cysts were curiously about one macrophage cell diameter (15 ± 5 µm; n = 90; Table 3). It is likely the most active phagocytosis in these areas occurred prior to our sample time of 3 weeks as cavitated regions of white matter did not contain the dense accumulation of macrophages that were observed at the focal region of spinal cord damage. In three of the eight spinal cords containing degenerate white matter tracts, these regions were nearly free of ED1 labeled cells.

Computer assisted two dimensional counting allowed an approximation of the total unit area of cysts at the lesion site, since large cavities within the region of damage were color transformed and their unit area measured in pixels in the same manner as performed with stained macrophage cells (see methods). The total unit area of these cysts ranged from about 0.025 - 0.1 mm^2 within any one histological section of a lesioned cord. Figure 13 shows three representative examples of such measured cysts (A) and a summary for all
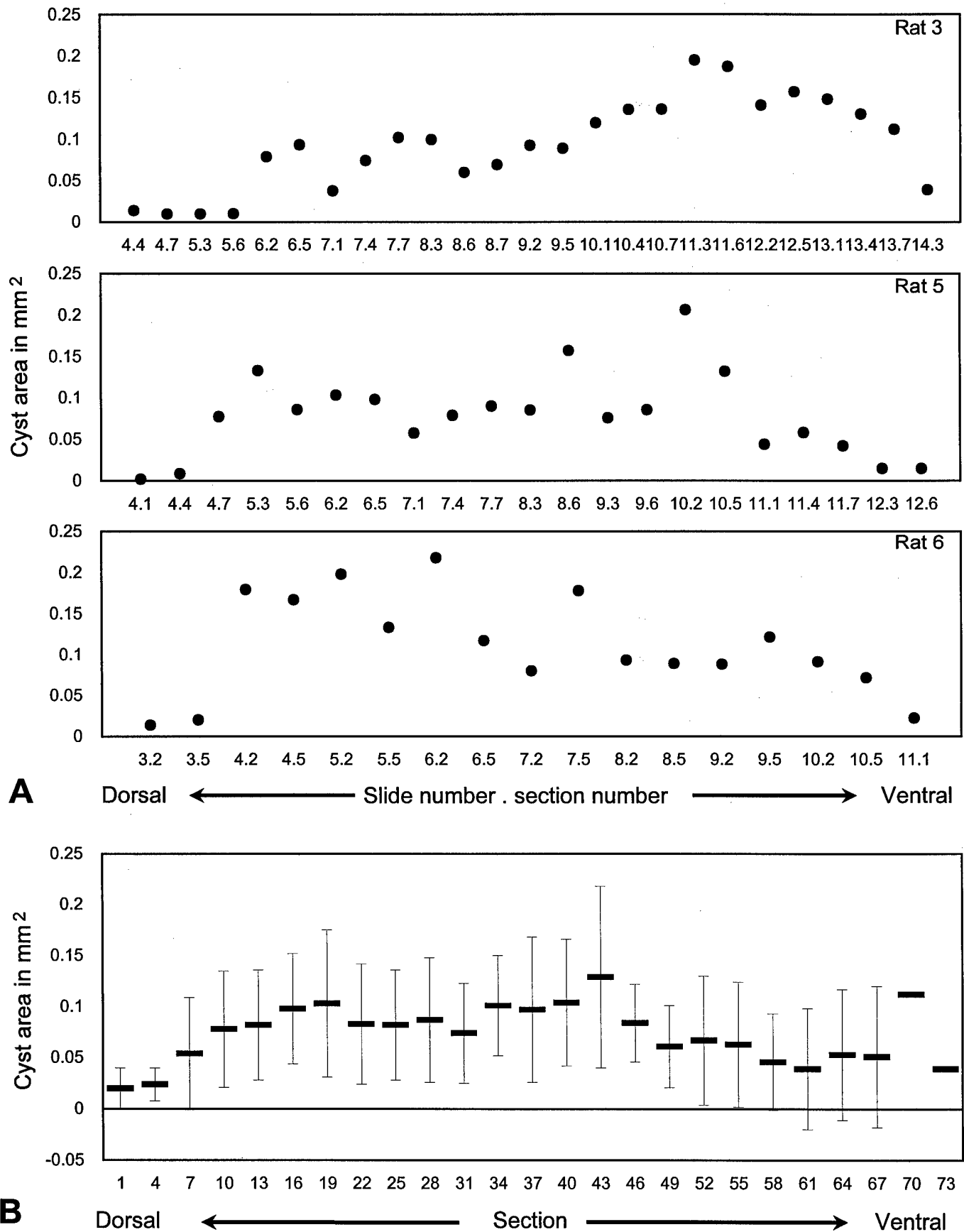
Figure 13 *Cyst area by histological section. (A) shows examples of area plots for rats 3, 5, and 6. (B) shows the means and S.D.'s of all 8 rats.*

eight spinal cords studied (B). Note that in contrast to the character of macrophage accumulations, the regions of spinal cord containing the greatest density of cysts does not correlate with the region of greatest experimental compression.

Defining the area of the lesion

If we are to evaluate the peak accumulations of macrophages relative to the size of the histological lesion at three weeks post injury, we must first define what the "lesion" is. In one scheme, we can define the lesion as that region of damaged parenchyma bounding macrophage accumulation that as well contains fluid filled cysts. This would be the more routine way an examiner would usually circumscribe the boundary of a "lesioned area" on any one histological section. It would be fair to include cysts within this region since many contain aggregations of phagocytic cells which may be ingesting—or at least obscuring—damaged parenchyma (see as well such "floating" macrophage accumulations in citation 18). However, there are usually islands of relatively intact parenchyma, well defined by background staining within such an area of injury. In another scheme, one might consider this relatively intact parenchyma (free of macrophages) as uninjured, and define the lesion as the area composed of macrophages and cavitated parenchyma, but not including internal zones - or islands - of relatively intact grey and white matter. Figure 14A shows a summary graph of the area of damaged, macrophage infested, and cystic spinal cord parenchyma. Figure 14B shows a similar graph in which undamaged parenchyma contained within this zone has been deleted from the calculation of unit area. A simple inspection of the ordinates demonstrates this difference in unit area of lesion to be substantial.

Macrophages per unit area of lesion at Three Weeks post injury

Figure 14C shows total counts of macrophages per unit area of lesion. In Figure 14D the data represents macrophages within lesions *in which islands of relatively undamaged parenchyma are not included.* Note that accumulations within the damaged dorsal

hemisphere of the spinal cord range from 4000 - 7000 cells per mm² of lesion using the latter definition of the lesion. The more routine way of defining the lesion (which does not take into consideration zones of apparently healthy parenchyma) shows the macrophage accumulations to be less than half of this amount (Fig. 14C).

Three Dimensional Surface Reconstruction: The subacute lesion as defined by Phagocytes

Three dimensional surface reconstructions involve management of the digitized image to emphasize boundaries and topology. Moreover, the algorithms we used to produce these reconstructions enable quantification of the region of interest[8]. Figure 15A-C shows the solid surface rendering of the macrophagic lesion embedded within its histological section. Furthermore, these views reveal the correct registration of the lesion surface with the plane of the sections. In Figure 16A a wire frame surface is used to reveal the injury zone within the spinal cord segment. The lesion can also be rendered semi-transparent to reveal this same anatomy, providing more details of the cysts at the expense of the lesion encompassing them (Fig. 16B and C). In Figure 16B, the addition of a "raft" or island of macrophages contained within a cyst is shown. Table 6 provides surface area and volumetric data derived from these two 3-D surface reconstructions.

These 3-D views show a lesion surface of complex shape. The surface area of the lesion in the two spinal cords shown are between 20-40% as large as the surface area of the entire segment of spinal cord containing it. The more severe injury occupies a volume approaching 18 % of the cord segment, the less severe injury approximately 6%. The more extensive regions of very small cysts could not be imaged at low power, and were not reconstructed.
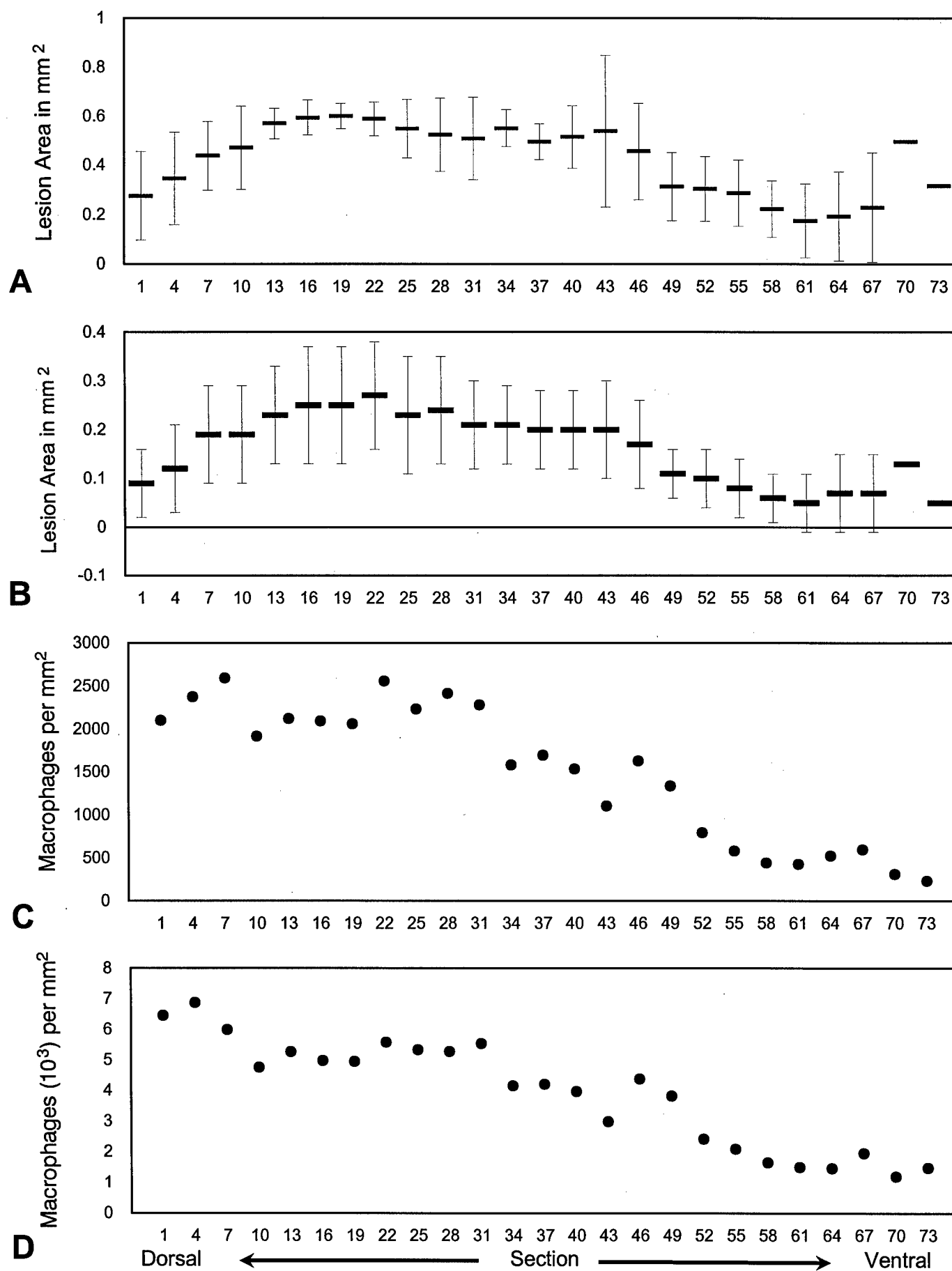
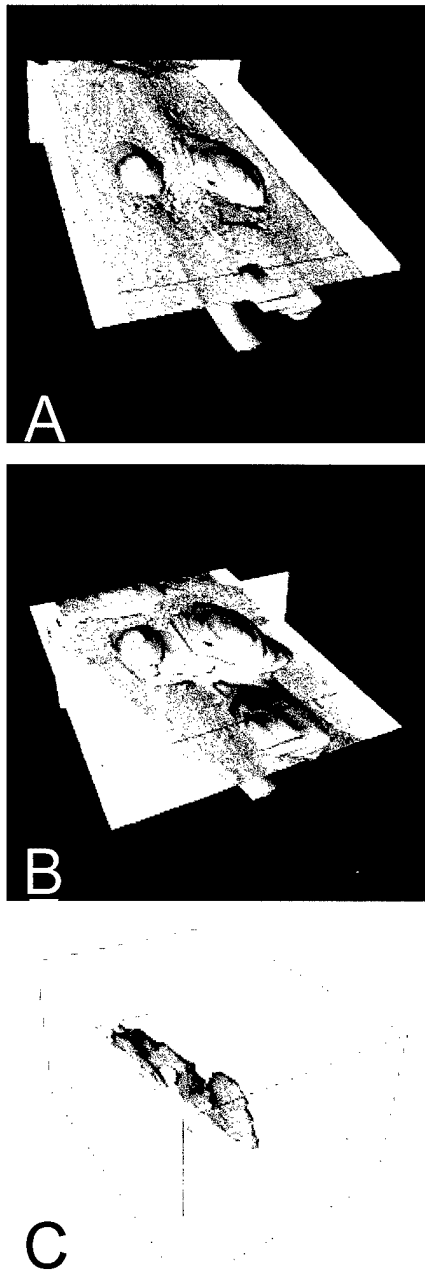**Figure 14** *Lesion area and macrophage density.*

Figure 15

Figure 16

Figure 15 *Registration of Surface reconstructions. (A) and (B) are 3-D surface reconstructions of the zone of injury superimposed within two orthogonal slices of the original data set. The lesion boundary was defined by ED1 labeled macrophages. The ventral surface of the cord is facing upward, rostral forward. Note the registration of the surface model within the histological section, and that the horizontal slice in (B) is more dorsal than in (A). (C) is a similar image, reconstructed from another injured spinal cord injury, oriented caudal forward, ventral up.*

Figure 16 *Surface Reconstruction of Digitized Images. (A) and (B) show surface reconstructions of the region of spinal cord injury defined by the boundary of labeled phagocytes. In A, the red wire frame model is the outside perimeter of the spinal cord segment containing the lesion. The most ventral sections have been removed, allowing an unobstructed view of the injury imbedded within it (rostral forward). In B, the same lesion as shown in A is visualized, but is made semi-transparent revealing the cystic structure (in red) within. The green mass within the large dorsal cyst is an island or raft of floating macrophages. This image has been rotated 180° along the long axis from that shown in A. In C, another reconstructed lesion containing cysts is shown by rendering the lesion surface semi-transparent. The lesion is oriented dorsal up and rostral forward.*

Table 6 Quantification of spinal cord segments, lesions, and cysts: comparative evaluation between 3-D surface reconstructions, geometric equations, and 2-D morphometry.

Rat #	Three Dimensional Morphometry[1]						Comparative Data[2]			
	A	B	C	D	E	F	G	H	I	J
	Cord Volume in mm^3	Cord Surface Area in mm^2	Lesion Volume in mm^3	Lesion Surface Surface Area in mm^2	Cyst Volume in mm^3	Cyst Surface Area in mm^2	Cord Volume[3] in mm^3	Cord Surface Area[4] in mm^2	Lesion Volume[5] in mm^3	Lesion Volume[6] in mm^3
Rat 1	9.2	46.3	1.7	20.2	0.2	9.2	9.4	30.1	1.1	4.3
Rat 7	14.3	62.5	0.9	13.0	0.1	6.9	17.0	38.3	0.9	1.1

1. The values in columns A-F are derived directly from 3-D surface reconstructions shown in Figures 9 and 10.
2. The values in columns G-J are derived from the application of different methods of quantification.
3. Volumes (V) shown are derived from a modification of the elliptical area formula for spinal cord area used by Blight (1985), where

$$V = [(\pi ab) \times h]$$

and a and b are one-half the major and minor axes of the ellipse (cord) and h is the length of the cord segment being measured.

Column G values are not significantly different from those in column A (P = 0.45, paired students' T, two tailed).

4. Surface areas (S) shown are derived from the formula for an approximation of an elliptical cylinder, where

$$S = 2\pi \left[\sqrt{\frac{a^2 + b^2}{2}} \, h + 2\pi ab \right]$$

and a and b are one-half the major and minor axes of the ellipse (cord) and h is the length of the cord segment being measured.

Note: The values in column H are not significantly different from those in column B (P = 0.12. paired students' T, two-tailed).

5. The volume of the lesions for each rat were derived from adding all surface area data obtained by 2-D morphometry for serial histological sections x the section thickness. That data (column I) is not significantly different than the data in column C (P = 0.5, paired students' T, two-tailed).

6. This volume (V) data is derived from a formula based on a frustum model of the spinal cord lesion, after Bresnahan et al. (1991),

$$V = 1/3h[B_1 + B_2 + (B_1 * B_2)^{1/2}]$$

where B_1 and B_2 are the areas of the cone bases, h is the distance between bases.
The volumes in column J are not significantly different from the data shown in column C (P = 0.45, paired students' T, two-tailed).
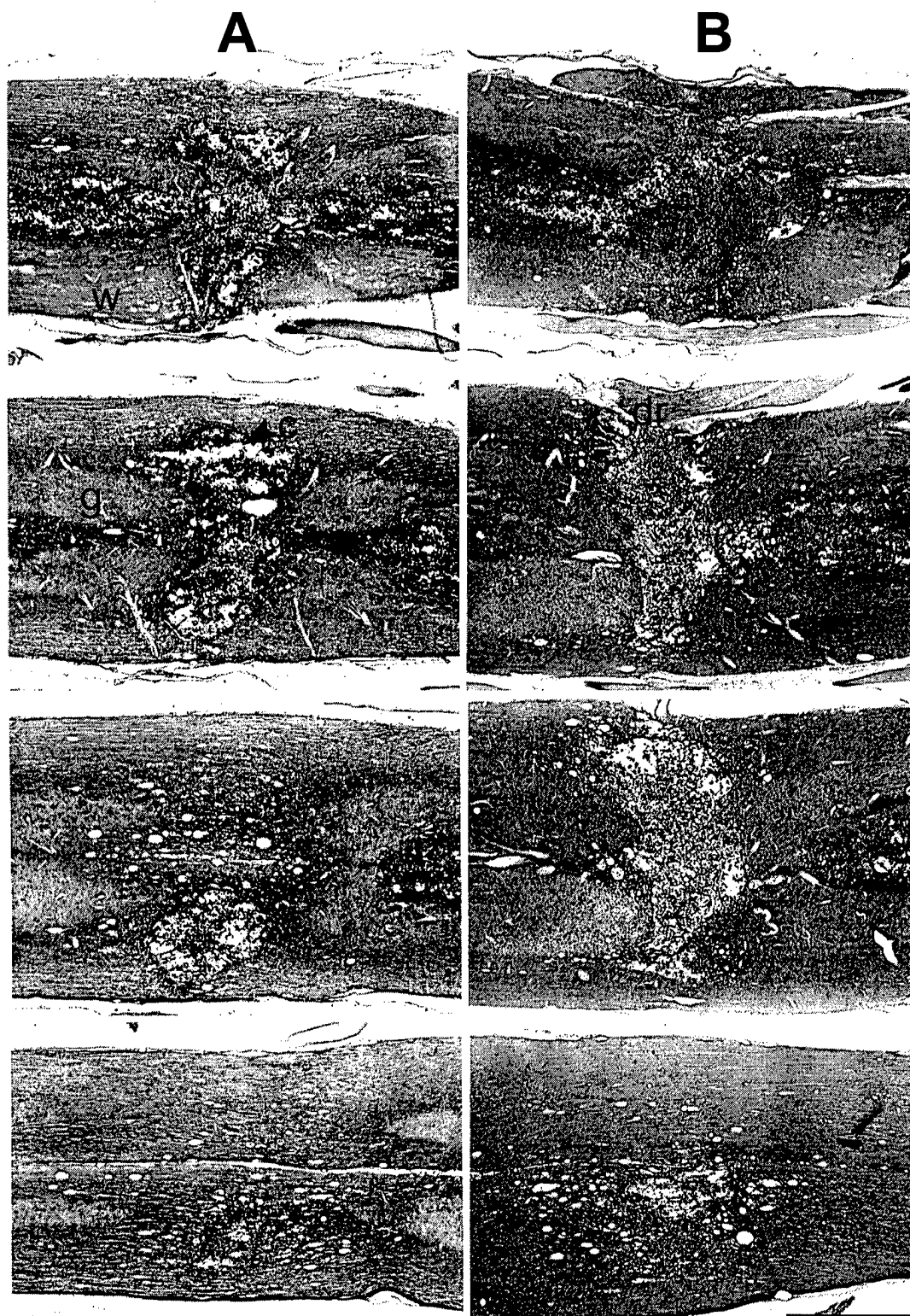
C. Electric Fields on Secondary Injury

<u>The anatomy of the subacute lesion at three weeks post injury</u>

In all spinal cords, the most numerous cell type occupying the lesion was the macrophage. These cells were of typical size (12-16 μm diameter), vesiculated, and positive for the surface antigen, ED1. Given the dorsal approach, followed by a dorsal compression of the spinal cord, the lesions were largely located in the dorsal half of the cord. In two controls and two experimentals the lesions were so shallow that the ventral half of the spinal cord was largely undisturbed. Such "intact" spinal cord parenchyma showed well defined cell borders, stained effectively with hematoxylin, was free of macrophages and large fluid filled cysts. In all spinal cords, the central lesion was largely defined by fluid filled cavities (cysts), clots of blood cells, and macrophages. These latter cells were so localized that it was not difficult to scribe the boundary of the lesion, delineating it from the immediately adjacent and relatively undamaged grey and white matter. The longitudinal extent of the central lesion was approximately one vertebral segment or less (measured in citation 104). Within the lesioned area, islands of intact parenchyma could be found, and within the larger cysts, even "rafts" of macrophages were observed (see also citation 16). Extending away from the central region were cavitated tracts of white matter undergoing Wallerian degeneration. (Curiously, however, caudal projections of the corticospinal tract appeared remarkably intact.) At the time point studied damaged white matter nearest to the central lesion was, as well, choked with macrophages and markedly cavitated, appearing similar to the central lesion (Fig. 17A). Such macrophage accumulation and cavitation was much less apparent with distance from the central lesion. The most severe degeneration of white matter projections were rostral to the lesion (i.e., the dorsal columns and lateral sensory columns). The same long tracts were largely intact, and free of cavitaties caudal to the lesion. Figure 18 shows two typical examples of lesions in an experimental and a control spinal cord. We emphasize that we were unable to detect differences in the anatomy of these two groups, either during blinded evaluation or later by unblinded review.
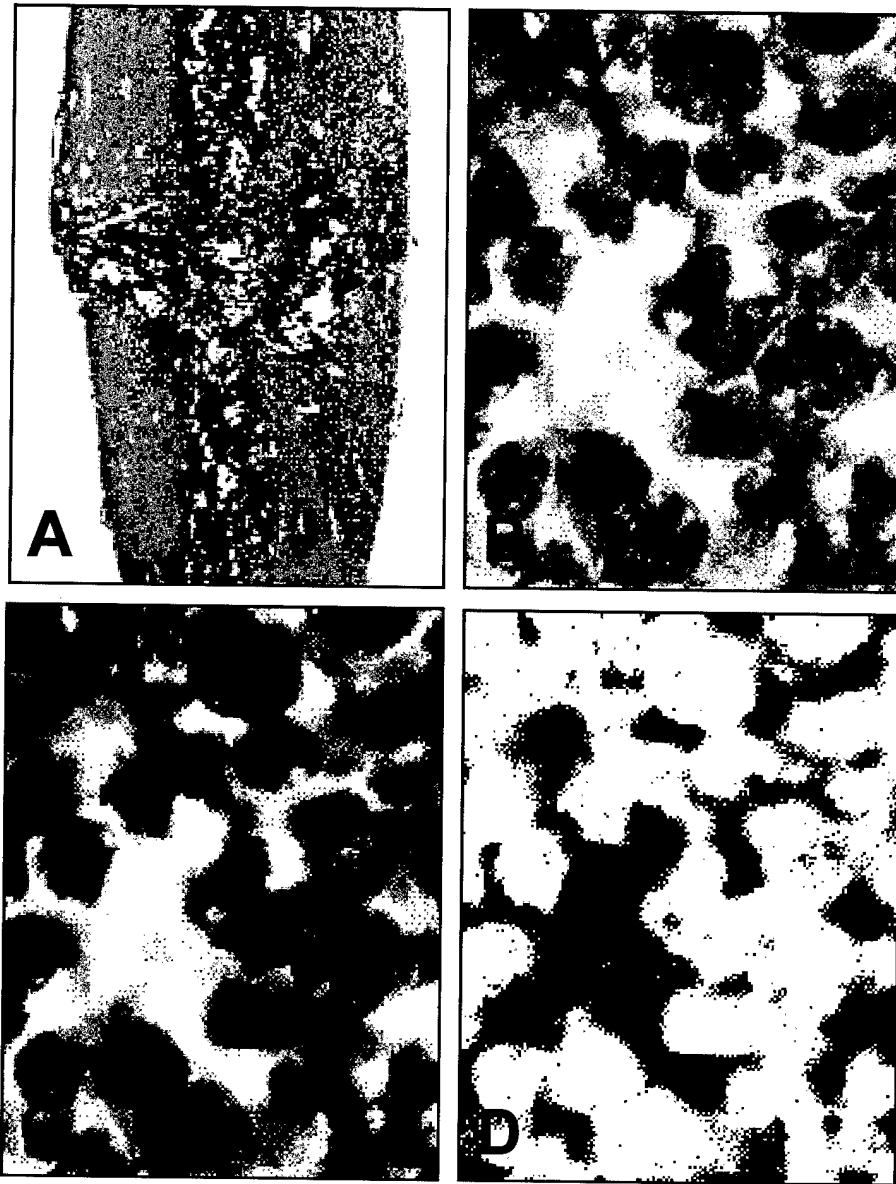
Figure 17 Computer Morphometry (A) Longitudinal horizontal section of a rat spinal cord, oriented rostral to the top and caudal towards the bottom. The section is approximately 2 mm at its widest. This digitized image is as it appears on the video monitor following capture from the histological section. The dark purple/brown staining is the region of labeled macrophages delineating the centrally located spinal cord lesion. The spinal cord is counter-stained with hematoxylin. Such compression lesions at 3 weeks were usually cystic (C). (B) A similarly digitized high magnification view of individual ED1 labeled macrophages within the injury site of the spinal cord shown in A. Note the vesiculated appearance of some of the labeled phagocytes and the background staining of parenchyma. Scale Bar = 20 μm. (C) The identical image shown in B. The pixel values showing the overall range of brown staining (labeled macrophages and portions of macrophages) has been converted to a single pixel value (green) in preparation for binarization and computer assisted counting. Note the exclusion of the blue stained parenchyma shown in B. (D) The identical image shown in B and C. To facilitate counting, the image is binarized where the pixel value of 1 (white) is ascribed to the macrophages and all other color values = 0 (black). The computer assisted program of counting then derives the unit area in white pixels. At any given magnification, the unit area in pixels is further converted to the unit area in micrometers.

Figure 18 *Experimental and Control Spinal Cord Injuries. The four images in column A are individual sections of the same experimental cord showing the progression of a compression lesion from dorsal (top of page) to ventral (bottom of page), and similarly in B, a control cord. Both cords are oriented rostral to the left and caudal to the right. Note in both spinal cords the dark regions of labeled macrophages in white and grey matter is usually localized in and around cysts at the site of compression injury. Note the characteristic "+" shape of the lesion in the most dorsal images, showing heavy macrophage labeling, and cysts which extend into the dorsal columns. In more central, and ventral sections, the lesion is less extensive, and more localized to the injury area. This is due to the dorsal focus of compression. The scale bar at the bottom of column B is for both cords and = 1 mm, w = white matter, g = grey matter, c = cysts, and dr = dorsal root.*
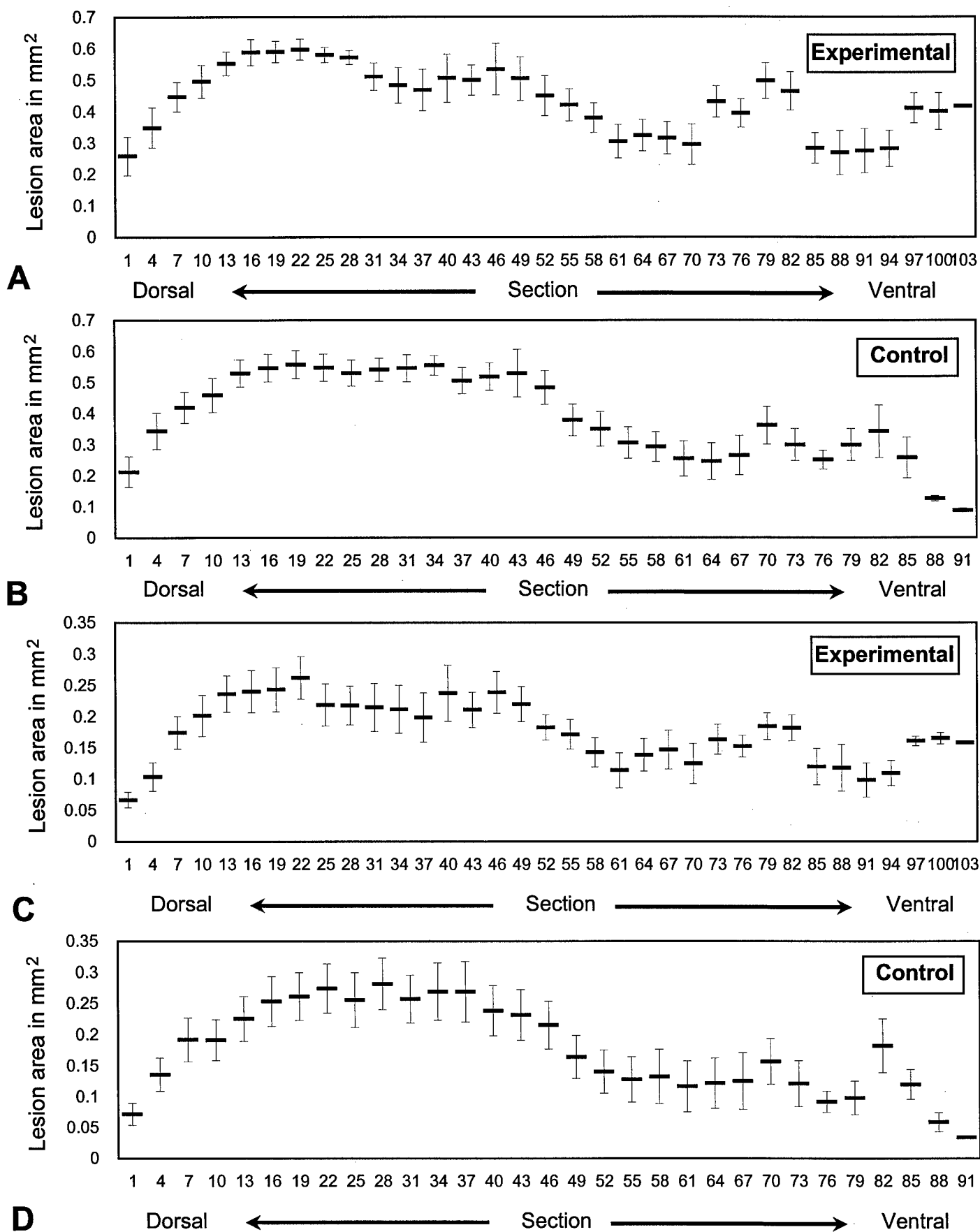
Defining the Lesion

As mentioned, the boundary or perimeter of the injured region of spinal cord was discernible due to heavy labeling by ED1 allowing a determination of its unit area. Furthermore, most lesions contained variable amounts of relatively intact spinal cord parenchyma. Thus, one could define the lesion in two ways: 1) the overall region of damaged parenchyma containing cysts and aggregations of macrophages within a defined perimeter, and 2.) this same region minus the unit area of relatively intact and normal appearing parenchyma[104].

In experimentally treated spinal cords, the mean areas of lesions within any one histological section ranged from about 0.26 mm^2 to 0.60 mm^2 including regions of "intact" tissue (Fig. 19A). When these regions are excluded from the calculation of unit area, the range was 0.07-0.26 mm^2 (Fig. 19C). In control spinal cords, these unit areas were 0.09-0.56 mm^2, and 0.03-0.28 mm^2, respectively (Fig. 19B and D). When the mean lesion areas per section are statistically compared, there is no difference between the data sets ($P = 0.11$, lesion including normal appearing parenchyma; $P = 0.98$, lesion excluding normal appearing parenchyma. Unpaired Student's T, Table 7). Thus, lesion size, independent of how it was defined, was not affected by the experimental treatment.

Macrophage numbers and their Density

As mentioned, the largest accumulation of phagocytes was in the dorsal hemisphere of the spinal cord, corresponding to the dorsally located lesions. Their mean numbers in the central region of the lesion ranged from about 800 to 1500 cells per 15 μm thick histological section. The maximum density of these cells was approximately 6000 macrophages per mm^2 in the control population and 5800 cells per mm^2 in the experimental population - excluding regions of intact parenchyma from the calculation of the unit area of the lesion.

Figure 19 A and B show the mean and standard error per section of the lesion area in the control and experimental groups when the lesion is defined as including the macrophage stained areas, and all cystic areas. C and D show the same as A and B, however, the lesion is defined as excluding hematoxylin stained "intact" parenchyma

(The density of macrophages was about 50% less when regions of intact parenchyma were included in the calculation.) Figure 20 provides the numbers and unit area of macrophages

		CONTROL		EXPERIMENTAL		Student's T, unpaired[6]
		N	Mean ± SEM	N	Mean ± SEM	
A	Lesion[1] Area (mm^2)	12	9.7 ± 0.9	12	11.1 ± 1.1	P = 0.33
B	Macrophages Area (mm^2)[2]	12	2.6 ± 0.5	12	2.4 ± 0.4	P = 0.80
	Percent (%)[4]	12	26.4 ± 3.7	12	22.0 ± 3.0	P = 0.36
C	Cysts and Cavities Area (mm^2)[2]	12	1.9 ± 0.3	12	2.1 ± 0.3	P = 0.60
	Percent (%)[4]	12	18.6 ± 2.0	12	18.3 ± 1.3	P = 0.91
D	Cysts and Macrophages Area (mm^2)[3]	12	4.4 ± 0.7	12	4.5 ± 0.5	P = 0.96
	Percent (%)[5]	12	45.0 ± 3.8	12	40.2 ± 3.3	P = 0.36

Table 7 A comparision of control and experimental lesions for all spinal cords

1. Row A shows the mean unit area in mm^2 of the lesion [defined to include macrophage accumulation, cysts, and relatively "intact" parenchyma (see methods)].

2. The unit area in mm^2 of macrophage accumulations (row B) and cavitation (row C) respectively.

3. The unit area in mm^2 of macrophage accumulations and cavitation (row D).

4. The percent of macrophage unit area per unit area of the lesion (row A), and the percent of cystic cavities unit area per unit area of the lesion (row A).

5. Total percent of cavitation and macrophage accumulation unit area per lesion (row A).

6. The statistic used was the two tailed, unpaired student's T: comparing experimental vs. control means. Note there is no significant difference between these groups.

determined for both experimental and control lesions, while Figure 21 illustrates the densities of these cells (in both groups), defining the lesion in both ways. Statistical evaluation of the mean areas of macrophages per section failed to demonstrate a difference between these groups (P = 0.80, unpaired Student's T, Table 7).

Cysts and Cavities

We quantified the amount of cystic cavitation of the central hemorrhagic lesion for all spinal cords. In the control population, cysts occupied a mean of 1.8 mm^2, SEM = 0.3 mm. In the experimental population, 2.1 mm^2, SEM = 0.3 mm^2. Figure 22 provides the means and standard errors of areas of cystic cavitation per histological section for all spinal cords studied. There was no statistical difference between these values when experimental and control groups were compared.

## D. Electric Fields and Polymeric Guidance Channels

General Procedure

Animals tolerated the surgical procedures well, and the minor mortality was not significantly different between the experimental and control groups. All stimulator units were functional at the time of their removal (the battery would not be exhausted for another week or more of continuous operation). Though both ends of the tube were visually confirmed to be imbedded in the parenchyma of the spinal cord at surgery, in 5 cases (4 control, 1 experimental), one end worked out of the cord at the dorsal incision allowing evaluation of only one end of the guidance channel. The number of ends of the channels that remained imbedded in spinal cord parenchyma at the end of the experiment is given in Table 8. In nearly every case, longitudinal horizontal sections defined where the walls of the silastic tube had been. Sections were cut at 15 μm, and the thin sheet of silastic remaining as the
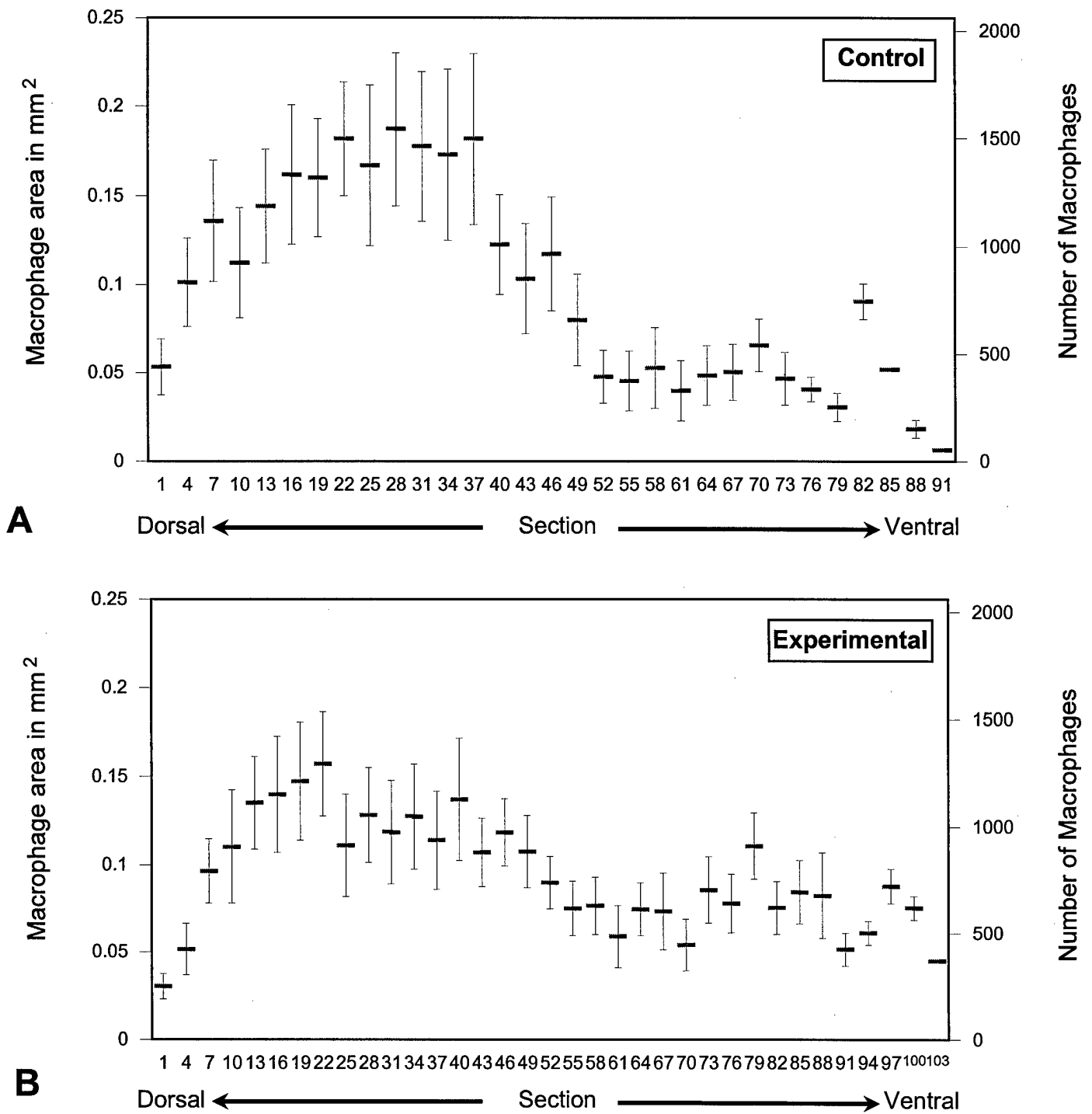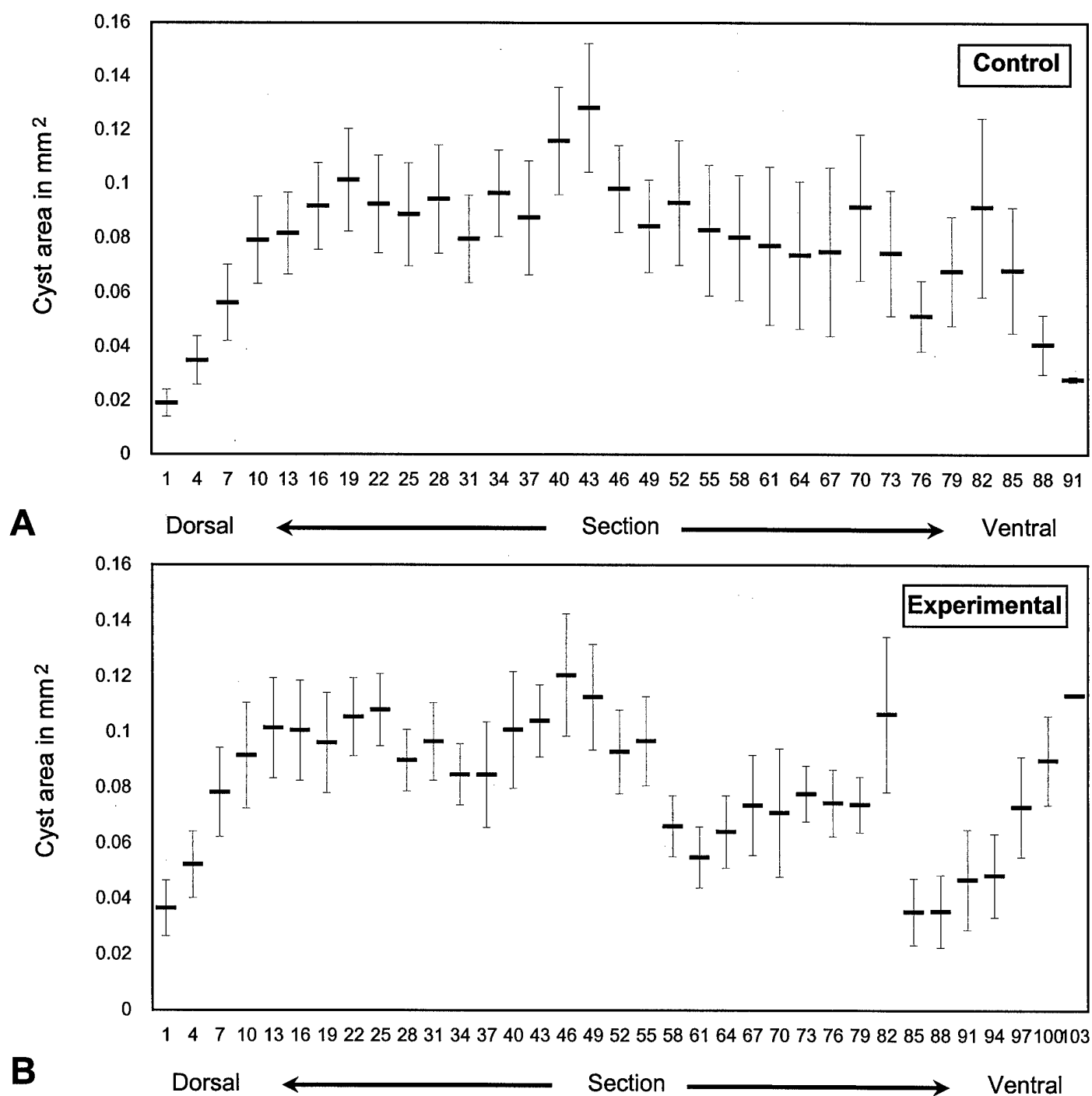
Figure 20 A and B show the mean and standard error per section of the macrophage area and macrophage count in the control and experimental groups respectively
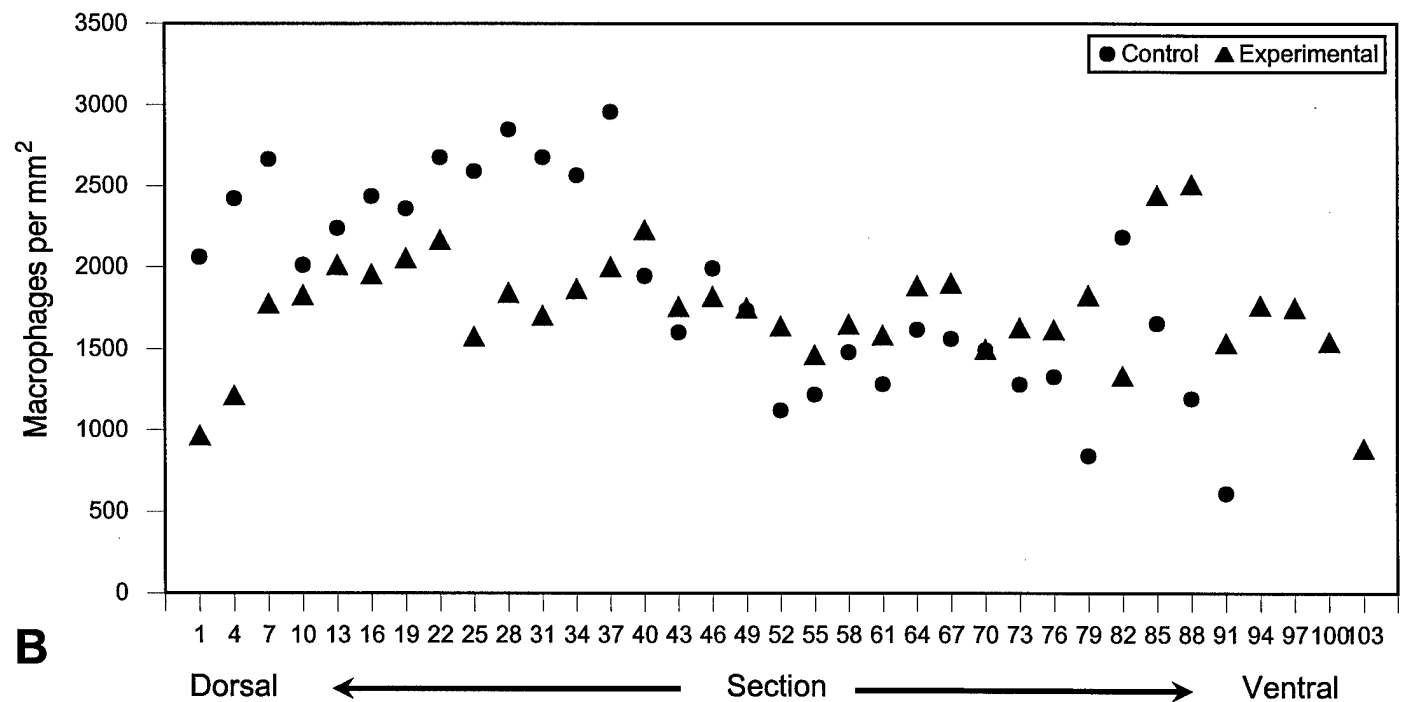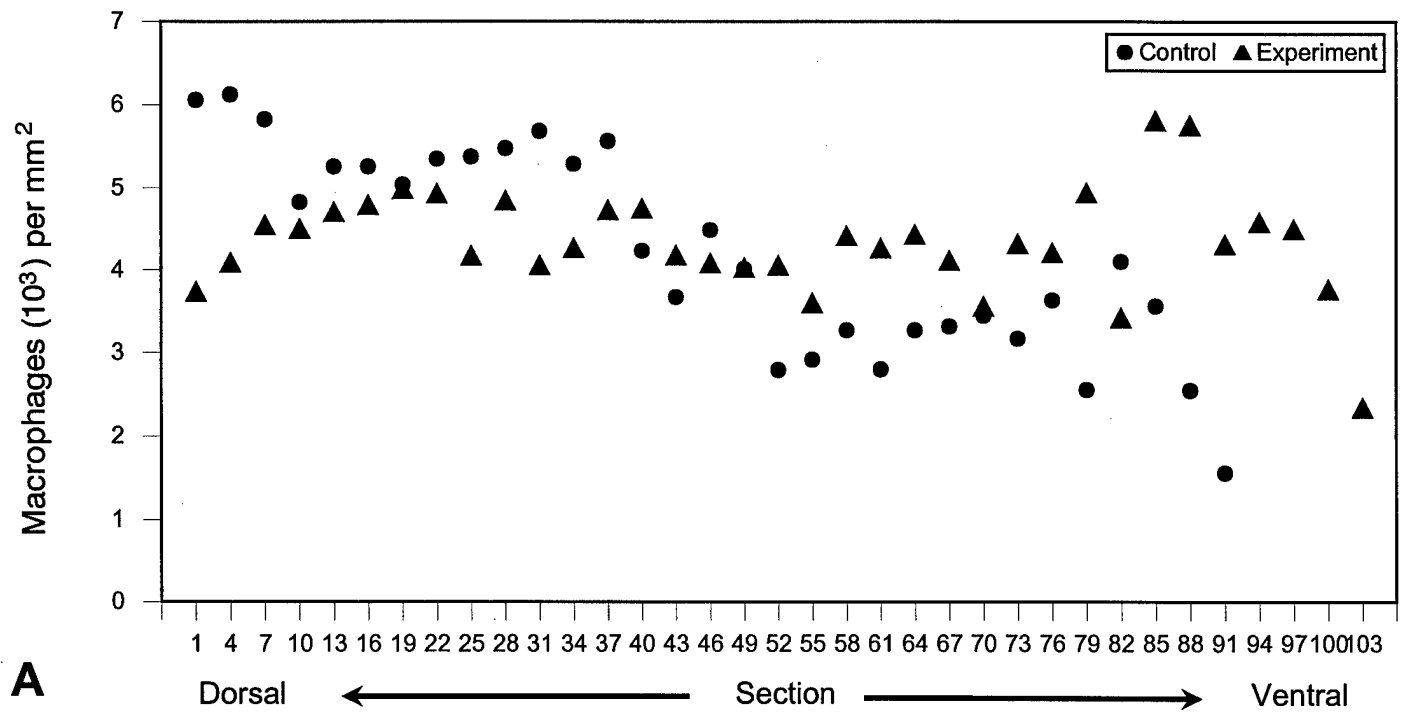
Figure 21 *A shows the number of macrophages per mm2 when the lesion is defined as the area composed of macrophages and cysts. B shows the number of macrophages per mm2 when the lesion is defined as above, but also including well stained "intact" parenchyma*

Figure 22 *A and B show the mean and standard error per section of the cystic area in the control and experimental groups respectively*

"wall" on either side of the tissue plug was usually lost during tissue processing for histology (Fig 23 and 25). During the first week after insertion, conventional histology confirmed that the hollow tube had filled for a distance of 1-2 mm with blood, loose connective tissue, and a more dense material, probably formed from clotted blood. By two weeks to one month post surgery, this forming plug of tissue contained many types of cells typically found in penetrating CNS injuries [10,12,16,104] including endothelial cells, macrophages, fibroblasts, and astrocytes, and their associated extracellular matrix (ECM) (Fig 23 A, C). By two months, the tissue plug was dense and usually extended far into the tube on both ends (Fig 25). The insertion of the silicone tube causes substantial damage to the delicate CNS tissues. A cavitated and vascularized "scar" tissue surrounded the tubes for a variable distance of up to several hundred microns rostral and caudal to its ends , with less tissue damage observed along its sides by two months post surgery. This scar tissue appeared similar to the tissue that intruded into the tube's open ends (Fig 23 B) and typical as well of the cicatrix described in other studies of spinal injury [10,16,68,81,121,123]. Though the scar tissue "plugs" sometimes extended deeply (ca. 2 mm) into the tube, in no instance did they meet at its center. In a few cases, a plug of tissue did not form within the end of the tube, the end being sealed with the capsule of scar tissue forming around it (Table 8). The insertion of the tube caused considerable damage to particularly white matter tracts. The dorsal column was usually transected, accompanied by the focal dissolution and delayed separation of ascending and descending lateral tracts (Fig 24).

Table 8

.	# Cords	Both ends of tube in cord	One end of tube in cord	Total ends studied	Ends contain-ing tissue plugs	Sharp[1] ends	Blunt[2] ends	Statistic 3
Exp	20	19	1	39	30	16	14	P = 0.0023
Cont	16	12	4	28	20	2	18	

Appearance of tissue plugs within the guidance channels (anterograde fills).

1. Tissue plugs were slender and pointed (refer to Fig 6).
2. Tissue plugs were blunt and rounded (refer to Fig 4).
3. The difference in proportion between the cases in which tissue plugs were sharp vs. blunt was significant, Fisher's Exact Test, two tailed.

Anterograde Tract Tracing: Control Preparations

Fig 25 shows a tissue plug extending into one end of a guidance channel typical of those found within tubes that contained a sham electrode. Axon profiles were not observed within the tissue plug in 14 of the 16 control implantations. In one of the two exceptional cases, 3 axon profiles were observed within the plug of tissue inside the channel (in one end of the tube only). In the second case, only one poorly filled axon was attached to, and coursed along the wall of, a small blood vessel penetrating the channel's interior. Overall, the *shape* of the tissue plug that formed within control applications was similar. Like a cork in a wine bottle, the plug usually filled the inside diameter of the hollow tube and was smooth and/or blunt at its terminal end (Fig 25A and B). This was in contrast to the shape of the tissue plugs that formed in most of the electrically facilitated implants (Table 8).
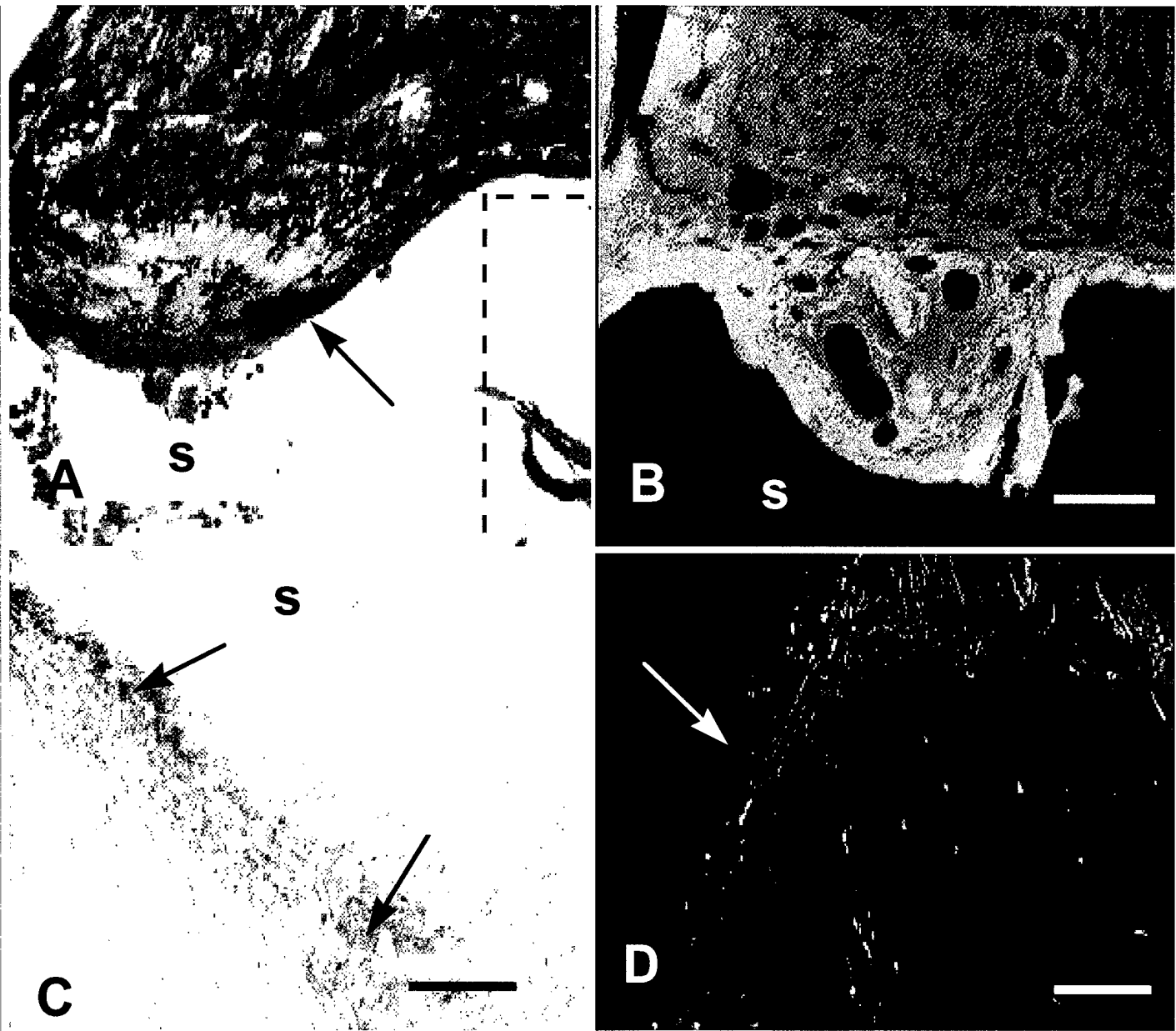
Figure 23 *Tissue formation within the guidance channel, one month post surgery. In A, the arrow points to a bulge of spinal cord "scar" tissue which protruded slightly into the open bore of the implanted guidance channel. The walls of the channel (hatched line) were invariably lost during histological preparation (refer also to Fig. 25 A). The blue/green stain (Masson's Trichrome), reveals the collageneous region of scar tissue, produced by fibroblasts which moved into the compromised CNS tissues. The space inside the channel is marked (s). In B, bright blue/violet fluorescent illumination reveals that the character of the tissue protruding into the mouth of the channels was cystic and cavitated, appearing similar to the fibroglial scar that encapsulated the guidance channel (barrier/excitation wavelengths in nms = 495/AFCY475). The scale bar = 120 μm. In C, the arrows point to a band of GFAP positive staining that also encapsulated the implanted silicone guidance channel. Such reactive gliosis, together with fibrous scar (lower left corner, and A.) above produced by invading fibroblasts, is typical of penetrating injury to the mammalian spinal cord. GFAP monoclonal immunochemistry, neutral red background stain. Scale bar = 80 μm; for C and A. In D, the arrow points to a spinal root, unmistakable when labeled. All labeled roots were between 50-100 μm from the site of tetramethylrhodamine injection and were never observed near the site of implantation. The scale bar = 30 μm.*

Figure 24. *Transected columns of axons 2 weeks following surgery. The low magnification dark field montage in the center shows the region of spinal cord surrounding an implanted guidance channel (scale bar = 1 mm). The arrows point to plugs (p) of tissue beginning to intrude into the caudal (top) and rostral (bottom) ends of the tube by this time (refer to Fig 23A and 25). The two high magnification images at the top (A, B) were captured in the region of the termination of the ascending dorsal column, marked by a hatched circle. The bottom two images (B and C) were captured from transected descending lateral columns, the region marked as well by the hatched circle. Note the free "end bulbs" [36,121] and swollen retraction clubs. End bulbs and retraction clubs demonstrate that portions of these tracts, originally projecting towards the guidance channel, were so damaged by the surgery that their axons underwent focal dissolution and eventual separation, or were acutely transected by the implantation surgery. The scale bar in D = 40 µm, for A-D.*
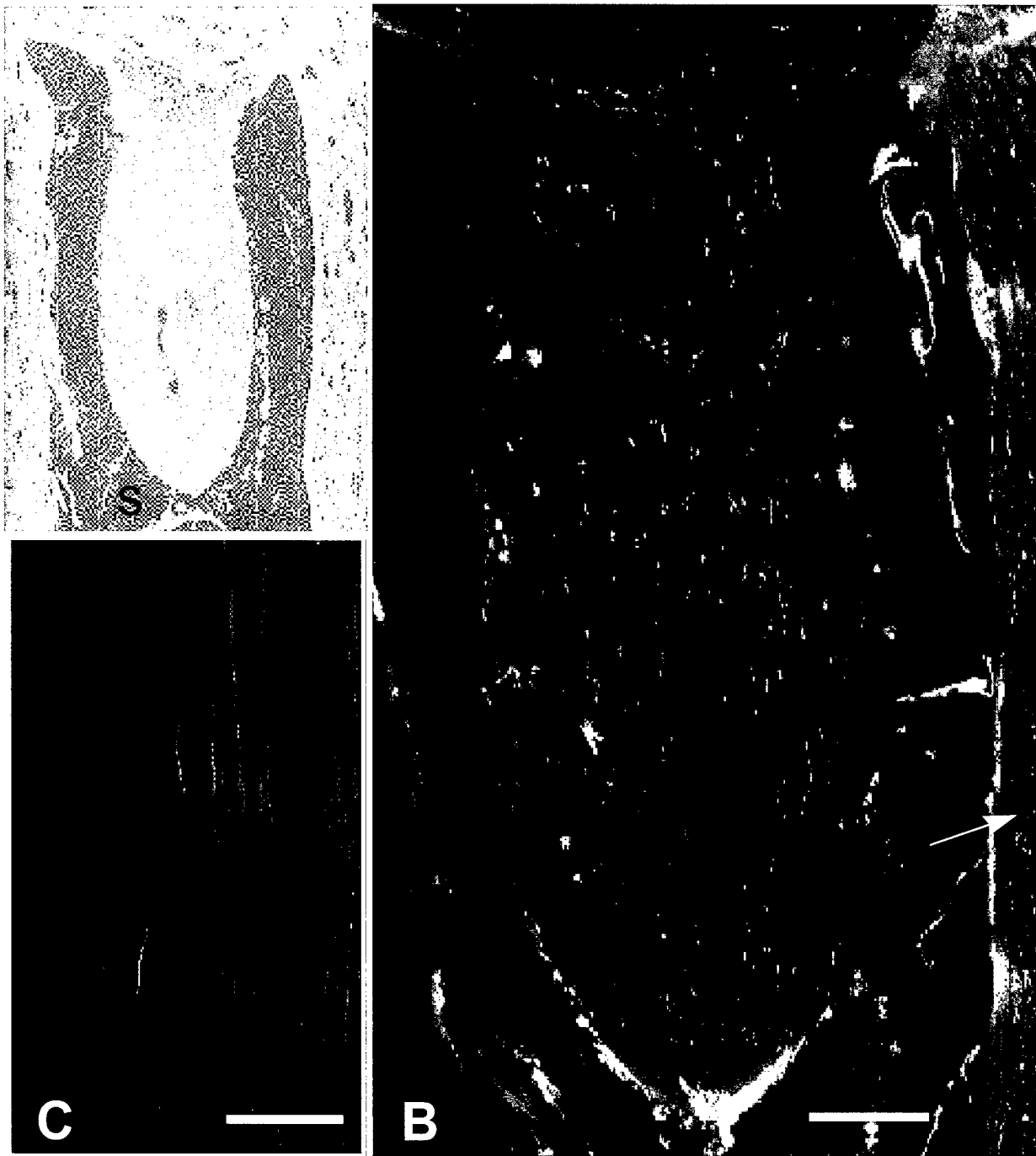
Figure 25 *Anatomical responses characteristic of sham treated (control) tubes two months post surgery. In A the tissue plug protruding into a guidance channel is shown. The space formerly occupied by the walls of the tube is approximated by the hatched lines. These walls were lost during histological processing. In B, a high magnification darkfield fluorescent montage of a different section of the same plug of tissue in A is shown. Note the complete lack of fluorescently labeled axons within it (compare with Figures 26 and 27). Injections of tetramethylrhodamine dextran were made approximately 1 cm from this location, and well filled long tract axons could be observed in the spinal cord surrounding the guidance channel (C, same section, approximately 100 µm to the right of the arrow shown in B). The scale bar in B = 125 µm, in C = 15 µm.*

## Anterograde Tract Tracing: Electrically Facilitated Implantations

Prior to describing the frequency and appearance of axons found within the experimental tubes, it is important to again emphasize that the shape of the tissue plug was markedly different in experimental applications compared to controls. In the experimental channels, the plug narrowed to a pointed, even relatively sharp, appearing tip. The plug did not usually fill the inside diameter of the tube, but tapered to a slender slip of a tissue, (compare Fig 25 and 27; Table 8). This difference in the shape of the scar plug was statistically significant between the two groups (P = 0.0023, Fisher's Exact Test, two tailed).

At one month post surgery, 4 of 6 experimental tubes did not contain axons within the plug of tissue, while 2 of these did . In both of these latter cases, regenerating fibers branched numerous times at their tips, projecting to the base of the plug, but not deeply into it (Fig 26). In 12 of 20 experimental tubes (2 months post surgery), axon profiles were clearly evident coursing throughout the entire length of the tissue plug inside the tube (Fig 27; Table 9). This difference in proportion between the experimental and control applications was statistically significant (P = 0.006, Fisher's Exact Test, two tailed; Table 8).

In four cases, approximately 10-20 axons penetrated deeply into the tissue plug. In the balance it was impossible to estimate the number of axons as they were too numerous, and clustered and intertwined together. Fluorescently filled axons entered the tube from both the outer (pial facing) margin as well as the central (gray matter facing) margin of the tube. These axons curved abruptly at the mouth of the tube, projected through the scar tissue that always surrounded it, and projected into the tissue plug.

On the basis of only the anterograde fills, it is likely that most axons entering the tubes were of spinal long tract origin. They were labeled intensely and appeared similar to the axons labeled within the adjacent tracts filled for long distances alongside of the channels. There was no evidence that peripheral axons were labeled by the anterograde technique except for those spinal roots at the site of dye injection (Fig 23D). There was no evidence of any axons entering the cord at the lesion (that might have become labeled by
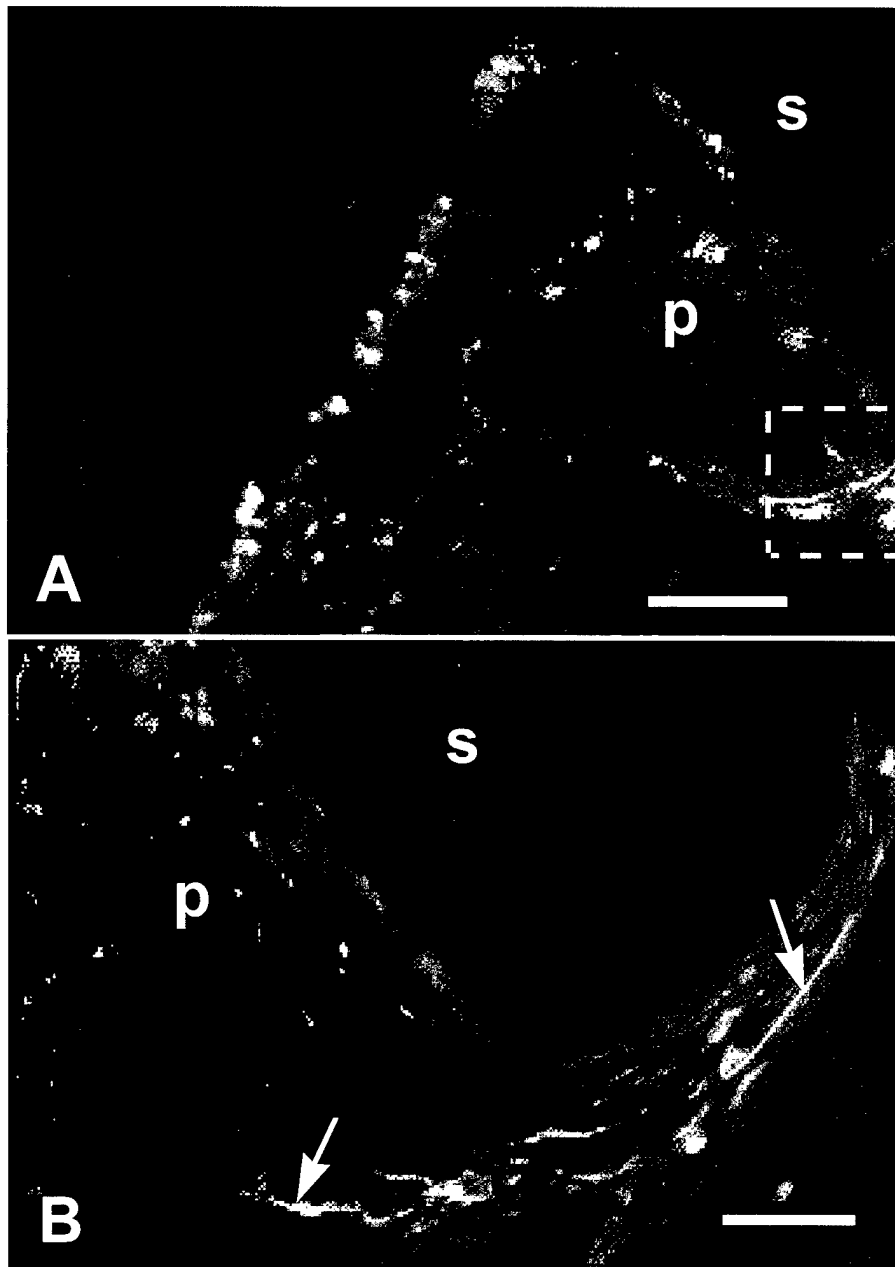
Figure 26 *Anatomical responses of an electrically facilitated guidance channel at one month post implantation. In A, a tissue plug (P), forming within the mouth of the guidance channel (refer to Fig 23) is seen in fluorescent darkfield. The space between the plug and channel wall is marked (s). A projection of rhodamine dextran labeled axons entering the plug (hatched box), is shown in a high magnification montage in B. The scale bar = 60 µm. In B, the arrows point to one of several branching axons that had projected into the scar tissue plug (p). The scale bar in B = 170 µm*
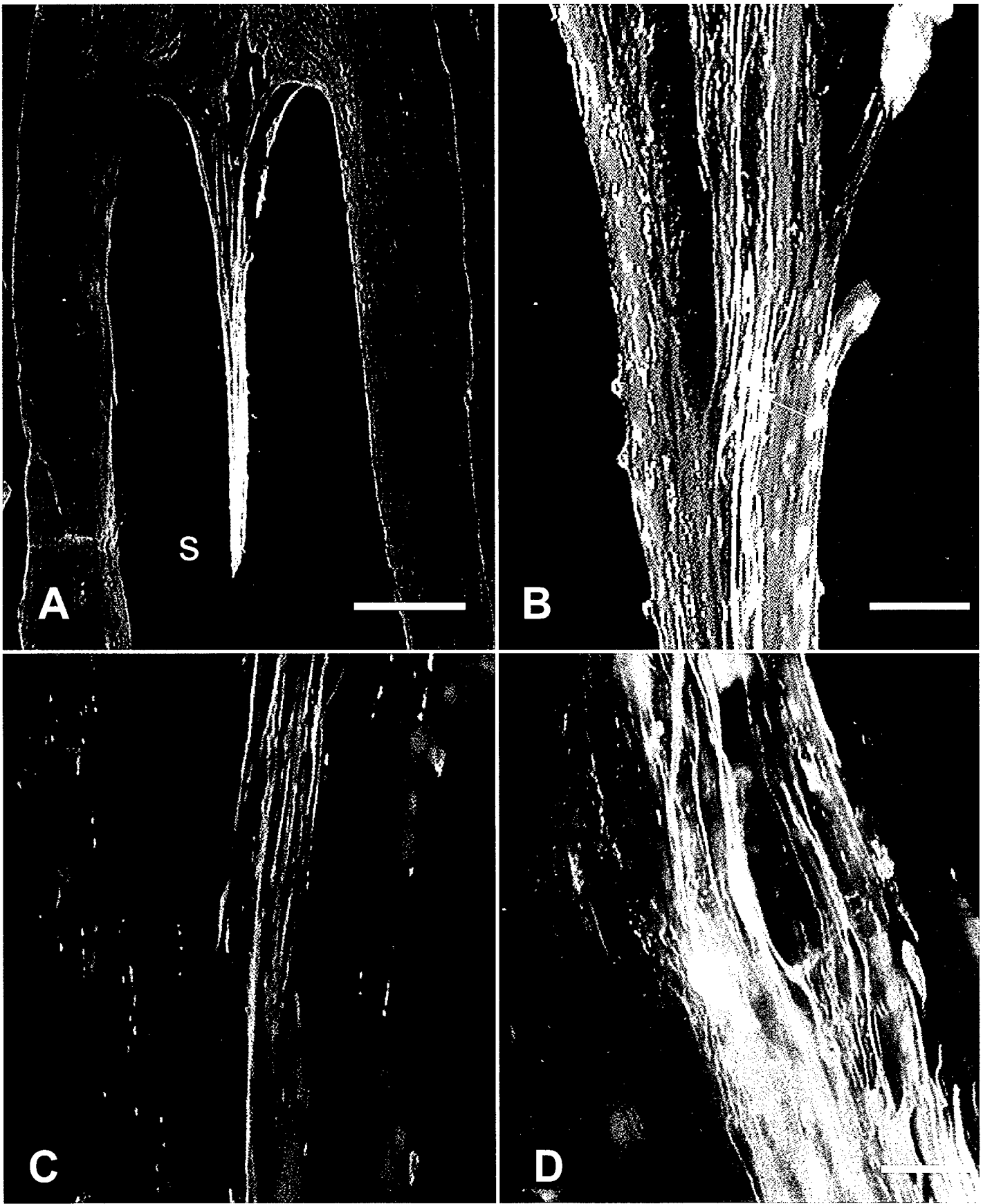
Figure 27 *Anatomical responses typical of electrically facilitated guidance channels at two months post implantation: Anterograde labeling of spinal axons. In A, a low magnification image of the sharp and thin plug of tissue protruding into the channel is shown (compare with Fig. 24). Higher magnification images B, C, and D are from the upper third, middle, and tip of the plug respectively (same section). Note the numerous labeled axons (arrow) traced to project from the mouth of the guidance channel to the end of the scar plug forming tangles of axons at the tip. The scale bars for A = 170 μm, B = 50 μm, and C and D = 30 μm*

extradural diffusion of the marker). This lack of extraneous labeling near the implanted tube was likely due to the small volume of marker injected into the spinal cord and the long distance from the lesion where the injection was made.

	Cords Studied	Axons in[1] both ends	Axons in[2] only one end	Total	Statistic[3.]
experiment.	20	2	10	12	p = 0.006
control	16	0	2	2	

Table 9.
*Occurrence of anterogradely filled axons within the guidance channels at 2 months post surgery.*
1. The tissue plug at both ends of a single implanted channel contained axons.
2. The tissue plug at only one end of the channel contained axons.
3. The occurrence of axons within the experimental guidance channels was significant (Fisher's Exact Test, two tailed).

Retrograde Tract Tracing

The retrograde tract tracing studies were undertaken in response to the impressive number of axons discovered entering the tubes in which DC current was pulled. Since therewas only one case of sixteen where more than one axon was found within the control tubes, these retrograde studies utilized only *active DC current applications* . This component of the investigation was attempted to further evaluate the origins of axons whose growth and guidance was facilitated by the extracellular voltage gradient.

The retrograde procedure worked well. The surface of the tissue plug within the tube was strongly labeled as the cells at the surface of the plug were exposed to the fluorescent marker confined to the interior of the tube (Fig 28A, insert a; and C). Cells surrounding the tube were not labeled as leakage of the dye was minimized by the insertion of crystals (and not of a solution of tetramethylrhodamine dextran) and the rapid sealing of the hole with silicone elastomer through which the crystals were inserted.

Most retrogradely labeled fibers could be traced towards white matter columns adjacent the tube on the pial facing side of the channel. Comparatively few fibers could be traced into
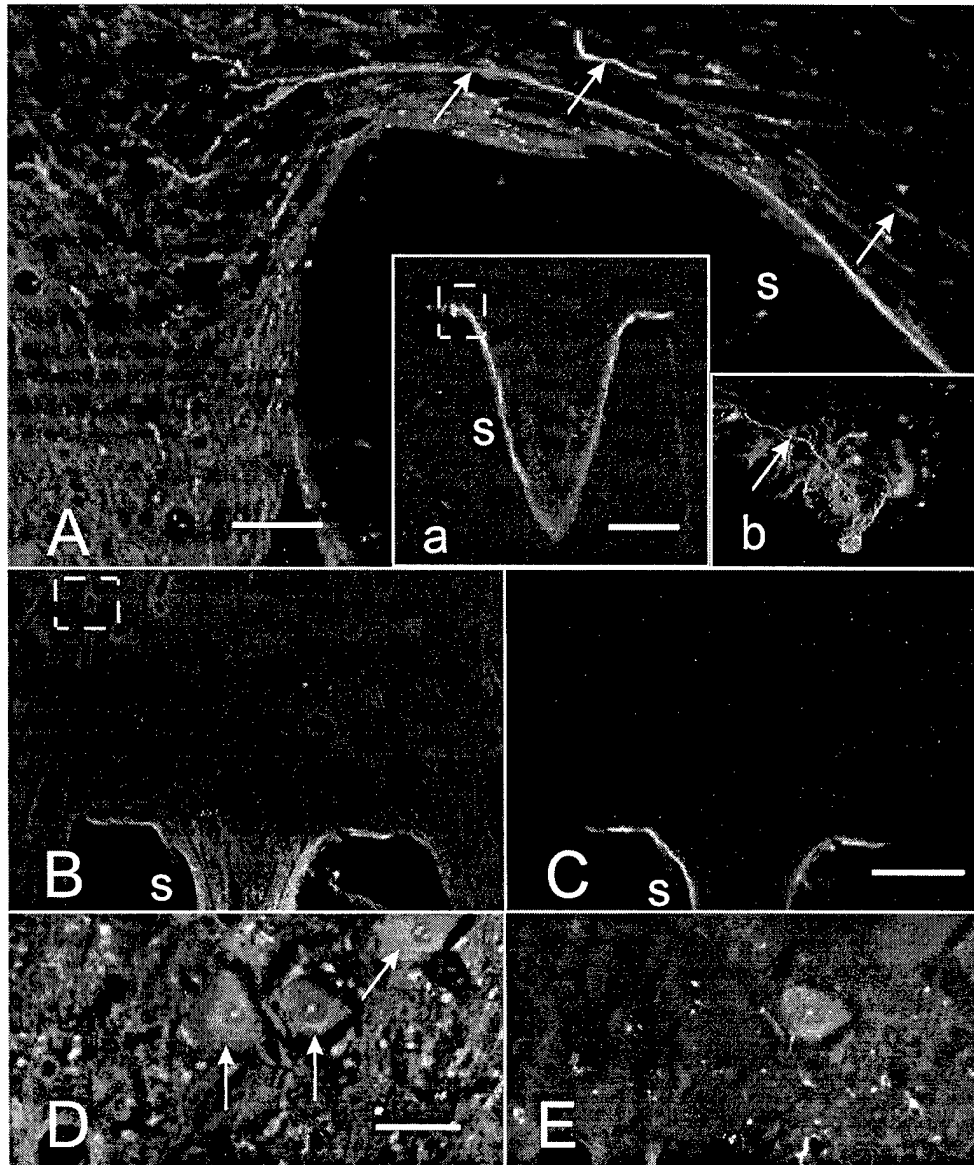
Figure 28 *Anatomical responses of electrically facilitated guidance channels at two months post implantation: retrograde labeling of spinal axons. The horizontal longitudinal sections in this figure, seen in darkfield fluorescent illumination, are similar in preparation to Figs 24 -26, however, labeling of axons was by retrograde uptake of the intracellular marker. Crystals of tetramethylrhodamine dextran were sealed within the center of the guidance tube approximately 14 hours prior to fixation of these tissues. In A, the arrows points to several retrogradely labeled axons at the mouth of the guidance channel, at the medial, or gray matter, facing aspect of the tube. Note the microcavitations of the scar tissue in this region. The space between the tissue plug and the channel wall is marked "s". The hatched box within the inset (a marks the region of the captured image seen in A. Note that only superficial cells of the surface of the tissue plug within the channel took up the dye confined inside the tube. The long expanse of a single axon shown in A projected out of the tube and caudally for approximately 200 μm in the adjacent gray matter. The brightly filled neuronal cell body in inset (b) was in the path of this projection, and out of the photographic field of A. This cell's arborization is out of the focal plane chosen to reveal the axonal process (arrow). In B, another low magnification view of spinal cord tissue adjacent the mouth of a guidance channel and tissue plug is shown in blue violet illumination, and in C with rhodamine specific illumination. Note that the marker labeled only the surface of the tissue plug inside the channel similar to A above. Numerous neuron cell bodies could be observed in the adjacent intact gray matter using blue violet illumination, three of which are shown in D (arrows). In this spinal cord, only two cell bodies were labeled with the intracellular marker applied within the tube. One of these is shown in E, within the group of neurons shown in D. Images D and E are identical views, however E was illuminated with fluorescent illumination specific for the rhodamine label. The cell bodies in D and E were located in the region marked with a hatched box in B. (The scale bars for A = 125 μm, B = 40 μm, for C and D = 20 μm.*

gray matter adjacent the medial (gray matter) side of the channels (Fig 28A). These axons made sharp bends within the scar tissue at the mouth of the tube, or made sweeping curved projections to enter the channel. In 5 cases, a few identifiable neuronal cell bodies within the adjacent gray matter were also labeled (Fig 28A, insert b; and E) though it was not possible to trace an individual axon to an individual labeled cell body through the scar tissue surrounding the implantation site. The labeling of neurons of gray matter adjacent the implanted tube was not observed in any experimental or control spinal cord filled by the anterograde technique.

E. Effects of DC Fields on Canine Paralegia

A total of 40 dogs were enrolled into the study meeting the strict entry requirements. Of these, only 1 dog was judged to have not met entry requirements by the final evaluation of medical records and the video taped neurological exam. A second dog was eliminated from the study due to its overall poor medical condition (emaciation, lack of owner compliance with home care). Four other dogs were lost to the study due to a lack of two or more of the early medical examination periods beginning just prior to surgery to, and including, the 6 week recheck exam. Table 10 lists the balance of 34 dogs, their experimental status, and other group characteristics. There was no statistical difference between the control and experimental group when these general characteristics were compared. Two additional dogs were lost to follow up after the 6 week recheck, one of them dying at 12 weeks to an unrelated heart ailment. Of the 34 dogs reported below, 15 % were of mixed breeds, 50 % were Dachshund, 12 % Spaniel, 6 % Welsh Corgi, and 17 % were of other pure breeds.

Table 10

	N	age	male/female	weight	vertebral level of injury	time to surgery[4] (days)
exp.	20	3.9±0.3[1]	11/20[2]	18.9lb±2.0[3]	T 12/13; range; T 11-L 2	4.28±1.10
con.	14	4.8±0.4	9/14	18.14lb±2.3[3]	T 12/13; range; T 11-L 3	3.18±1.17

Characteristics of Animal Groups
The characteristics for the OFS treated (exp) and sham treated (con) groups are provided. The age (1; in years) was not stastically different; P = 0.12, Students T test. The porportion of male to female dogs in each group was not stastically different (2; P = 0.72, Fisher's Exact Test). The average weight in lbs was not significantly different between groups (3; P = 0.86, Students T test). The average time from the onset of paraplegia to surgery was also not significantly different between the groups (4; P = 0.56, Students T test). The level of injury was nearly identical in each group.

Clinical Complications

Only one dog died during the course of this investigation, as mentioned This death was unrelated to stimulator implantation, in fact the animal had shown steady improvements in neurological function until its demise. The video records for this animal were scored with other animals, and its medical records reevaluated prior to the breaking of the experimental code. These data were included in the 6 week recheck period data set. There was no evidence of clinical complication during the 16 week period of OFS stimulation in any dog.

The safety of these various procedures is in part due to the numerous (>259) paraplegic dogs managed by the veterinary medical team in experimental clinical trials since 1987. In the present study, the OFS implant was located beneath the skin, and removed using general anesthesia following the clipping of the medical grade insulated stainless steel electrodes (a portion of the lead and PIIR electrodes were left in place). We did not experience any complications to arise from this procedure as well.

Radiological Observations

We observed no complications or untoward effects related to the radiographic procedures. There was no radiographic evidence of corrosion or migration of the electrodes or the OFS device in any of the study animals. Two principal types of myelographic changes were associated with intervertebral disc herniation: 1) Dorsal displacement of the ventral subarachnoid contrast column and 2) circumferential obliteration of the subarachnoid contrast columns due to cord swelling. Extensive spinal cord malacia was typified by uptake of (opacification) of contrast medium by the cord parenchyma, and 5 dogs were excluded from the study because of severe malacia.

Urological Exam and Local Reflex Response to Injury

Paralyzed dogs with upper motor neuron sequalae (UMN paraplegia) possessed intact urethral and detrusor reflexes indicating a UMN bladder. This was characterized by

an inability to empty the bladder completely—secondary to a failure to relax the urethral sphincter sufficiently during detrusor contraction. Obstruction in normal micturation due to UMN bladder syndrome also developed increased bladder compliance, detected by the CMG. Complete functional recovery of bladder control and micturation could have become evident on follow up exams, however we did not observe full functional recovery of urinary continence in any dog evaluated in this study. Rather, the Urodynamic evaluation was quite useful in identifying problems requiring therapy for urinary retention. For example, since the internal urethral sphincter is under α–adrenergic control, phenoxybenzamine (an α–adrenergic antagonist) was sometimes administered to facilitate the relaxation of the internal urethral spincter during micturation. In particular, the urodynamic evaluation proved useful in identifying animals with compromised lower motor neurons , or LMN sequalae. Such animals completely lack the urethral or detrussor reflex.

Local Reflexes were evaluated to judge the status of the dog, particularly if lower motor neurons were compromised due to continuing secondary injury—especially spreading myelomalacia. All dogs demonstrated normal to sometimes hyperascetic lower limb reflexes such as the myotactic and inverse myotactic stretch reflex, while the crossed extensor reflex could at times also be exaggerated[136,41]

Changes in Neurological Functioning

There were five types of examinations that provided functional data useful to the measurement of clinical outcome: Superficial Pain Appreciation, Deep Pain Appreciation, Conscious Proprioception, Ambulation, and the conduction of nerve impulses across the lesion as measured by SSEP. In every behavioral evaluation and at every time point studied, a larger proportion of OFS treated dogs received higher scores—*with no reverse trend* . The individual functions were sometimes statistically significant between groups at each time point evaluated, or showed a trend towards significance. Below we provide a comparative description of experimentally treated and sham treated controls at the 6 week

and 6 month recheck examinations and finally a comparison of the Combined Neurological Scores derived from these data.

Electrophysiological Tests for Recovered Conduction: The Somatosensory Evoked Potential

Evoked potential tests were used both to define neurologically "complete" animals at admission, and as a means to follow possible improvements in conduction. As described above, to enter this study, dogs could not show any evidence of an SSEP at the initial exam as part of the entry criterion. Evoked Potential measurement technique, equipment, and electrode functioning was checked at each examination by stimulation of the medial nerve of the forelimb as a control procedure. The CNS conduction pathway in continuity with the Median nerve of the forelimb would not be compromised by spinal injury at the thoracolumbar area. Fig. 29 B, D, and F shows a typical example of a median nerve stimulation, demonstrating a typical SSEP of approximately 15-20 ms latency. Fig. 29 shows a presurgical, 6 week, and 6 month SSEP electrical record (Fig 29 A, C and E respectively) demonstrating the complete lack of a cortical potential, characteristic of most dogs evaluated during the coarse of this study. Fig. 30A shows another negative baseline record (and its control median nerve record, B) and a recovered SSEP at 6 weeks and at 6 months. This recovery of the SSEP was recorded from an experimentally treated dog. Recovered potentials could be normal to late arriving in latency, sometimes showing dampened amplitudes. Recovering cortical potentials were on the order of 100 - 300 μV in amplitude and 25 - 50 ms in latency. In the experimental dogs, 3 of 15 dogs evaluated showed recovered conduction at 6 weeks and 7 of 17 evaluated at the 6 months recheck showed a recovery of conduction through the cord injury. In the sham treated group, a cortical potential was observed in 2 of 13 dogs studied at the 6 weeks recheck, and in 2 of 14 dogs evaluated at the 6 months recheck period. (For various practical reasons, including sensitivity to anestheia, every dog in the study was not able to undergo evoked potential

testing at test period). Though the number of experimental animals recovering an SSEP was more than double that of the control group by the end of the study, this was not statistically significant given the low number of animals evaluated (P = 0.13, Fisher's Exact Test, Two tailed).

<u>Superficial Pain</u>

At the 6 weeks recheck period only 4 of the 20 experimental dogs did not respond to painful stimuli applied below the level of the lesion, while 10 of 14 control dogs were unresponsive. The proportion of dogs that recovered the ability to perceive superficial pain at the 6 weeks recheck period compared to those that did not, was statistically significant (P = 0.04, Fisher's Exact test, two tailed). This difference accompanied a strong trend towards significance in the neurological scores between the two groups (P = 0.06, Mann-Whitney, two tailed). Removal of high outlier scores from each group showed the cluster of data points near the mode to be statistically significant even at the 6 week recheck (P = 0.04, Mann-Whitney, two tailed). This difference in the response to superficial pain stimuli continued to improve in the experimental group so that the 6 month recheck period, 15 of the 18 OFS treated dogs showed a response to painful stimuli, while only 2 of the 14 controls did. This difference in proportion was strikingly significant (P = 0.0002, Fisher's
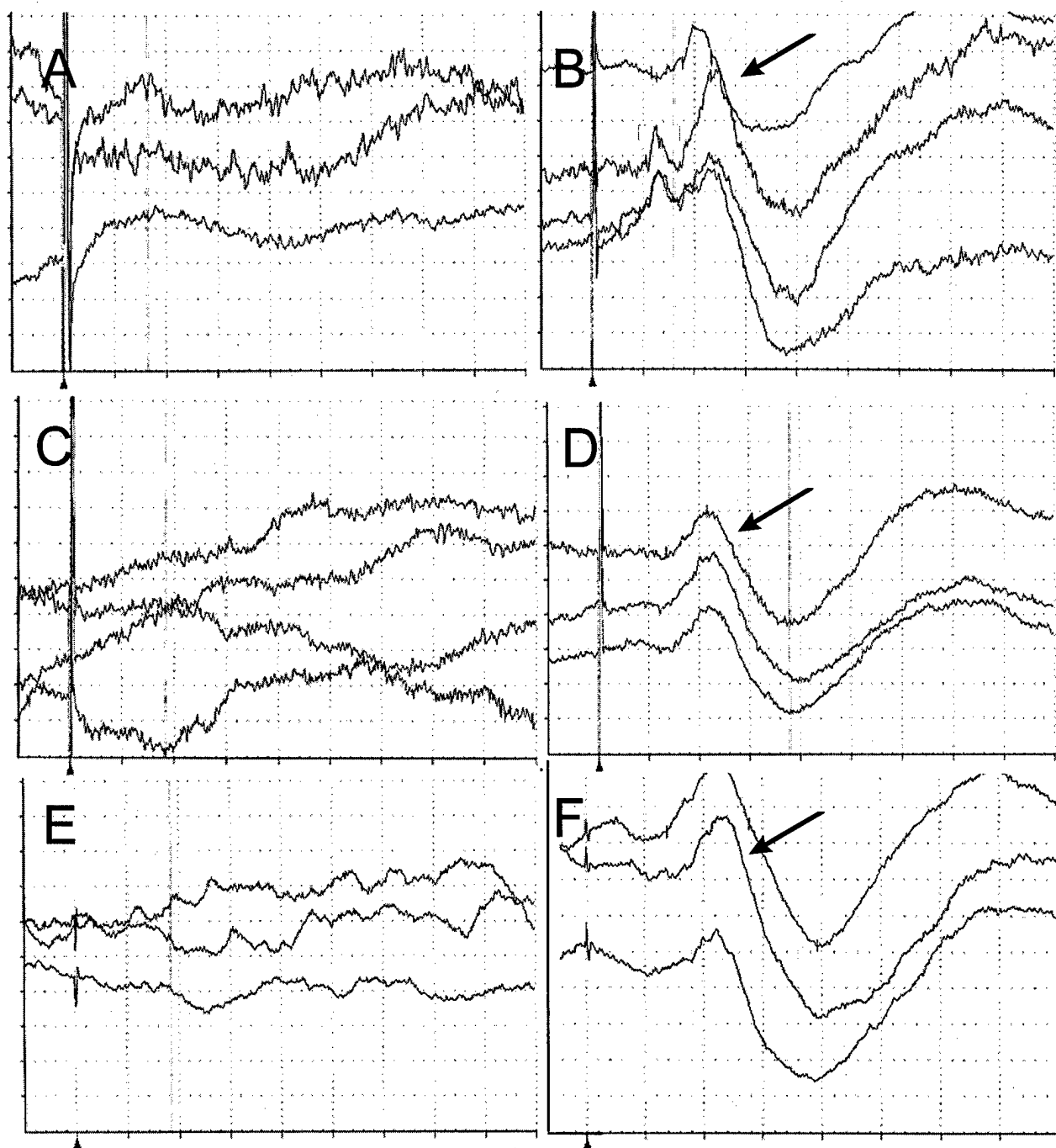
Figure 29 *Somatosensory Evoked Potential (SSEP) Records obtained in a Sham Treated Dog. This series of evoked potentials records obtained from sham treated dog (case # 680-292) shows the complete absence of conduction through the injured spinal cord following stimulation of the tibial nerve of the hindleg, recorded at the somatosensory cortex (see text). Three or four sets of averages (of 200 stimulations each) are shown for each electrical record. The small arrowhead in the lower left corner of each electrical record denotes the stimulus artifact. In A, the presurgery baseline measurement is shown, and in B, the cortical response to a medial nerve (forelimb) control stimulation is shown – obtained at the same measurement period as A. Records C and E were taken at the 6 week recheck and 6 month recheck respectively, and the median nerve control stimulation, performed at the same time, is shown adjacent them (D and F). Note the complete absence of cortical potentials at all three time points. These failures in conduction (A, C, and E) were typical of all SSEP records in all dogs that did not respond to tibial nerve stimulation. Cortical potentials in response to medial nerve stimulation of the forelimb (arrows) were typically of 20 ms latency. In records B - F, the time base was 50 ms/div. and in A, 30 ms/div. Amplitudes were 62 μV/div. in B - F, and 15 μV in A.*
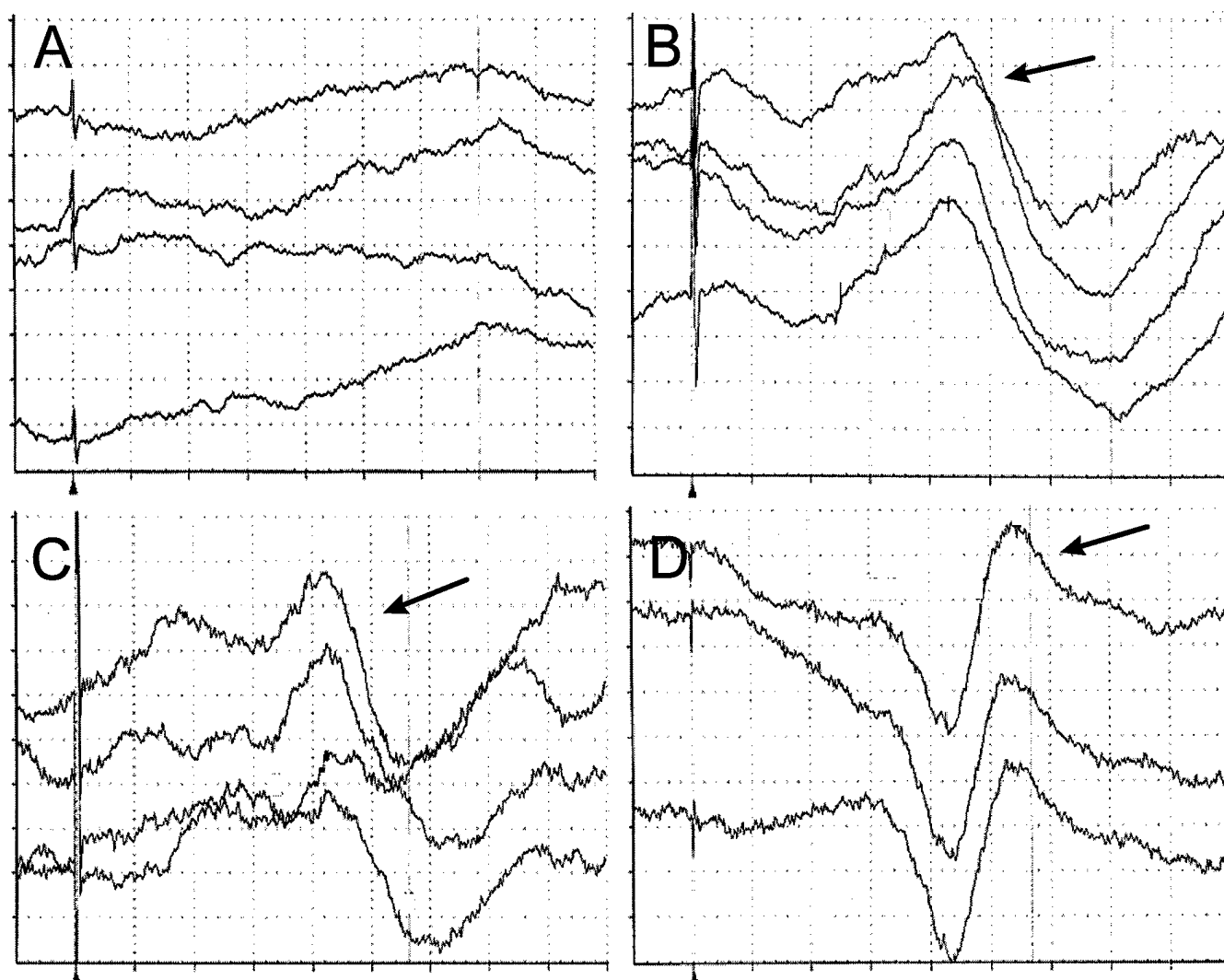
Figure 30 SSEP records obtained from a recovering OFS treated Dog. This series of evoked potentials were obtained from an electrically treated dog (case # 679-704). As in Fig. 29, A shows the presurgery baseline recording which did not reveal a cortical response to tibial nerve stimulation, and B shows the median nerve control record obtained at the same measurement period. Note the clear cortical potential of about 18 ms latency (arrow) in B when the conduction pathway was entirely rostral to the lower thoracic level of this injury. Evoked potential recordings in response to hindlimb tibial nerve stimulation are shown in C and D, taken at the 6 week and 6 month recheck periods respectively. Note the clear recovery of conduction through the lesion at these time points (arrows). All conventions are the same as in Fig. 29. The time base and amplitude in A, B = 3 ms/div., and 62 µV/div. respectively; in C, D = 5 ms/div., and 31µV/div., respectively.

Exact, two tailed), as was the comparison between the superficial pain neurological scores (P = 0.0009, Mann-Whitney, two tailed).

Deep Pain

A comparison of the neurological scores for deep pain recognition revealed a trend towards significance at the 6 week recheck period (P = 0.07, Mann-Whitney, two tailed). Removal of one outlier score from each group showed significance about the mode at this time point (P = 0.04). However, the perception of deep pain continued to improve in control dogs so that by 6 months, there was no longer a significant difference between sham treated and OFS treated animals (P = 0.11, Mann-Whitney, two tailed). Removal of one outlier neurological score from both groups at this time still revealed a trend towards significance in this behavioral evaluation (P = 0.07). Fig 31 summarizes these data for both Deep and Superficial Pain appreciation.


Conscious Proprioception and Ambulation

Though OFS treated animals always received higher average neurological scores in both the proprioceptive placing test and in blinded evaluation of ambulation, these differences were not statistically significant at either the 6 weeks or 6 months evaluation periods. Fig. 32 summarizes these data for both conscious proprioception and ambulation.

Total Combined Neurological Score

The total neurological score between the two groups, derived as an average of each of the 4 graded behavioral assessments (excluding SSEP), showed a trend towards significance even at the 6 week recheck (P = 0.08, Mann-Whitney, two tailed). The overall improvement in scores with time in the OFS treated group relative to the sham treated group was apparent, and the Combined Neurological Score between them reached statistical

significance at the 6 months recheck examination period (P = 0.047, Mann-Whitney, two tailed).
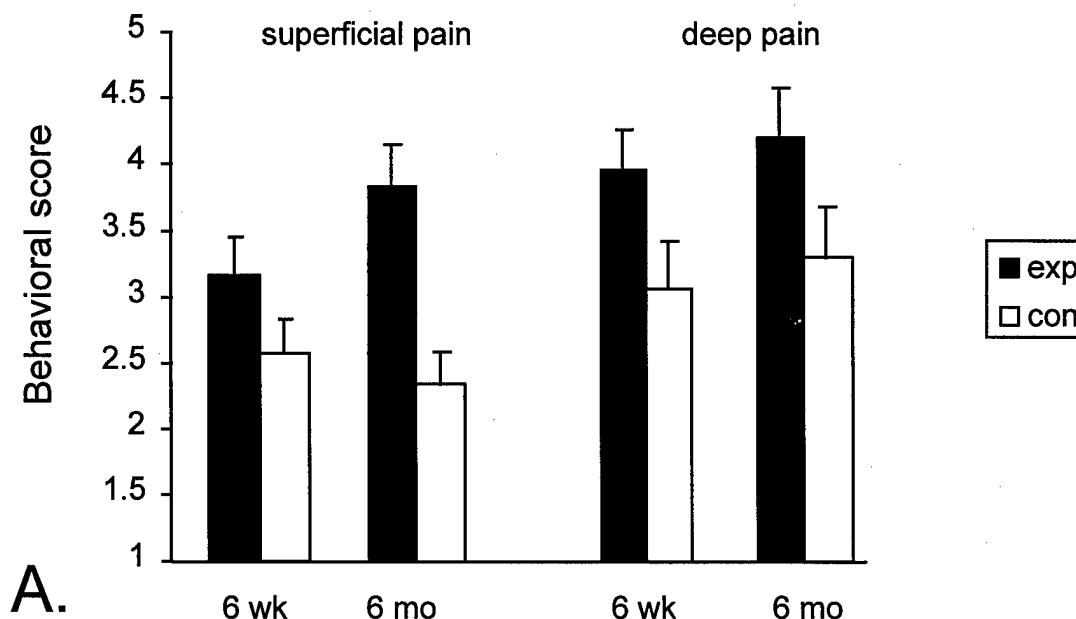
	group	recheck time	N[1]	$\bar{X}^2$	SD	range	statistic; p-value[3] OR[4]	
Superficial pain	exp.	6 wk.	20	2.2	1.3	1-4.2	**0.04**	0.06
	con.	6 wk.	14	1.6	0.9	1-3.8		
	exp.	6 mo.	18	2.8	1.3	1-4.2	∅	**0.0009**
	con.	6 mo.	14	1.3	0.9	1-4.0		
deep pain	exp.	6 wk.	20	2.9	1.4	1-4.8	**0.04**	0.07
	con.	6 wk.	14	2.1	1.3	1-4.8		
	exp.	6 mo.	18	3.2	1.6	1-4.9	0.08	0.11
	con.	6 mo.	14	2.3	1.4	1-4.8		

Figure 31 Behavioral Data : Appreciation of Deep and Superficial Pain. In A, the 6 week and 6 month behavioural scores for OFS treated (exp) and sham treated (con) dogs are graphed. Error bars are standard errors of the mean. The abcissa, the possible behavioural scores from the lowest (1) to the highest (5; see text), and the ordinate, the 6 week and 6 month time points. The table in B provides all of the data including the number of animals evaluated at each time point for experimental and control dogs. (1), the mean behavioural score (2), standard deviation and range of the data, and the P value (3) of the statistical comparison between groups at each time point. This value was derived using the nonparametric Mann Whitney, two tailed test, and significant scores are shown in bold. Comparisons following the removal of the highest score from each group (4, or outlier removed; OR) are also shown.
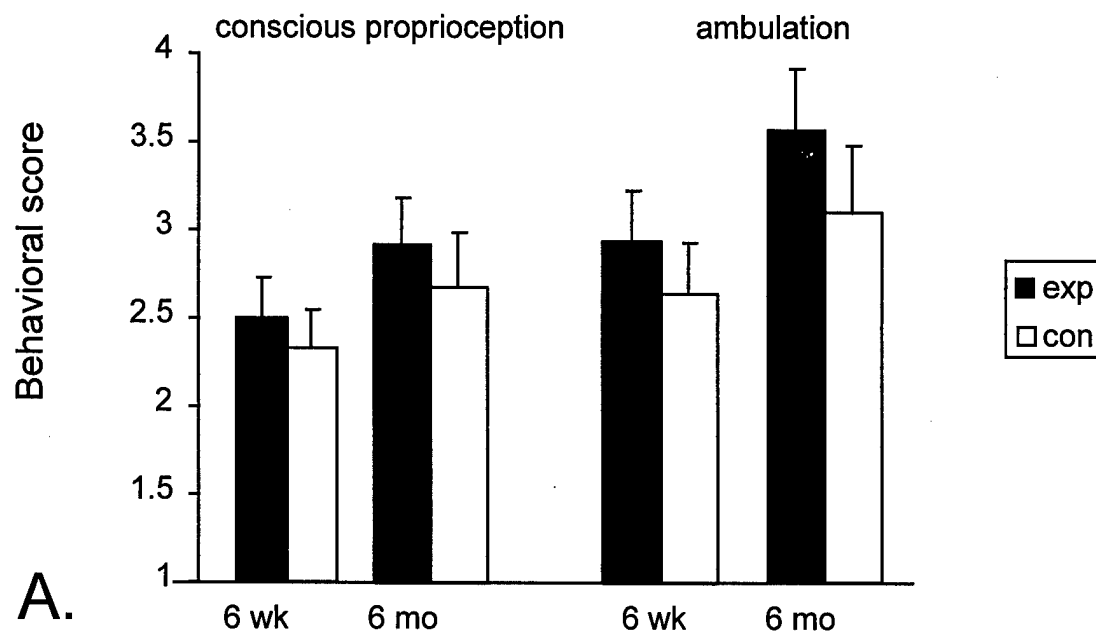
	group	recheck time	N[1]	$\overline{X}$[2]	SD	range	statistic; p-value[3] OR[4]	
conscious proprioception	exp.	6 wk.	20	1.5	1.1	1-4.8	0.58	0.67
	con.	6 wk.	14	1.3	0.9	1-4.0		
	exp.	6 mo.	18	1.9	1.1	1-4.7	0.44	0.43
	con.	6 mo.	14	1.6	1.1	1-2.4		
ambulation	exp.	6 wk.	20	1.9	1.2	1-3.8	0.76	0.87
	con.	6 wk.	14	1.6	1	1-3.7		
	exp.	6 mo.	18	2.5	1.5	1-4.3	0.16	0.22
	con.	6 mo.	14	2.1	1.4	1-4.3		

Figure 32 Behavioral data : Concious Proprioception and Ambulation.
The conventions for A and B are the same as in Fig. 31.

III. Conclusions

A. Sensory Projections, DC Fields, and Fluorescent Tract Tracing

We have shown that a rostrally negative, weak (ca. 0.4 mV/mm), electrical field, applied for approximately one month by means of an indwelling stimulator unit, can alter the anatomy of transected ascending long tract axons within the adult mammalian spinal cord. In electrically treated spinal cords, axons or their branches may project towards the center of the lesion at the plane of transection. A few fine (< 1 μm) processes may actually cross the transection at this level, sometimes projecting though dense "scar tissue" at the lesion, and pass into the rostral segment of the spinal cord. We made no attempt to count fibers in these critical regions of the injured cord since there were no comparable projections with which to compare in the control population. Furthermore, given their extremely complicated trajectories, one would be uncertain if counts were of separate axons or branches of the same axons.

We also confirm earlier observations of large caliber axons circumnavigating the lesion through undamaged parenchyma[37]. These axons turn laterally and branch repeatedly as they pass into the rostral segment. This level of branching was not observed in our previous reports.

In control (sham-treated) spinal cords, the severed proximal segments of sensory afferents undergo retrograde degeneration, and their terminal ends were rarely found near the most caudal region of the lesion. If the interesting projections of labeled axons were in response to mechanical displacement during lesioning, the placement of the marker, or during final handling of the tissues–similar anatomies should have been observed in controls, in both this and prior study[36,37,40]. They were not.

To this point we have avoided using the term "sprouting" when referring to fine, regenerating, axonal processes. This is to escape confusion over the nature of the axonal response to the applied electric field. Endogenous sprouting, that is, the production of axonal processes from *intact* axons can be a normal response to injury in the adult

mammalian CNS[75,76]. We did not observe evidence of such sprouting in control preparations in response to the hemisections performed here, however, we can not *exclude* sprouting mechanisms as a means to produce some of the fine branches that we have described. We emphasize that if sprouting of intact axons had occurred, it would as well have been facilitated by the imposition of the electric field, since the presence of fine axonal processes within the lesion was not observed in control spinal cords.

Our ability to describe this anatomy was enhanced not only because of the greater resolution of the laser confocal microscope, but as well because the use of small molecular weight rhodamine conjugated dextrans which work exceptionally well as anterograde tracers. These tracers fill the smallest bore axons and their processes over great distances, and revealed the curious trajectories and patterns of axonal regrowth that *were not revealed by* the relatively high molecular weight (> 40,000 MW) peroxidase tracers that we had formerly employed[36,37,40].

Inhibiting, Guiding and Confusing Factors

It is well know property of crushed or cut axons to branch luxuriously, producing many fine axonal processes. This was described by Ramon y Cajal in crushed peripheral nerve[121], and documented in many other systems where axons regenerate in response to injury, for example in regenerating Lamprey reticulospinal axons[127,142], in leach giant fibers[105], and in the regenerating spinal cord of the immature opossum[137]. It is also clear that these axonal processes can, in some cases, assume roughly normal projections, or may become entirely confused, and regenerate in very abnormal directions. This has usually been interpreted to be due to the disrupted terrain of the scar tissue (as in peripheral nerve regeneration, or in the crushed connective of the Leech CNS)–but not always. Lamprey giant axons may branch following retrograde dieback at the point where the cut end is in relatively undisturbed parenchyma. Some of the regenerating processes may become disoriented and project back towards the brain[142]. This characteristic is indicative

of regenerating spinal axons in a variety of other species[12,5]. It also defines the dominant response of the long tract axons to the applied voltage in this study, and suggest to us this response to be axonal regeneration.

The cellular composition at the site of traumatic injury in both non mammalian and mammalian CNS injuries is complex, including ependymal "tubes" in infra mammalians, astroglia, oligodendrocytes, various blood cells, the glial limitans, basal laminae, and fibrous connective tissue (a component of the scar produced by invading extramedullary fibroblasts)[12,91,50,123,122,81]. These cells and their molecular products can provide pathways that appear to inhibit regeneration, or guide or confuse regenerating axons. It is not surprising that axons in this study, and more commonly their finer branches, followed the margins of the dense scar at the plane of transection, or projected inwards (centrally) or outwards (laterally) at the marker holes encased in a capsular fibrous scar. The upregulated presence of extracellular matrix molecules and cell adhesion receptor systems coincident with the injury reaction (and "scar" formation) would produce an exceptionally rich source of adhesivity choices for growing axons.

Possible Non-Neuronal Targets of the Field

In the mammal, the reactive gliosis that occurs in response to injury has long been debated to provide a physical[123], physiological[95], and more recently chemical[139] impediment to central axon regeneration (although this is not supported by all tests[13,81]). We have no basis to speculate on the possible interaction between the effects of an applied voltage and such guiding, inhibiting, or confusing molecules that are relevant to regeneration. However, we can speculate that one possible effect of the applied field may be to impose a novel cellular architecture on critical non-neuronal cells accumulating at the injury zone.

As discussed above, glial cells may form fasciculation pathways in inframammalians which may facilitate axonal regeneration through the injury. Could the imposed field in the

mammal produce a more "permissive" orientation of glia? An imposed electric field can effect cell shape, migration, and orientation of a variety of cells (reviewed by citations 109 and 29). In particular, GFAP positive cortical astrocytes *in vitro*, will switch from a more fibrous character to a bipolar form and will assume an orientation perpendicular to an applied voltage gradient (50-500 mV/mm)[43]. This response is observed in nearly <u>all cells</u> of the population and it occurs within a few hours after application of field strengths over 250 mV/mm. This magnitude of electric field is orders of magnitude greater than that used in this study. Another cell type which eventually dominates the acute and subacute spinal cord lesion is the macrophage. Furthermore, this cell, its molecular products, and the nature of inflammatory response, are now being recognized to play a critical role in CNS regeneration or more properly, the lack of it[114,16,94]. Interestingly, in culture macrophages preferentially migrate in an applied voltage gradient[11].

B. Two and Three Dimensional Morhometry of SCI

Even though several weeks have passed following a spinal cord injury, macrophage numbers are impressive, dominating the cellular makeup of the injury zone and defining the boundaries and overall shape of the subacute lesion. Their density within the unit area of the central lesion approaches the theoretical limit imposed on such isodiametric cells of approximately 12 μm diameter. Given this average diameter, about 8000 cells could be squeezed into a cross sectional area of approximately 1 mm^2. If we define the area of the lesion as that containing only compromised parenchyma inundated with phagocytes plus cystic regions, significant portions of the lesions in this study come very close to this upper limit. In the balance, up to 68% of this theoretical limit is occupied by macrophages.

Blight[16] found little evidence for a substantial fall in the numbers of macrophages from between 7 days and over 3 months. This fact accounted for our choice of a sample time (3 weeks post-injury) where numbers of these cells would have peaked, and unlikely to

have declined since the insult. This temporal peak also corresponds with that of hydrolytic enzymes found in the central lesion (reviewed by Blight[16]). The large numbers of these cells shown here supports Blight's hypothesis of macrophage mediated "bystander damage" as an important contribution to "secondary" injury--even if only based on their exclusion of other cell types at the injury site.

The Method

To our knowledge, immunocytochemical identification of macrophage cells has not been coupled to a procedure aimed at rigorously determining their numbers, density, or to provide volumetric data in a CNS lesion. There are a number of markers for the macrophage, such as labels for the accumulation of acetylated low density lipoprotein[117,74]. We have chosen the monoclonal antibody ED1 for a variety of reasons; 1) its commercial availability, aiding possible replicatory studies, 2) it is one of the most studied of this group, widely used, with a long history of use, and particularly reliable in technical preparation, 3) it predominantly recognizes mononuclear phagocytes of myelomonocytic lineage (as well as monocytes in blood and their precursors in marrow), 4) ED1 expression is associated with the activated state, or phagocytic status, of these scavenger cells[55], 5) it does not recognize several subtypes of macrophages (metallophilic spleen and subsinusoidal lymph node macrophages, resident macrophages of peripheral connective tissue)[61,118,55]. Particularly relevant for our purposes, ED1 does not recognize the inactivated resident microglia of the CNS. This monoclonal antibody identifies a glycolated protein, 90,000-110,000 MW, ubiquitously expressed in the cytosol (probably associated with phagolysosomal machinery) and weakly on the plasma membrane[55]. Altogether, we believe ED1 to be the best choice for discrimination of immigrant mononuclear phagocytes invading the CNS injury and their resident scavenger colleagues, transformed ameboid microglia, which may be indistinguishable from the activated macrophages[72].

The methodology used here samples nearly all (ranging from 90 - 100%) of the lesion in any one histological section of the injured spinal cord. If we counted cells in every section, this would over represent cell number (since many cleaved cells would lie within the thickness of one section). Counting the macrophages within the lesion in every third 15 μm thick section (roughly the diameter of a single macrophage) estimates the number of these cells throughout the injury zone, while counting every 4th section would under represent the actual numbers of these cells. Using profile counts of cells of a similar, or smaller, diameter to the section thickness could over represent the number due to object splitting[52], however, we have calibrated this by comparing computer assisted cell counts to actual counts made by a naive investigator. Furthermore, there was little actual difference (and no statistical difference) between the visual counts of cells made by an investigator and by the computer. Comparisons between the volume and surface area data generated by different software (2-D and 3-D) provides additional support for the overall quantitative evaluation. For example, compilation of 2-D surface area data to provide volumes of two spinal lesions was not significantly different than that data derived by 3-D morphometry.

To our knowledge, the last attempt at establishing the numbers of macrophages within the whole spinal cord lesion at several time periods post injury was performed over a decade ago[16]. This study employed a) a visual identification of macrophages in semi-thin toluidine blue stained sections and b) counting by a line sampling technique[14]. Cell counts were made along 24 sample lines for each half cord. These estimates were expressed per unit area of the whole cord segment studied, and given as well for the outer 200 μm circumferential rim of the lesion. These macrophage counts in the guinea pig are strikingly lower than those reported here for 3 weeks in the rat. Since the method used by Blight showed only a doubling (or less) in the peak numbers of macrophages between one week and 3 months, the differences between the two reports is probably *not* a function of the temporal dynamic of macrophage accumulation, rather, a difference produced by the method of counting cells or a species difference between rat and guinea pig (see citation

24). This difference was unlikely to be due to injury severity since his lesions were more severe than ours, compromising the entire cord. There have been other attempts quantifying macrophage number within restricted sample region in the injured CNS[74,73]. These counts have been used to compare the effect of treatments aimed at reducing macrophage numbers and not applied to determining the overall number or density of macrophages within the lesioned area.

Shape Reconstruction of the Subacute Injury

Modern graphics hardware can quickly render an assembly of simple surface primitives, such as triangles or other polygons into 3-D images. Furthermore, the surface area and volume of a closed shape represented by a collection of primitives can be calculated. Our algorithms use polygons to represent the contours of a sliced object, and thereafter reconstruct 3-D shapes from such contours. These algorithms more accurately meet the computational demands of evaluating soft tissue injury than other commercial or public domain software.

It is commonplace to conceive of the mature injury to the spinal cord as something of a tube within a tube. Said another way, a central core of necrosed parenchyma surrounded by a thin rim of sparing. This view is almost always seen in drawings of transverse sections through the injury zone, common to the older literature, and still prevalent in modern reports[108,22]. Bresnahan et al.[45] provided the first computer assisted three dimensional reconstruction of the injury, defined by creosyl violet histology, and imaged by the amalgamation of transverse drawings made every 0.5 mm through the spinal segment of injury. The three dimensional reconstruction and volumetric quantification algorithms applied here, both confirm and extend some aspects of this work. The actual shape of the subacute injury defined by the boundaries between uninjured (macrophage free) and abnormal parenchyma is extremely complex with an extended surface area. We have applied the Bresnahan et al.[45] formula for lesion volume to this subacute injury. This

models the lesion as a frustum. Assuming that the early ischemic lesion (their data) is as complicated a shape as the macrophagic lesion (our data), their formula provides reasonable predictive power. Volume and surface area data derived by modeling the cord as elliptical (after Blight[16]) also appears useful. Overall, the application of such simple models may be helpful in approximating such extremely complicated topologies, when more sophisticated computational power is either not available or demanded.

The Macrophage in CNS Injury and Reconstruction

The macrophage is uniquely suited to mediate critical processes of healing, tissue reconstruction, and regeneration. The cells are highly mobile and recruited to injury sites, as well as differentiating from circulating monocytes that are known to cross the blood brain barrier and other epithelial/endothelial "barriers" by unknown mechanisms[113,77]. Macrophages are well known to be "professional scavengers" playing a sometimes dominant role in the cytolysis and engulfment of dead and dying cells and their debris at the injury zone. This role also includes the removal of myelin debris in damaged nervous tissue, a job once assumed to be restricted to Schwaan Cells in peripheral nerves[113]. The various intracellular products such as hydrolytic enzymes, and other moieties that contribute to this cellular clean up operation have been well discussed[58,77]. This process of cellular debridment, especially the removal of myelin debris, appears important to the rate if not the success of peripheral nerve regeneration. Temporal differences in this phase of inflammation may lie at the basis of differences in outcome when comparing regeneration of the neural elements of the PNS and CNS[113].

Macrophages also mediate reconstructive phases of healing - not just the removal of cell debris following injury. The production of various cytokines such as interleukin 1 (IL -1), are known to regulate various aspects of immune and non-immune mediated processes and subsequently, the reconstruction phase following inflammation and healing[132]. Macrophages may also contribute to a "persuasive" microenvironment in the CNS favoring

axonal regeneration[57]. In CNS tissue, macrophage synthesis of IL-1 and transforming growth factor beta (TGFß) together with activated amoeboid microglial scavengers is associated with increased neoangiogenesis and astroglial proliferation[72]. Astrocytes also synthesize these same compounds which together with macrophage cell specific products may oppose the activity of basic fibroblast growth factor (bFGF) (which facilitates fibril scarring and endothelial proliferation). It is likely that reactive gliosis and hypervascularity in CNS lesions is not helpful to reconstruction and functional outcome following CNS injury[123,122,22,94]. Recently Lazarov-Spiegler et al.[94] suggest a biochemical suppression of the activated state of macrophages by the CNS. Perhaps the extraordinary numbers of macrophages in the subacute lesion reported here may be a function of a relatively poor phagocytic capability.

The Macrophage and Cystic Cavitation

As expected, the dominating presence of macrophages is associated with cavitation of the spinal cord and Wallerian degeneration of white matter at distance from the focus of the injury. Regions of so called "microcavitation"[89] are characterized by extensive small holes in the parenchyma, each curiously the size of a single macrophage (these data). While some of these holes may be capillaries in cross sections (also on the order of 10 μm in diameter) the large numbers and localization in white matter does not suggest a major component of "cavitated" parenchyma to be due to the presence of vascular elements (see citation 22). Perhaps such cavitation (particularly in white matter) may be formed by restricted phagocytosis of parenchyma by single cells. Interestingly however, the regions of severe cavitation within the spinal segment containing the lesion are not restricted to the dorsal part of the spinal cord - the site of peak macrophage numbers and the experimentally produced injury. This supports the view that several mechanisms of cavity formation, including phagocytosis, act in concert to destroy parenchyma at the site of injury. However, the extensive inclusions of macrophages within forming cysts, even floating within these

cysts as "rafts" (these data and citation 22) leaves no doubt that the activity of these cells leads to the cavitation and cyst formation within CNS soft tissue.

C. Electric Fields on Secondary Injury

Spinal cord injury is an extremely complex pathophysiological event. The functional deficits that occur secondary to spinal injury are produced by many temporally dynamic processes including ionic imbalance in the acute injury, neuronal cell death and separation of axonal processes, progressive demyelination of spared but physiologically inactive axons, and a secondary injury cascade leading to a delayed and more extensive dissolution of spinal cord parenchyma[16,143,144]. Many species of non-neuronal cells play a role in the pathophysiology of spinal cord injury; macrophages, reactive astrocytes at the site of the insult, oligodendrocytes (possessing particular molecules inhibitory to nerve regeneration), Schwaan cells and fibroblasts that invade the compromised intramedullary compartment[23,122,81,129]

We have tested if macrophage accumulations within a three week old spinal injury may be affected by an applied voltage gradient of about 400 μV/mm. This time point was chosen since macrophage accumulation at the lesion site peaks by about 1 week, and shows little substantive decline for some months thereafter[16]. Thus, at the time point chosen we could expect maximal concentrations of macrophages within the injury zone in control preparations. A robust presence of phagocytes at the central hemorrhagic lesion in spinal cord has been implicated to be deleterious, contributing to progressive injury processes and a reduced functional outcome[18]. As discussed below, a reduction in the numbers of phagocytes is associated with a better functional outcome from spinal cord and brain injury. We have imposed an extracellular DC voltage across these lesions using prior methods sufficient to produce both regenerative changes in long tract spinal axons[36,40,30] and recoveries of function following experimental spinal cord injury[38,40] in laboratory

rodents. Our hypothesis was that if the applied voltage gradient directed a migration of phagocytes towards the electrodes, and <u>away from the central lesion</u>, this may contribute to a better functional outcome. We have determined that an imposed voltage sufficient to affect both nerve regeneration and functional recovery does not appear to affect peak macrophage accumulations at the lesion, the size of the lesion, or the amount of cystic cavitation of tissues of the central lesion.

Cellular Basis for Functional Recovery from Spinal Injury by Applied Electric Fields

We have previously shown that a rostrally negative applied electrical field can produce a recovery of function in an anatomically and physiologically defined sensorimotor reflex, i.e., the cutaneous trunci muscle reflex (CTM), when permanently eliminated by transection of its ascending CNS afferent projections[38,40]. Furthermore, an imposed voltage gradient, whose polarity is inverted every 15 minutes, can facilitate functional recovery in naturally produced canine paraplegia[41]. We have attributed these recoveries of function to a facilitated regeneration of damaged axons within the spinal cord for several reasons. First, there is now an extensive modern literature detailing both galvanotactic and galvanotrophic responses of nerve processes to imposed voltage gradients (reviewed by Borgens and McCaig[31]; Borgens[29]. Secondly, in guinea pigs, the recovery of function of CTM receptive fields (permanently rendered areflexive by transection of central ascending afferents) would require regeneration of these rostrally projecting fibers. The tips of growing or regenerating axons are directed towards the cathode of an applied field[28]. This polarity does affect the regrowth of ascending afferents in guinea pig spinal cord, but not the opposite polarity[37]. Finally, the opposite polarity of the applied electric field (i.e., anode rostral to the lesion) is not associated with a recovery of function of the CTM reflex[39].

There is a growing list[110,39] of non-neuronal cells whose migration or architecture is strikingly affected by an imposed weak voltage gradient such as embryonic fibroblasts[109,63], neural crest[53,125], myoblasts[85], astrocytes[43], osteoclasts and

osteoblasts[66]. One report details the responses of peritoneal macrophages to a relatively large (> 1 V/cm) external voltage gradient. Macrophage motility was defined by a directed pseudopodial activity, which usually occurred towards the positive pole of the applied field[111]. Pseudopodial activity is a quite indirect measure of oriented cell migration, and the magnitude of the applied field used in this report is much larger than endogenous fields associated with injury or regeneration or the field strengths used in most other experiments (1-500 mV/mm). This report also stands apart since most cells tested migrate to the negative pole of the applied field. Still, this data suggested to us that an extracellular voltage gradient might provide migrational cues to macrophages that could possibly dominate other tropic cues leading to a depletion of these cells at the lesion.

The Macrophage in Spinal Injury and Functional Recovery

We chose to test macrophage responses to the applied field in vivo due to its emerging role as a cell species directly implicated to affect nerve regeneration in the PNS and CNS, and a contributor to bystander damage during the initial inflammatory reaction to spinal insult[16,18,114,113,115,]. We chose the ED1 label since it is particularly associated with activated phagocytes[55]. There are several lines of evidence suggesting that regeneration in the PNS is in part due to an early and robust macrophage mediated removal of myelin and other byproducts of Wallerian degeneration of dying distal nerve segments[113,115]. In the CNS, macrophage recruitment to degenerating white matter appears to be delayed, and less robust than in PNS lesions. The difference in regeneration may not just be due to a relative paucity of cells, but to a specific characteristic of activated macrophages imparted to them by their environment. Thus, optic nerve regeneration is facilitated by implanted macrophages preincubated with damaged peripheral nerve[94]. Peak numbers of phagocytes occur in the central spinal lesion (as opposed to distal segments of injured nerve processes) by about a week post injury. The numbers of cells invading this area are impressive[16,104] and correlate with peaks in the levels of hydrolytic enzymes and

other cytotoxins liberated in this region, presumably in part by macrophages[16,18,20,23]. This further suggests that the inflammatory reaction in damaged brain and cord may contribute to delayed and progressive secondary injury following the initial insult. This is supported by the observation that administration of specific macrophage toxins (such as silica dust) is associated with a less severe response to injury and better functional outcome[73,20].

In summary: In spite of the obvious opportunity for interaction between electric fields and macrophages in studies where applied voltages are used to produce a better functional outcome from spinal injury, we found no evidence for such an interaction. If applied fields do exert an effect on CNS responses to injury via the macrophage, we suggest this must be on a more subtle level - such as affecting the state of activation or phagocytic capability of phagocytes[94].

D. Electric Fields and Polymeric Guidance Channels

This report demonstrates that a weak electric field imposed within a damaged adult guinea pig spinal cord can both induce the regeneration of axons, and guide their growth, into the ends of a hollow silicone rubber tube inserted into the dorsal half of the cord. This is because a pair of electrodes produced a DC voltage gradient within the injured spinal cord, with the cathode located within the experimental tubes. This negative electrode drew current into the open ends of the tubes, producing increasingly steep voltage gradients near to, and within, these hollow guidance channels. This was the pathway of numerous regenerating axons. It was rare to find any axons within the control applications.

Anterograde as well as retrograde labeling with a low molecular weight intracellular marker demonstrated that axons within the experimental tubes were of CNS origin. Labeled axons of lateral white matter columns, and other axons associated with neurons of central

gray matter (both interrupted by the surgical insertion of the tube) were found inside the electrically facilitated guidance channels.

There was no evidence that peripheral axons were labeled by these techniques. It is clear that some Peripheral Nervous System (PNS) axons can regenerate into the adult mammalian spinal cord when the CNS and PNS compartments are mixed following a piercing injury [10,68]. It is possible that such putative PNS axons entered the lesion and were also induced to grow into the guidance channel by the extracellular voltage gradient. However these fibers were not observed within experimental tubes, because they were not labeled. It is also possible that some of the axons observed inside the experimental channels arose from collateral sprouts from adjacent intact long tract projections. This issue has been discussed before[30]. Briefly, this response to an applied electric field is also unlikely since axonal branching is not observed in well labeled lateral column or dorsal column projections in electrical field or control treated spinal cords[30,36,37]. Moreover, there is no clear evidence from other in vitro or in vivo studies that applied voltages can induce substantial sprouting from intact axons. The observations reported here support the hypothesis that an extracellular electric field can not only induce axonal regeneration within the mammalian spinal cord [30,37], but likely help guide it as well in concert with other factors associated with the extracellular matrix[4,81]. It is this regenerative response to an applied extracellular gradient of voltage that probably lies at the basis of a behavioral recovery from spinal cord injury in both laboratory models of spinal trauma[40,38] and in a veterinary clinical model—naturally produced paraplegia in dogs[42].

Nerve Regeneration in Silicone Tubes

In studies of peripheral nerve regeneration into silicone guidance channels, the implanted tubes fill with a clear extracellular fluid containing fibrin and neurotrophic factors[138]. These localized molecular and ECM components are associated with a significant increase in the ability of axons of the proximal nerve stump to cross the gap to

the distal nerve stump[84,96,38]. It is likely that in this study, cells that invaded the CNS compartment following implantation of the guidance channel also contributed ECM and soluble molecular components conducive to nerve regeneration, though the rare occurrence of axons within control tubes suggest the abortive regeneration of CNS axons[12,91,121] was not altered or overcome significantly. The presence of a collageneous scar capping the tube by one month post-implantation suggests that immigrant cells from the peripheral environment may instead have produced even more of an impediment to CNS regeneration[125].

A steady DC field has been used in conjunction with a silicone cuff or sleeve to enhance sciatic nerve regeneration[90]. The effect was real, but very modest, perhaps in part due to the lack of current regulating components in the circuit. Other studies[1,67,139] suggest piezoelectric guidance channels (i.e. channel material with trapped electrical charges) may also enhance nerve regeneration. These latter applications are not likely related to steady voltage gradients, distributed over large distances within the spinal cord by an active DC circuit as reported here.

The Nature of the Stimulus

There are two components of the electrical circuit that we should consider: that component outside the tube, and that component within it. The magnitude of the electrical field inside the tube is the least difficult to estimate. Given a cross sectional area of 0.2 mm^2, a resistivity of the (initially) loosely organized tissue and fluids within the tube (on the order of 500 Ω cm), and a total current of 0.1 μA, we should expect the voltage gradient within the tube to be on the order of 2.5 mV/mm. To attempt to estimate the field at distance from the channel with any precesion would be difficult, given various and many uncertainties—such as the exact current path within the extracellular space and the resistivity along these extracellular pathways[26,32,87].

The failure of axons to grow into some experimental tubes could be due to several factors including an early and more complete closure of the mouth of the channel with dense connective tissue[125] prior to the arrival of axons, or some subtle failure in the circuit following implantation. It is interesting that axons usually do not enter both ends of the experimental tubes. This suggests that the developing tissue plugs at both ends may become unequal in their electrical characteristics. Soon after implantation, current flow could be mostly directed through one end to complete the circuit due to a climbing resistance to current flow at the other end of the tube. The failure of tissue plugs to form within some tubes also suggest the ECM (including collageneous and glial scar) at the ends of the tube may be quite variable influencing not only the character of the electrical circuit, but even the access of cells to the interior of the guidance channel.

There are many choices of tubal fasciculation pathways or guidance channels to help sustain and direct nerve regrowth. These include silastic (silicone rubber), poly (DL-lactide-episilon-caprolactone (PLLA/PCL) tubes, polyacrylonitrile/polyvinylchloride (PAN/PVC) guidance channels, polygalactin, polypropylene, and polyethylene guidance tubes, to name only a few[59,60,67,84,106,138]. The mechanical or surface character of these various materials can also improve peripheral nerve regeneration alone, or in combination with transplanted cells and growth factors[2,3,46,78,141].

Silicone rubber was used in this study due to its historically good coaptation with nervous system tissues[25,71,96], and its electrical insulating capability[25]. The latter allows the tube to not only aggregate regenerating axons, but permits the use of an inserted (and likewise silicone rubber insulated) electrode to draw current into the channel's open bores completing a circuit from an external anode. The stable bonding of a silicone based adhesive to the electrode's silicone insulation eliminated an alternate current pathway through the hole in the center of the tube where the electrode was originally inserted.

It is important to emphasize that in all tests of the regeneration or growth of neurites to an applied electrical fields under physiological conditions, cell responses are mediated by

the cathode[26,30,33,35,88,97-100,112,126]. Axons grow towards cathodes, and away from anodes. Indeed, axons or neurites facing the anode usually undergo marked retrograde degeneration or turn away from it[26,99,126]. Therefore, to induce axonal growth towards and into the silicone rubber channel, a cathode was located within it's center. The opposite polarity could not be tested however. At the anode, electrode products produced by electrolysis are cytotoxic (and in this study, trapped inside the tubes). Cathodes, on the other hand, are relatively innocuous at modest levels of direct current[31]

The Cellular Targets of the Stimulus

The low magnitude of the imposed electrical field in spinal cord tissues bears directly on the question of what were the most likely molecular or cellular targets of the applied voltage? There are three reasonable possibilities: 1.) axons themselves, 2.) other non neuronal and more isodiametric cells at the injury site, and 3.) the molecular products of such cells (such as components of the ECM). Such low field responses support the notion that the axon is the principle target of the applied voltage[26,31,87]. The geometry of long cellular processes such as white matter axons extending parallel with the voltage gradient makes them particularly attractive targets, as they are potentially permeable to the applied current[31,87]. The results of this study suggest that axons could be the main targets of the field. Small numbers of branching, regenerating fibers were first detected at the mouth of the experimental tubes soon after the circuit was removed. These early arriving fibers could have provided a fasciculation pathway for fibers arriving later in larger numbers. It was fortuitous to have labeled these few axons with a localized and distant injection of marker. Even fewer axons, arriving at the channels during the application of the electric field, may have escaped labeling and observation.

Glial cells are known to form natural fasciculation pathways during development of the nervous system, and during its regeneration in some species[50,81]. It is possible that the electrical field imposed an orientation on glia or their processes in the region

sorrounding the tube. This may have helped guide regenerating axons to it. We have tested the responses of mammalian cortical astrocytes to an externally applied voltage in vitro. These cells showed marked orientational responses to potential drops on the order of 50 - 100 mV/mm over a few hours of observation[42]. So called "fibrous" astrocytes lost their extensive cellular processes, and became exclusively bipolar. They always changed their orientation in the presence of the applied field such that their long axis was perpendicular to the voltage gradient[42]. It is not known if much weaker voltage gradients than that tested in vitro, but imposed for many days or weeks, would also lead to such architectural changes in vivo. The overall shape of the plugs, which was curiously different between the control and experimental applications, could also reflect a voltage mediated effect on the migration and/or orientation of other types of non neuronal cells gathering and proliferating in the lesion.

Such an orinted cellular architecture, formed during the period of exposure to the voltage gradient, could provide a local enviroment helping to guide regenerating axons into the tube. It is less likely that the applied field could directly reorganize the molecular components of the substrate or ECM once these are layed down. Most critical ECM molecules that might be suggested to establish a preferential orientation for nerve growth would not be expected to be responsive to voltage gradients on the order of 0.01-10 mV /mm. For example, studies of electrically induced birefringence changes in collagen molecules required applied voltages on the order of tens to hundreds of volts per cm[87]. Finally, the combined use of a guidance channel and electric field aggregates responding cells in a local region, and thus amplifies the interpretative opportunities for the investigator. This model may provide an ideal means to better evaluate the factors critical to the electrical facilitation of spinal cord regeneration.

E. Effects of DC Fields on Canine Paraplegia

In this blinded clinical trial, we have learned that the application of a weak electrical field whose polarity reverses every 15 minutes can improve the functional recovery from severe, acute, and neurologically complete, paraplegia. This improvement in function was evidenced by: 1.) a marked trend for an improvement in function in every category of neurological of evaluation in only OFS treated dogs with no reverse trend; 2.) the statistically significant improvement in the Combined Neurological Scores between OFS treated and control (sham-treated) dogs at the end of the 6 month period of evaluation; and 3.) distinct improvements in individual categories of evaluation–particular in the appreciation of pain and the recovery of SSEP conductionin the experimentally treated group. This study has corroborated the results of an earlier clinical trial of OFS which also used naturally injured paraplegic dogs[41]. The positive results of that trial prompted our narrowing of the entry criterion to only those animals that could be treated within 18 days of the onset of paraplegia, and the development of a new generation of OFS implantable stimulators that would be suitable for eventual human testing.

Oscillating Field Stimulation and Canine Paraplegia

As mentioned, this is the second test of OFS in canine paraplegia, and largely mirrors the results obtained in the first blinded clinical trial[41]. In that study, statistical significance between the experimental and sham treated groups was reached at the first (8 week) recheck period. Though there was a strong trend towards significance at the 6 week recheck period in the present study, it was not reached until the end of the study period, 6 months post injury. Differences in the conduct of the two trials included 1.) the higher output of the stimulators used in the present study, 2.) the delayed activation of the stimulator for a period between 48-96 hours after surgical decompression of the spinal cord, and 3.) the addition of measurements of urinary continence, monitored by cystometry and urethral pressure profilimetry, in the present study.

1.) Though the magnitude of the field was chosen with an eye on eventual clinical use in humans as explained above, this represented a 3 fold enhancement in the applied voltage gradient as used previously. We have not observed an enhanced recovery from the application of the larger field strength in this trial. It may be that: a) this range of stimulation (200-600 μV/mm) is optimal; b) small increases in function in the behavioral categories evaluated would require a greater number of study animals, or c.) this level of functional recovery can not be increasingly facilitated by the use of applied voltages alone. In our previous trial, we noted a window of time (the first 2 weeks following injury) in which OFS treatment should be made.

2.) The delay in activation of the units was designed to distinguish the relative contribution of the surgical decompression vs. the application of the electrical field to the recovery of function. Twelve dogs in both the experimentally treated and sham treated group could be compared to examine this issue. These 24 dogs remained negative for deep pain following surgical decompression, and prior to the activation of the electrical field in the experimental group. At the 6 month recheck, the combined neurological score was not significantly different between the two groups, but showed a strong trend in this direction (P = 0.07; Mann Whitney, two tailed). This suggests the electrical field by itself may be the most significant of the two clinical procedures in producing recovery of function.

3.)The tests of urinary continence turned out not to be a good indicator of functional recovery as these physiological measurements did not discriminate between dogs that showed behavioral evidence of voluntary micturation (based on owner reporting and the observations of technicians on kenneled dogs) and those that remained incontinent.

It is both interesting and revealing to combine and compare the neurological data derived from both canine clinical trials of OFS--even given the differences in the application noted above. This provides both an overview of our total experience to date using this form of treatment in acutely injured dogs, and provides a larger number of animals with which to compare outcomes (6-8 week n = 33 exp., 25 cont.; 6 month n = 31, and 25 respectively).

Of the five categories of assessment , the difference in porportion between recovering and non-recovering dogs was significantly different in three of them at the 6 month recheck period (superficial pain, ambulation, and the recovery of conduction of the SSEP; $P \leq 0.02$; Fisher's exact test for proportions, two tailed). Interestingly, only 2 dogs of 4 recovered appreciation of superficial pain at the 6 month recheck period , while over half of all OFS treated study animals recovered this sensation (19 of 31; $P = 0.0001$, Fisher's Exact Test). In spite of its use as a prognosticator of functional recovery in canine paraplegia[134,136,41] deep pain appreciation turned out to be a less sensitive indicator in these trials as numerous animals in both groups recovered this sensation by 6 months post surgery (12 of 25 controls; 22 of 31 experimentals). Fig. 33 summarizes these comparisons of the two combined clinical trials.


A Human OFS Application as Tested in the Dog

The present study employed a new type of OFS stimulator that would meet the requirements for phase one human use—which is the next step in our development of this technology. To be able to achieve a similar magnitude of imposed voltage gradient at the lesion as that previously found sufficient to improve functional recovery from spinal cord injury in the naturally injured dog (i.b.i.d.) required a complete redesign of the implantable OFS unit. Since the cross sectional area of a human patient would be about three fold that of the small to medium sized dogs used in our earlier trials, the current density required to produce a similar imposed voltage gradient across the lesion in the human would need to increase by about 3 fold. This requirement led to the present design in which three individual, and similar circuits deliver between 500-600 uA total current between three pairs of electrodes whose polarity reverses in synchrony. This circuit design maintains current density levels at each electrode at safe levels as used previously. Other designs where the increased magnitude of total current would be delivered by only one or even two pairs of electrodes in order to meet this objective was viewed as unacceptable. This was based on

6 week - 8 week
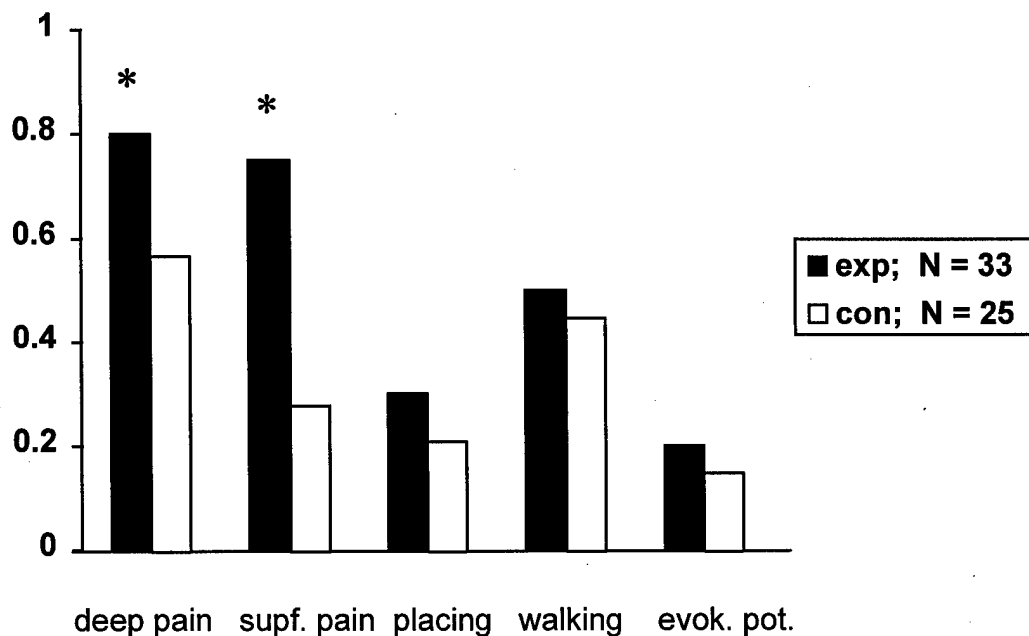
6 month
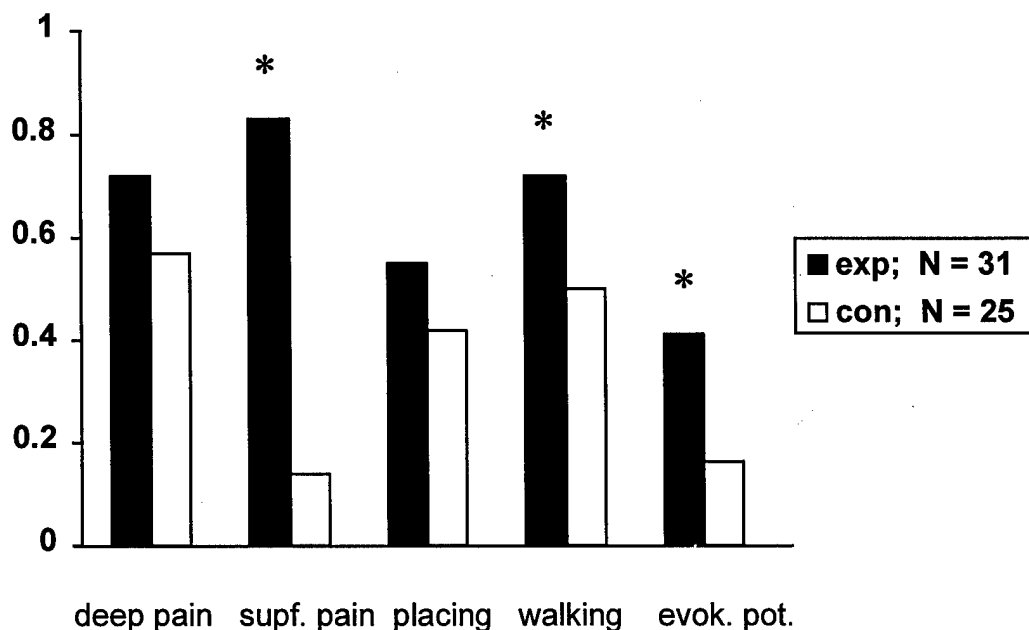
Figure 33 *Behavioral Recovery: Combined Trial Comparisons. The porportion of dogs that showed detectable recovery of function in each of the behavioural evaluations for OFS treated (exp.) and sham treated (con.) groups. This data was obtained by summing the number of recovering and non recovering dogs in each group observed in this and a previous clinical trial of OFS treatment of canine paraplegia (see Fig. 6 in Borgens et al., 1993a). All dogs represented here were treated within 18 days of their spinal cord injury. All dogs admitted to both clinical trials were required to meet the same entry criterion and were neurologically complete paraplegics. An asterisk denotes a paired comparison which was stastically significantly different ($P \leq 0.05$, Fishers Exact Test, two tailed).*

the fact that higher current densities at each electrode might lead to an enhanced potential for soft tissue damage adjacent the site of electrode implantation. Human testing would require functioning "fail-safe" circuitry that would shut off the operation of the stimulator implant coincident with non-nominal output. In particular, a failure to oscillate would result in the stimulator output to lock onto a DC application, which would pose certain risk of soft tissue damage at the positive pole (anodal electrode; refer to discussion in citation 28. All of these needs were met by the present stimulator design which functioned well during the coarse of this investigation.

The Paraplegic Dog as a Model for Human Spinal Cord Injury

The pathophysiology of human SCI is similar to that produced accidentally in the canine. Human injury is characterized by a central hemorragic necrosis of gray and white matter at the site of impact produced by acute compressive force; a continuing dissolution of this compromised spinal cord parenchyma with time following the injury, and variable amounts of sub pial sparing of white matter that may or may not be physiogically functional. In contrast to laboratory induced models of SCI in small animals (usually rodents), humans are rarely unconscious or anesthetized at the time of injury, and their injuries are "closed"– that is the spinal cord is not directly exposed to the insult. Anesthesia alone improves functional outcome from spinal injury[128], and the use of a laboratory induced "closed" injury–particularly in primates–has become financially and politically untenable. We have critically questioned the degree to which experimental results observed in laboratory rodent models of SCI can, or should, be extrapolated to human SCI[29].

The acute, traumatic compression of the canine spinal cord by intervertebral disc herniation in the canine however, closely models that described above for human traumatic spinal cord injury. Paradoxically, disc herniations in humans rarely result in spinal cord damage since discs move outwards, away from the central foramen, compressing nerve roots and producing pain. There is greater ligamentous support of the vertebral column in

dog relative to man, thus disc material is projected into the foramen causing direct damage to the spinal cord[41,136]. This severe compressive force causes local hemorrhage and sometimes laceration of the parenchyma when disc material penetrates the spinal cord– mirroring that which may occur secondary to traumatic burst fracture of the vertebrae in the human accident. Spinal cord swelling and a progressive, continuing deterioration of the tissue at the site of impact has been followed by myelographic examination. An exaggerated example of so called "secondary injury" is clinically observed in the dog as Ascending/Descending Myelomalacia. This progressive deterioration of the spinal cord does not respond to clinical management, forcing euthhanasia of the animal. Spinal cord injuries in the dog are also evaluated with many of the same clinical assessments as used in humans and conventional management of the injury is the same in those cases where owners will go forward with relatively expensive Veterinary medical treatment (acute methylprednisolone therapy followed by surgical decompression of the spinal cord and stabilization of the vertebral column). All control animals in this study received this current and recognized standard of care for acute SCI[136].

Finally, while an uncoordinated form of "spinal walking" can occur in the dog, completely paraplegic animals that require support of the hindquarters by a wheeled cart for several months following the injury rarely recover use of the hindlimbs, remaining paraplegic and incontinent for their lifetime. We have evaluated over one hundred "chronically" paraplegic dogs, ranging from 3 years to 11 years post injury and have observed little improvement in their clinical presentation. Locally controlled and generated ambulation is common to small animal laboratory models of SCI leading to the generation of elaborate means of discriminating subtle differences in walking[49], or indirect means of evaluation of hind limb control such as inclined plane performance testing[64]. These problems have prompted us to utilize a long tract sensorimotor reflex in the rodent as a index of spinal cord behavioral recovery (instead of ambulation) because damage to the intramedullary afferent white matter serving this relex produces a permanent loss in behavior for the life of the

animal[18,38,40,29]. We do not attempt to identify such locally controlled and patterned stepping during the behavioral scoring of ambulation in the canine, focussing on a comparison of the animals relative ability to walk and Ito climb stairs[41]. Altogether these considerations make the naturally injured dogs a most useful "preclinical" model for human SCI (see also citations 22, 82, and79 for a progression from the paraplegic dog SCI model to phase one human clinical trials in SCI).

The Response of the Injured CNS to Oscillating Electrical Fields

The use of an oscillating electrical field was originally based on these observations, particularly one by Colin McCaig in 1987. He documented that the growth responses of Xenopus neurites in vitro facing the cathode (negative pole of the applied field) were immediate, while the initiation of resorption of neurites facing the antipode took nearly an hour[99]. Thus we reverse the polarity of the imposed field within this window of time to influence regeneration of long tract axons within the white matter in both directions–while not encouraging retrograde dieback of axons facing the anode[41,28]. We have recently documented axonal response to oscillation of the field in the adult guinea pig using miniature OFS stimulators and a double label technique for fluorescent tract tracing of regenerating ascending and descending projections (Borgens and Bohnert, unpublished observations). In another related experiment, an applied voltage gradient was used to initiate regeneration of severed adult guinea pig spinal axons–and to direct these regenerating fibers into a silastic tube, surgically implanted into the spinal cord. In control tubes,labeled axons were very rare. In experimental tubes, large numbers of spinal axons were easily identified by both anterograde and retrograde intracellular labeling. Since the applied field was present for only 1 week, and since regeneration of axons into tubes occurred between 1-2 months post surgery, the voltage gradient must have influenced the ordering of some component of the extracellular matrix to allow regenerating axons a "memory" of where to project after the electrical cue was no longer present[30]. In summary

we believe that the behavioral recovery reported here in response to the clinical use of applied voltage gradients is in part mediated by the well described growth responses of injured axons to applied fields (refer to the Introduction) and other more subtle effects that could also influence their regeneration and/ or their direction of growth.

REFERENCES:

1. Aebischer P., Valentini R.F., Dario P., Domenici C., and Galletti P.M. (1987) Piezolelectric guidance channels enhance regeneration in the mouse sciatic nerve after axotomy. *Brain Research* **436**, 165-168.

2. Aebischer P., Guénard V., Winn S.R., Valentini R.F., and Galletti P.M. (1988) Blind-ended semipermeable guidance channels support peripheral nerve regeneration in the absence of a distal nerve stump. *Brain Research* **454**, 179-187.

3. Aebischer P., Salessiotis A.N., and Winn S.R. (1989) Basic fibroblast growth factor released from synthetic guidance channels facilitates peripheral nerve regeneration across long nerve gaps. *J. of Neuroscience Research* **23**, 282-289.

4. Aguayo A.J., Bray G. M., Rasminsky M., Zwimpfer T., Carter D., and Vidal-Sanz M. (1990) Synaptic connections made by axons regenerating in the central nervous system of adult mammals. *J. exp. Biol.* **153**, 199-224.

5. Anderson, M.J., and S.G. Waxman (1983) Regeneration of spinal neurons in inframammalian vertebrates: Morphological and development aspects. *J. Hirnforsch* **24**, 371-398.

6. Bajaj, C. and G. Xu. (1992) *A-Splines: Local Interpolation and Approximation using Continuous Piecewise Real Algebraic Curves.* Computer Science Technical Report, CAPO-92-44, Purdue University.

7. Bajaj, C. and G. Xu. (1994) Data Fitting with Cubic A-Splines. In *Proceedings of Computer Graphics International '94*, pages x-y, Melbourne, Australia.

8. Bajaj C., Coyle C. and Lin K. (1996) Arbitrary topology shape reconstruction from planar cross sections, *Graphical Models and Image Processing* **58, 6**: 190-211.

9. Bajaj, C., E. Cole and K. Lin (1996b) Boundary and 3-D triangular meshes from planar cross sections, Proceedings of the 5th International Imaging Roundtable, Sandia National Labs, Report SAND 96-2301, VC-405, 1996, pp.169-178.

10. Beattie, M.S., Bresnahan, J.C., Komon, J., Tovar, C.A., Van Meter, M., Anderson, D.K., Faden, A.I., Hsu, C.Y., Noble, L.J., Salzman, S., and Young, W. (1997) Endogenous repair after spinal cord contusion injuries in the rat. *Exp. Neurol.,* **148**, 453-463.

11. Bernstein, J.J., M.R. Wells, and M.E. Bernstein (1978) Spinal cord regeneration: synaptic renewal and neurochemistry. In Cotman, C.W. (ed): Neuronal Plasticity. Raven Press, New York, pp 49-71.

12. Berry, M. (1979) Regeneration in the central nervous system. In *Recent Advances in Neuropathology.* W.T. Smith and J.B. Cavanaugh (Eds) New York: Livingstone. pp. 67-111.

13. Berry, M., S. Hall, L. Rees, J. Carlile and J.P.H. Wyse (1992) Regeneration in the optic nerve of the adult Browman-Wyse (BW) mutant rat. *Journal of Neurocytology.* **21**, 426-448.

14. Blight, A.R. (1983) Cellular morphology of chronic spinal cord injury in the cat: analysis of myelinated axons by line sampling. *Neuroscience.* **2**, 521-543.

15. Blight, A.R. (1984) Inflammatory responses following experimental spinal cord injury: A destructive effect of macrophages on axons and myelin? *Society for Neuroscience Abstracts.* **10**, 887.

16. Blight, A.R. (1985) Delayed Demyelination and Macrophage Invasion: A Candidate for Secondary Cell Damage in Spinal Cord Injury, *Central Nervous System Trauma.* **2**, 299-315.

17. Blight A.R. (1991) Morphometric analysis of a model of spinal cord injury in guinea pigs, with behavioral evidence of delayed secondary pathology, *Journal of the Neurological Sciences* . **103**, 156-171.

18. Blight A.R. (1992) Macrophages and Inflammatory Damage in Spinal Cord Injury, *Journal of Neurotrauma* . **9**, s83-s91.

19. Blight A. (1993) Remyelination, Revascularization, and Recovery of Function in Experimental Spinal Cord Injury. In: *Advances in Neurobiology: Neural Injury and Regeneration Vol 59* F.J. Seil (Ed.) pp. 91-103.

20. Blight, A.R. (1994) Effects of silica on the outcome from experimental spinal cord injury: Implication of macrophages in secondary tissue damage. *Neuroscience* . **60**, 263-273.

21. Blight, A.R., M.E. McGinnis, and R.B. Borgens (1990) Cutaneus Trunci Muscle Reflex of the Guinea Pig. *Journal of Comparative Neurology* . **296**, 614-633.

22. Blight, A.R., J.P. Toombs, M.S. Bauer and W.R. Widmer (1991) The effects of 4-Aminopyridine on neurological deficits in chronic cases of traumatic spinal cord injury in dogs: A phase I clinical trial. *J. of Neurotrauma* **8**, 103-119.

23. Blight, A.R., Saito, K., and Heyes, M.P. (1993) Increased levels of the excitotoxin quinolinic acid in spinal cord following contusion injury, *Brain Res.* **632**, 314-316.

24. Blight A.R., E. Carwile Leroy, Jr., M.P. Heyes. (1997) Quinolinic acid accumulation in injured spinal cord: time course, distribution, and species differences between rat and guinea pig. *J. Neurotrauma* . **14**, 89-98.

25. Bloch, B., and G. W., Hastings *Plastic Materials in Surgery*, C.C. Thomas, Pub. Springfield, IL (1972)

26. Borgens, R.B. (1982) What is the role of naturally produced electric current in vertebrate regeneration and healing? *International Review of Cytology* **76**, 245-298.

27. Borgens, R.B. (1988) Voltage gradients and ionic currents in injured and regenerating axons. In: Advances in Neurology, Vol. 47: Functional Recovery in Neurological Diseases. S.G. Waxman, Ed., (Raven Press, New York), pp. 51-66.

28. Borgens, R.B. (1989) Artificially controlling axonal regeneration and development by applied electric fields. In: Electric Fields in Vertebrate Repair. Co-authored by R.B. Borgens, K.R. Robinson, J.W. Vanable, Jr., and M.E. McGinnis. (Alan R. Liss, New York), Chapter 4. pp. 117-170.

29. Borgens, R.B. (1992) Applied Voltages in Spinal Cord Reconstruction: History, Strategies, and Behavourial Models. In Spinal Cord Dysfunction, Volume III: Functional Stimulation, Oxford University Press, Oxford, 1992, p. 110-145.

30. Borgens, R.B., D.M. Bohnert (1997) The Responses of Mammalian Spinal Axons to an Applied DC Voltage Gradient Experiemental Neurology, 145, 376-389.

31. Borgens, R.B. and C.D. McCaig (1989) Endogenous currents in nerve repair, regeneration, and development. In: Electric Fields in Vertebrate Repair. Co-authored by R.B. Borgens, K.R. Robinson, J.W. Vanable, Jr., and M.E. McGinnis. (Alan R. Liss, New York), Chapter 3. pp. 77-116.

32. Borgens, R.B. and C.D. McCaig (1989) Artificially controlling axonal regeneration and development by applied electric fields. In: Electric Fields in Vertebrate Repair. Co-authored by R.B. Borgens, K.R. Robinson, J.W. Vanable, Jr., and M.E. McGinnis. (Alan R. Liss, New York), Chapter 4. pp. 117-170.

33. Borgens R. B., and Shi, R. (1995) Uncoupling histogenesis from morphogenesis in the vertebrate embryo by collapse of the transneural tube potential. Dev. Dynamics , 20, 456 - 467

34. Borgens, R.B., L.F. Jaffe, and M.J. Cohen (1980) Large and persistent electrical currents enter the transected spinal cord of the lamprey eel. Proceedings of the National Academy of Science U.S.A. 77, 1209-1213.

35. Borgens, R.B., E. Roederer, and M.J. Cohen (1981) Enhanced spinal cord regeneration in lamprey by applied electric fields. Science 213, 611-617.

36. Borgens, R.B., A.R. Blight, and D.J. Murphy (1986a) Axonal regeneration in spinal cord injury: A Perspective and new technique. J. Comp. Neurol. 250, 157-167.

37. Borgens, R.B., A.R. Blight, D.J. Murphy, and L. Stewart (1986b). Transected dorsal column axons within the guinea pig spinal cord regenerate in the presence of an applied electric field. J. Comp. Neurol. 250,168-180.

38. Borgens, R.B., A.R. Blight, and M.E. McGinnis (1987) Behavioral recovery induced by applied electric fields after spinal cord hemisection in guinea pig. Science 238, 366-369.

39. Borgens, R.B., M.E. Metcalf, and A.R. Blight (1992) Delayed Application of Direct Current Electric Fields in Experimental Spinal Cord Injuries. *Rest. Neuro. Neurosci.,* **5**, 173-179.

40. Borgens R.B., Blight A.R. and McGinnis M.E. (1990) Functional Recovery After Spinal Cord Hemisection in Guinea Pigs: The Effects of Applied Electric Fields, *The Journal of Comparative Neurology* . **296**, 634-653.

41. Borgens, R.B., M.E. Metcalf, and A.R. Blight (1993a) Delayed Application of Direct Current Electric Fields in Experimental Spinal Cord Injuries. *Restorative Neurology and Neuroscience* Vol. **5**, 173-179.

42. Borgens, R.B., J.P. Toombs, A.R. Blight, M.S. Bauer, W.R. Widmer and J.R Cook. (1993b) Effects of Applied Electric Fields on Clinical Cases of Complete Paraplegia in Dogs. *J. Restorative Neurology and Neuroscience* (in press). manuscript included in appendix materials

43. Borgens, R.B., R. Shi, T.J. Mohr, and C.B. Jaeger (1994) Mammalian Cortical Astrocytes Align Themselves in a Physiological Voltage Gradient. *Exp. Neurology.* **128**, 41-49

44. Bracken, M.B., Shepard, M.J., Collins, W.F., et al. (1990) A randomized, controlled trial of methylprednisolone or naloxone in treatment of acute spinal-cord injury, *New Engl.J.Med.,* **322**, 1405-1461.

45. Bresnahan, J.C., Beattie, M.S., Stokes, B.T., and Conway, K.M. (1991) Three dimensional computer-assisted analysis of graded contusion lesions in the spinal cord of the rat. *J. Neurotrauma.* **8**, 91-101

46. Brushart T.M., Mathur V., Sood R., and Koschorke G.M. (1995) Dispersion of regenerating axons across enclosed neural gaps. *J. of Hand Surg.* **20**, 557-64.

47. Bunge R.P., W.R. Puckett, J.L. Becerra, A. Marcillo, and R.M. Quencer (1993) Observations on the Pathology of Human Spinal Cord Injury - A Review and Classification of 22 New Cases with Details from a Case of Chronic Cord Compression with Extensive Focal Demyelination. In: *Advances in Neurobiology: Neural Injury and Regeneration Vol 59* F.J. Seil (Ed.) pp. 75-89.

48. Chakers, W.D., Flickinger, F., Bresnahan, C.J., Beattie, M.S., Weiss, K.L., Miller, C., and Strokes, B. (1987) MR imaging of the acute spinal cord trauma. *Annual Journal of Neurological Research* . **8**, 5-10.

49. Cheng, H., Almström, S., Giménex-Llort, L., Chang, R., Ogren, S., Hoffer, B., And Olson, L. (1997). gait analysis of adult paraplegic rats after sinal cord injury. Exp. Neurol. **148**, 544-557.

50. Chernoff, E.A.G. and D.L. Stocum (1995) Developmental aspects of spinal cord and limb regeneration. *Developmental Growth and Differentiation.* **37**, 133-147.

51. Cliff, N. (1996). Alternatives to mean comparisons, in: Ordinal Methods for Behavioral Data Analysis. Lawrence Erlbaum Associates, Publishers: Mahwah, NY, pps 123-156

52. Coggeshall, R.E. and H.A. Lekan (1996) Methods for determining numbers of cells and synapses: a case for more uniform standards of review. *The Journal of Comparative Neurology*. **364**, 6-15.

53. Cooper, M.S. and R.E Keller (1984) Perpendicular orientation and directional migration of amphibian neural crest cells in DC electrical fields. *Proc. Natl. Acad. Sci. USA*. **81**, 160-164.

54. Currie, S.N., and J. Ayers (1987) Plasticity of fin command system function following spinal transection in larval sea lamprey. *Brain Researc* h. **415**, 337-341.

55. Damoiseaux, J.G.M.C., E.A. Dopp, W. Calame, D. Choa, G.G. MacPherson and C.D. Dijkstra (1994) Rat macrophage lysosomal membrane antigen recognized by monoclonal antibody ED1. *Immunology* **83** 140-147.

56. Davenport R.W. and McCaig C.D. (1993) Hippocampal Growth Cone Responses to Focally Applied Electric Fields, *Journal of Neurobiology*. **24**, 89-100.

57. David, S., O. Bouchard, O. Tsatas and N. Giftichristos (1990) Macrophages can modify the nonpermissive nature of the adult mammalian central nervous system. *Neuron* **5**, 463-469.

58. Davies, P. and R.J. Bonney (1979) Secretory products of mononuclear phagocytes: a brief review. *Journal of the Reticuloemdothelial Society* **26,** 37-47.

59. den Dunner W.F., Stokroos I., Blaauw E.H., Holwerda A., Pennings A.J., Robinson P.H., and Schakenraad J.M. (1996) Light-microscopic and electron-microscopic evaluation of short-term nerve regeneration using a biodegradable poly(DL-lactide-epsilon-caprolacton) nerve guide. *J. of Biom. Mat. Res.*, **31**, 105-15.

60. den Dunnen W.F., Van der Lei B., Schakenraad J M., Blaauw E.H., Stokroos I., Pennings A.J., and Robinson P.H. (1993) Long-term evaluation of nerve regeneration in a biodegradable nerve guide. *Microsurgery*. **14**, 508-15.

61. Dijkstra, C.D., E.A. Dopp, P. Joling, and G. Kraal (1985) The heterogeneity of mononuclear phagocytes in lymphoid organs: distinct macrophage subpopulations in the rat recognized by monoclonal antibodies ED1, ED2 and ED3. *Immunology* **54**, 589-599.

62. Dixon, W.J. (1950). Analysis of extreme values. Ann. Math. Stat. **21**, 488-506.

63. Erickson, C.A and R. Nuccitelli (1984) Embryonic fibroblast motility and orientation can be influenced by physiological electric fields. *J. Cell Biol.* **98**, 296-307.

64. Fehlings, M., And Tator, C. (1995). The relationships among the severity of spinal cord injury, residual neurological function, axon counts, and counts of retrogradely labeled neurons after experimental spinal cord injury. Exp. Neurol. **132**, 123-134.

65. Fehlings, M.G., C.H. Tator, R.D. Linden (1988) The effect of direct current field on recovery from experimental spinal cord injury. *Journal of Neurosurgery*. **68**, 781-792.

66. Ferrier, J., Ross, S.M., Kanehisa, J., and Aubin, J.E. (1986) Osteoclasts and osteoblasts migrate in opposite directions in response to a constant electric field. *J. Cell Physiol.*, **129**, 283-8.

67. Fine E.G., Valentini R.F., Bellamkonda R., and Aebischer P. (1991) Improved nerve regeneration through piezoelectric vinylidenefluoride-trifluoreoethylene copolymer guidance channels. *Biomaterials* **12**, 775-780.

68. Frisen, J., K. Fried, A.M. Sjogren and M. Risling (1993) Growth of ascending spinal axons in CNS scar tissue. *Intern.J. of Develop.Neurosc.* **4**, 461-475.

69. Gambardella, P.C. (1980). Dorsal decompressive laminectomy for treatment of thoracolumbar disc disease in dogs: A retrospective study of 98 cases. Veterinary Surgery. **9**, 24-26.

70. Geisler, F.H., Dorsey, F.C. and Coleman, W.P.(1991) Recovery of motor function after spinal cord injury - a randomized, placebo-controlled trial with GM-1 ganglioside, *New Engl.J.Med.*, **324**, 1829-1838.

71. Gibson K.L., Remson L., Smith A., Satterlee N., Strain G.M., and Daniloff J.K. (1991) Comparison of nerve regeneration through different types of neural prostheses. *Microsurgery*. **12**, 80-5.

72. Giulian, D. (1987) Ameboid microgila as effectors of inflammation in the central nervous system. *Journal of Neuroscience Research* **18**, 155-171.

73. Giulian, D. and C. Robertson (1990) Inhibition of mononuclear phagocytes reduces ischemic injury in the spinal cord. *American Neurological Association* **27**, 33-42.

74. Giulian, D., J. Chen, J. Ingeman, J.K. George and M. Noponen (1989) The role of mononuclear phagocytes in wound healing after traumatic injury to adult mammalian brain. *The Journal of Neuroscience* **9**, 4416-4429.

75. Goldberger, M.E. and M. Murray (1988) Patterns of sprouting and implications for recovery of function. In: *Advances in Neurology, Vol. 47: Functional Recovery in Neurological Disease*, S.G. Waxman (Eds.), 361-385.

76. Goldberger M.M., M. Murray, and A. Tessler (1993) Sprouting and Regeneration in the Spinal Cord - Their roles in Recovery of Function After Spinal Injury. In: *Neuroregeneration.* A. Gorio (Ed) Raven Press, New York pp. 241-264.

77. Gordon, S. (1995) The macrophage. *BioEssays* **17**, 977-986.

78. Guénard V., Kleitman N., Morrissey T.K., Bunge R. P., and Aebischer P. (1992) Syngeneic Schwann cells derived from adult nerves seeded in semipermeable guidance channels enhance peripheral nerve regeneration. *J. of Neuroscience,* **12(9)**,3310-3320.

79. Hansebout, R.R., Blight, A.R., Fawcett, S., And Reddy, K. (1993). 4-aminopyridine in chronic spinal cord injury: A controlled, double-blind, crossover study in eight patients. J. Neurotrauma.**10**, 1-18.

80. Hansen, H.J. (1952). A pathologic-anatomical study on disc degeneration in dog with special reference to the so-called enchondrosis intervertebralis. Acta Orth. Scand. Suppl. **11**, 1-129.

81. Hatten, M.E., R.K.H. Liem, M.L. Shelanski, and C.A. Mason (1991) Astroglia in CNS injury. *Glia.* **4**, 233-243.

82. Hayes, K.C., Blight, A.R., And Potter, P.J. (1993). Preclinical trial of 4-aminopyridine in patients with chronic spinal cord injury. Paraplegia. **31**, 216-224.

83. Henry, W.B. (1975). Dorsal decompressive laminectomy in the treatment of thoraco-lumbar disc disease, JAAHA. **11**, 627-635.

84. Henry E.W., Chiu T., Nyilas E., Brushart T.M., Dikkes P., and Sidman R.L. (1985) Nerve regeneration through biodegradable polyester tubes. *Experimental Neurology* **90**, 652-676.

85. Hinkle, L., McCaig, C.D. and Robinson, K.R. (1981) The direction of growth of differentiating neurons and myeloblasts from frog embryos in an applied electric field, *J.Physiol.,* **314**, 121-135.

86. Hoerlein, B.F. (1978). The status of the various intervertebral disc surgeries for the dog in 1978. JAAHA. **14**, 563-570.

87. Jaffe L.F. and Nuccitelli R. (1977) Electrical controls of development. *Ann. Rev. Biophys. Bioeng.* **6**,445-476.

88. Jaffe, L.F. and M.-M. Poo (1979) Neurites grow faster toward the cathode than the anode in a steady field. *Journal of Experimental Zoology.* **209**, 115-127.

89. Kao, C.C. and L.W. Chang (1977) The mechanism of spinal cord cavitation following spinal cord transection. Part 1: a correlated histochemical study. *J. Neurosurg.* **46**, 197-209.

90. Kerns J.M., Fakhouri A.J., Weinrib H.P., and Freeman J.A. (1991) Electrical stimulation of nerve regeneration in the rat: the early effects evaluated by a vibrating probe and electron microscopy. *Neuroscience* **40(1)**, 93-107.

91. Kiernan, J.A. (1979) Hypotheses concerned with axonal regeneration in the mammalian nervous system. *Biol Rev.* **54**, 153-197.

92. Krause, T.L., G.D. Bittner (1990) Rapid Morphological Fusion of Severed Myelinated Axons by Polyethylene Glycol. *Proc. Natl. Acad. Sci. USA,* Vol. 87, pp. 1471-1475.

93. Krause, T.L., H.M. Fishman, M.L. Ballinger, and G.D. Bittner (1994). Extent and mechanism of sealing in transected giant axons of squid and earthworms. *Journal of Neuroscience.* **14**, 6638-6651.

94. Lazarov-Spiegler, O., A.S. Solomon, A.B. Zeev-Brann, D.L. Hirschberg, V. Lavie and M. Schwartz (1996) Transplantaion of activated macrophages overcomes central nervous system regrowth failure. *The FASEB Journal.* **10**, 1296-1302.

95. Liuzzi, F.J. and R.J. Lasek (1987) Astrocytes block axonal regeneration in mammals by activating the physiological stop pathway. *Science.* **237**, 642-645.

96. Lundborg G., Dahlin L.B., Danielsen N., Gelberman R.H., Longo F.M., Powell H.C., and Varon S. (1982) Nerve regeneration in silicone chambers: influence of gap length and of distal stump components. *Experimental Neurology* **76**, 361-375.

97. McCaig, C.D. (1986a) Dynamic aspects of amphibian neurite growth and the effects of an applied electric field , J. Physiol., **375**, 55-69.

98. McCaig, C.D. (1986b) Electric fields, contact guidance and the direction of nerve growth, *J. Embryoll.Exp.Morph.,* **94**, 245-255.

99. McCaig, C.D. (1987) Spinal neurite reabsorption and regrowth in vitro depend on the polarity of an applied electric field, *Development,* **100**, 31-34.

100. McCaig C.D., and Rajnicek A.M. (1991) Electrical fields, nerve growth and nerve regeneration. *Exp. Physiol.,* **76**, 473-494.

101. Means, E.D., and D.K. Anderson (1983) Neuronophagia by leukocytes in experimental spinal cord injury. *Journal of Neuropathology and Experimental Neurology.* **42**, 707-719.

102. Metcalf, M.E. and R.B. Borgens (1993a) Steady Ionic Current Traverses the Neural Folds in Amphibian Neurulae *J. Exptl. Zoology* (submitted). manuscript included in appendix materials.

103. Moriarty L.J., And Borgens R.B. (1998). Macrophage accumulations within the acute spinal injury are not affected by an externally applied electric field. J. Neurologic. Sci., (under review).

104. Moriarty, L.J., Duerstock, B.S., Bajaj, C.L., Lin. K., and Borgens, R.B. (1998) Two and Three Dimensional Computer Graphic Evaluation of the Subacute Spinal Cord Injury. *J. Neurol. Sci.* **155**, 121-137.

105. Muller, K.J. and J.G. Nicholls (1981) Regeneration and Plasticity. In: *Neurobiology of the Leech,* K.J. Muller, J.G. Nicholls, and G.S. Stend (Eds.). 197-226.

106. Nicoli, A. N., Perego G., Cella G. D., Maltarello M. C., Fini M., Rocca M., and Giardino R. (1996) Effectiveness of a bioabsorbable conduit in the repair of peripheral nerves. *Biomaterials,* **17,** 959-62.

107. Nielson, G. and T. Foley. (1989) Knot Selection for Parametric Spline Interpolation. InT. Lyche and L. Schumaker, editors, *Mathematical Methods in Computer Aided Geometric Design,* pages 261-271. Academic Press.

108. Noble, L. and J. Wrathall. (1985) Spinal cord contusion in the rat: morphometric analyses of alterations in the spinal cord. *Exp. Neurol.* **88,** 135-149.

109. Nuccitelli, R. and C.A. Erickson, (1983) Embryonic cell motility can be guided by physiological electrical fields. *Exp. Cell Res.* **147,** 195-201.

110. Nuccitelli, R. (1988) Physiological electric fields can influence cell motility, growth, and polarity. *Adv. Anat. Embryol. Cell Biol.,* **2,** 213-233.

111. Orida and Feldman (1982) Directional Protrusive Pseudopodial Activity and Motility in Macrophages Induced by Extracellular Electric Fields. *Cell Motility .* **2,** 243 255.

112. Patel, N. and Poo, M-M. (1982) Orientation of neurite growth by extracellular electric fields, *Journal of Neuroscience .* **2,**483-496.

113. Perry, V.H. and B.C. Brown (1992) Role of macrophages in peripheral nerve degeneration and repair. *BioEssays* **14,** 401-406.

114. Perry, V.H., M.C. Brown, and S. Gordon (1987) The macrophage response to central and peripheral nerve injury: A possible role for macrophages in regeneration. *J. Exp. Med.* **165,** 1218-1223.

115. Perry, V.H., P.B. Anderson and S. Gordon (1993) Macrophages and inflammation in the central nervous system. *TINS* **16,** 268-273.

116. Perry, V.H., M.C. Brown, and P.B. Anderson. (1993) Macrophage Response to Central and Peripheral Nerve Injury. In: *Advances in Neurobiology: Neural Injury and Regeneration Vol 59* F.J. Seil (Ed.) pp. 91-103.

117. Pitas, R.E., Innerarity, J.N., Weinstein, J.N. and Mahley, R.W. (1981) Acetoacetylated lipoproteins used to distinguish fibroblasts from macrophages *in vitro* by fluorescence microscopy. *Arteriosclerosis* **1,** 177-185.

118. Polman, C.H., C.D. Dijkstra, T. Sminia, and J. Koetsier (1986) Immunohistological analysis of macrophages in the central nervous system of Lewis rats with acute experimental allergic encephalomyelitis. *J. Neuroimmunol* **11,** 215-222.

119. Povlishock, J.T. (1993) Traumatic Brain Injury The Pathobiology of Injury and Repair. In: *Neuroregeneration.* A. Gorio (Ed) Raven Press, New York pp. 185-216.

120. Pratt, V. (1985) Techniques for conic splines. *Computer Graphics*, 19(3):151-159.

121. Ramon y Cajal, S. (1928) *Degeneration and Regeneration of the nervous system.* Hafner Publishing Co. New York, NY.

122. Reier, P.J. and J.D. Houle (1988) The glial scar: Its bearing on axonal elongation and transplantation approaches to CNS repair. In: Advances in Neurology, Vol. 47: Functional Recovery in Neurological Diseases. S.G. Waxman, Ed., (Raven Press, New York), pp. 87-138.

123. Reier, P.J., L.J. Stensaas, and L. Guth (1983) Spinal Cord Reconstruction in: *The Astrocytic Scar As an Impediment to Regeneration in the Central Nervous System.* Kao C.C., Bunge R.P. and Reier R.J. (eds.); CC Thomas, Springfield, IL, pp. 163-195.

124. Robinson K.R. (1985) The responses of cell to electrical fields, a review. *J. Cell Biol.* **101,** 2023-2027.

125. Robinson, K.R., and R.F. Stump (1984) Self-generated electrical currents through *Xenopus* neurulae. *J. Physiol. 352*:339.

126. Roederer, E., N.H. Goldberg, and M.J. Cohen (1983) Modification of retrograde degeneration in transected spinal axons of the lamprey by applied DC current. *Journal of Neuroscience* **1**, 153-160.

127. Rovainen, C.M. (1976) Regeneration of Müller and Mauthner Axons after spinal transection in larval lampreys. *J. Comp. Neur.* **168**, 545-554

128. Salzman, S.K., Mendez, A.A., Sabato, S., et al., (1990). Anesthesia influences the outcome from experimental spinal cord injury. Brain Res. **521**, 33-39.

129. Schwab, M.E., J.P. Kapfhammer, and C.E. Bandtlow (1993) Inhibitors of neurite growth. *Annual Review of Neuroscience.* **16**, 565-595.

130. Selzer, M.E. (1978) Mechanisms of functional recovery and regeneration after spinal cord transection in larval sea lamprey. *J. Physiol.* 277:395-408.

131. Shi, R. and R.B. Borgens (1994) Embryonic neuroepithelium sodium transport, the resulting physiogical potential, and cranial developoment. *Dev. Biol.* **165**, 105-116

132. Stocum, D.L. (1995) Wound Repair, Regeneration and Artificial Tissues. ed.R.G. Landes Company.

133. Strautman, A.F., R.J. Cook, and K.R. Robinson (1990) The distribtion of free calcium in transected spinal axons and it modulation by applied electrical fields. J. Neuroscience **10(11)**, 3564-3575.

134. Tarlov, I.M. (1957). *Spinal Cord Compression: Mechanisms of Paralysis and Treatment..* Charles C. Thomas (ed), Springfield, Illinois pps. 1-147.

135. Tator, C.H. and M.G. Fehlings (1991) Review of the secondary injury theory of acute spinal cord trauma with emphasis on vascular mechanisms. *J. Neurosurgery* **75**, 15-26.

136. Toombs, J.P. And Bauer, (1993). M.S. in Textbook of Small Animal Surgery. D. Slatter, (ed) W.B. Saunders Company. pps. 1070-1087.

137. Treherne, J.M, S.K.A. Woodward, Z.M. Varga, J.M. Ritchie, and J.G. Nicholls. (1992) Restoration of conduction and growth of axons through injured spinal cord of neonatal opossum in culture. *Proceedings of the National Academy of Science USA* **89**, 431-434.

138. Valetini R.F., and Aebischer P. (1997) Strategies for the engineering of peripheral nervous tissue regeneration. In *Principles of Tissue Engineering*, (eds. Lanza R., Langer R., and Chick W.) 671-684. R.G. Landes Company.

139. Valentini R.F., Sabatini A.M., Dario P., and Aebischer P. (1989) Polymer electret guidance channels enhance peripheral nerve regeneration in mice. *Brain Research* **480**, 300-304.

140. Waibl, H. (1973) *Zur topographie der medulla spinalis der albinoratte (Rattus norvegicus)* Spronger-Verlag, Berlin, New York.

141. Williams L.R., Danielsen N., Müller H., and Varon S. (1987) Exogenous matrix precursors promote functional nerve regeneration across a 15-mm gap within a silicone chamber in a rat. *J. of Comparative Neurology* **264**, 284-290.

142. Wood, M.R. and M.J. Cohen. (1979) Synaptic regeneration in identified neurons of the lamprey spinal cord. *Science* **206**, 344-347.

143. Young, W. (1993) Secondary injury mechanisms in acute spinal cord injury, *J. Emerg. Med.* **11**, 13-22.

144. Young, W., P.P. Huang and J. Kume-Kick (1995) Cellular, ionic, and biomolecular mechanisms of the injury process. *Contemporary Management of Spinal Cord Injury*, pp 27-42 eds.AANS Publications Committee, Edward C. Benzel, MD, and Charles H. Tator, MD.

V. Publications

Borgens, R.B., D.M. Bohnert (1997) The Responses of Mammalian Spinal Axons to an Applied DC Voltage Gradient *Experiemental Neurology,* **145**, 376-389.

Borgens, R.B. (1998). Electrically mediated regeneration and guidance of adult mammalian spinal axons into polymeric channels. *J. of Neuroscience.* (in press).

Borgens, R.B., J.P. Toombs, G. Breur, W.R. Widmer, D. Waters, P. March, L. Adams, A.M. Harbath. (1998). An imposed oscillating electrical field improves the recovery of function in neurologically complete paraplegic dogs. *J. of Neurotrauma.* (under review).

Jenkins, L.S., Duerstock, B.S. and Borgens, R.B. (1996). Reduction of the current of injury leaving the amputation inhibits limb regeneration in the red spotted newt. *Developmental Biology.* **178**, 251-262.

Moriarty L.J., And Borgens R.B. (1998). Macrophage accumulations within the acute spinal injury are not affected by an externally applied electric field. J. Neurologic. Sci., (under review).

Moriarty, L.J., Duerstock, B.S., Bajaj, C.L., Lin. K., and Borgens, R.B. (1998) Two and Three Dimensional Computer Graphic Evaluation of the Subacute Spinal Cord Injury. *J. Neurol. Sci.* (in press).

Shi, R., and Borgens, R.B. (1998). Acute repair of crushed guinea pig spinal cord by polyethylene glycol. *J. of Neurophysiology.* (under review).

Shi, R., Blight, A.R., Borgens, R.B. (1998). Functional reconnection of severed mammalian spinal axons by a molecular surfactant. *J. of Neurotrauma.* (under review).

IV. Personnel

R. B. Borgens

J. P. Toombs

L. Adams

D. Bohnert

A. Harbath

H. Eddy-Harbath

W. R. Widmer

P. March